# PRELIMINARY LITHOLOGICAL AND STRUCTURAL FRAMEWORK OF EOCENE VOLCANIC ROCKS IN THE NECHAKO REGION, CENTRAL BRITISH COLUMBIA

Prepared for

Geoscience BC

Prepared by


Esther Bordet
Craig Hart
Dianne Mitchinson

University of British Columbia, Mineral Deposit Research Unit


April 2011

**TABLE OF CONTENTS**

**LIST OF FIGURES**

**LIST OF TABLES**

## Project Background

In July 2009, Geoscience BC issued a request for proposal to stimulate exploration activity and attract oil and gas investment in the Nechako Basin, British Columbia. The Mineral Deposit Research Unit (MDRU) submitted a successful proposal to address the following indicated Areas of Interest:

- Constraints on the distribution and thickness of the Eocene volcanic rocks from either direct sampling or remote sensing methods
- Development of regional tectonic models that integrate a wide variety of relevant geoscience datasets, including faulting history, and have the potential to indicate the thickness of Cretaceous and/or Eocene sedimentary rocks across the basin
- Heat flow and thermal evolution of the Nechako basin

The project, from January 2010 to April 2011, was led by MDRU Director Craig Hart. The project's main components, including field work, data collection, analytical work, and data integration and interpretations were conducted by Esther Bordet, an MDRU PhD candidate. Dianne Mitchinson, a Post-Doctoral Fellow at MDRU, was responsible for components related to physical property modelling and their integration with geological and structural data.

## Acknowledgements

Geoscience BC provided the main source of funding to the project, including field work expenses and analytical work. Geoscience BC also granted a scholarship to Esther Bordet. Additional support is provided through a Natural Science and Engineering Research Council of Canada Industrial Postgraduate Scholarship, in partnership with Golder Associates Ltd.

Significant scientific contributions and support were provided throughout the project by Mitch Mihalynuk and Janet Riddell of the BC Geological Survey. James Siddorn, from SRK Consulting, communicated his method for the interpretation of the structural framework using aeromagnetic maps. The project also contributed from discussions and data sharing with Graham Andrews, Kelly Russell, Randy Enkin, Jessica Spratt, Nathan Hayward, Jim Mortensen, Larry Diakow and Derek Thorkelson.

Julia Smith provided effective support during the 2010 field season. Chelsea Raley conducted wet-dry density measurements under the supervision of Betsy Friedlander and Kelly Russell.

## 1 Introduction

### 1.1 Project Location and Access

The Nechako region of central British Columbia has been defined as the area bounded to the east by the Fraser fault, to the west by the Coast Mountains and Yalakom fault, by the Skeena arch to the north and the Tyaughton Basin to the south (Figure 1.1; Ferri and Riddell, 2006).

The Nechako region is easily accessible by car. The drive on Highway 1 West from Vancouver to Cache Creek, and Highway 97 North from Cache Creek to Williams Lake or Quesnel takes about 7 hours. Highway 59 connects Quesnel to the community of Nazko about 130 km to the east. Around Nazko, a series of well-maintained active logging roads provide access to the main traverse areas described in this report. Secondary logging roads leading to inactive logging activities were used occasionally, but areas of difficult access where mostly covered by foot.

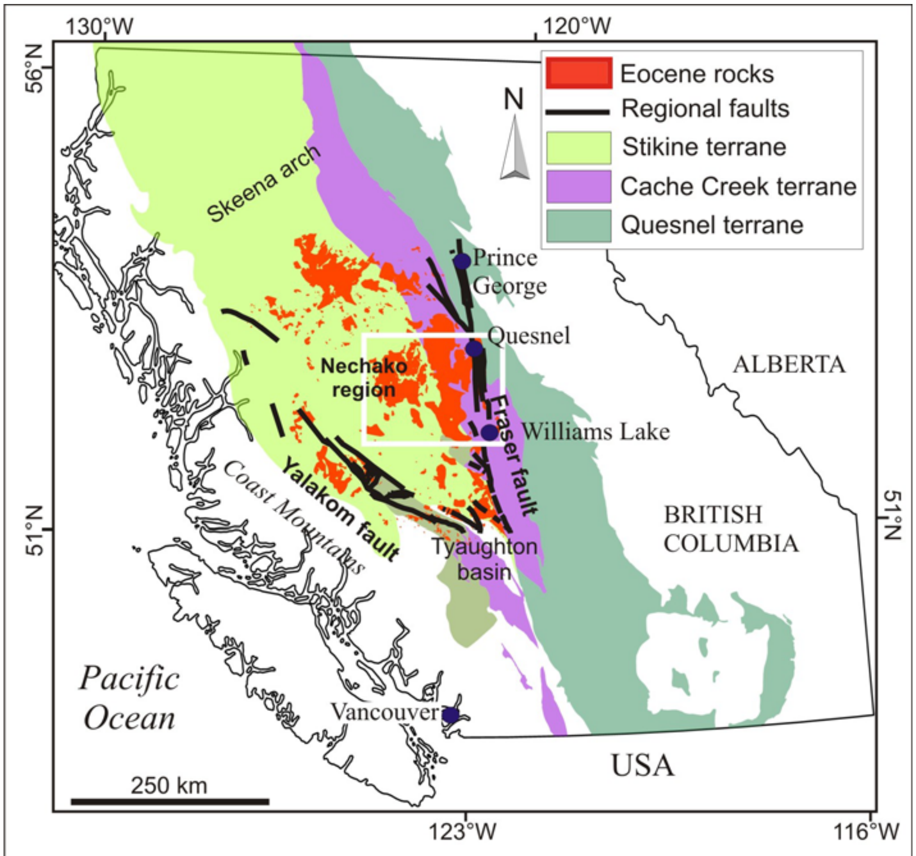


**Figure 1-1: Location of the Nechako region in central British Columbia and position of the region relative to the accreted terranes and regional structures (adapted from Massey et al., 2005). Extent of Eocene volcanic rocks is indicated in red. Summer 2010 field area is outlined by a white rectangle.**

Field surveys conducted in 2010 covered a large portion of the Nechako region, including the area around Nazko, parts of the Chilcotin Plateau to the south, and some selected traverses south and west of Quesnel and down to Williams Lake (Figure 1.2; Bordet and Hart, 2011). Additional traverses were conducted along an eastern portion of the seismic transect surveyed in 2009 as part of the BATHOLITHS Continental Dynamics Project (Wang et al., 2010) between Nazko and Quesnel (Figure 1.2).

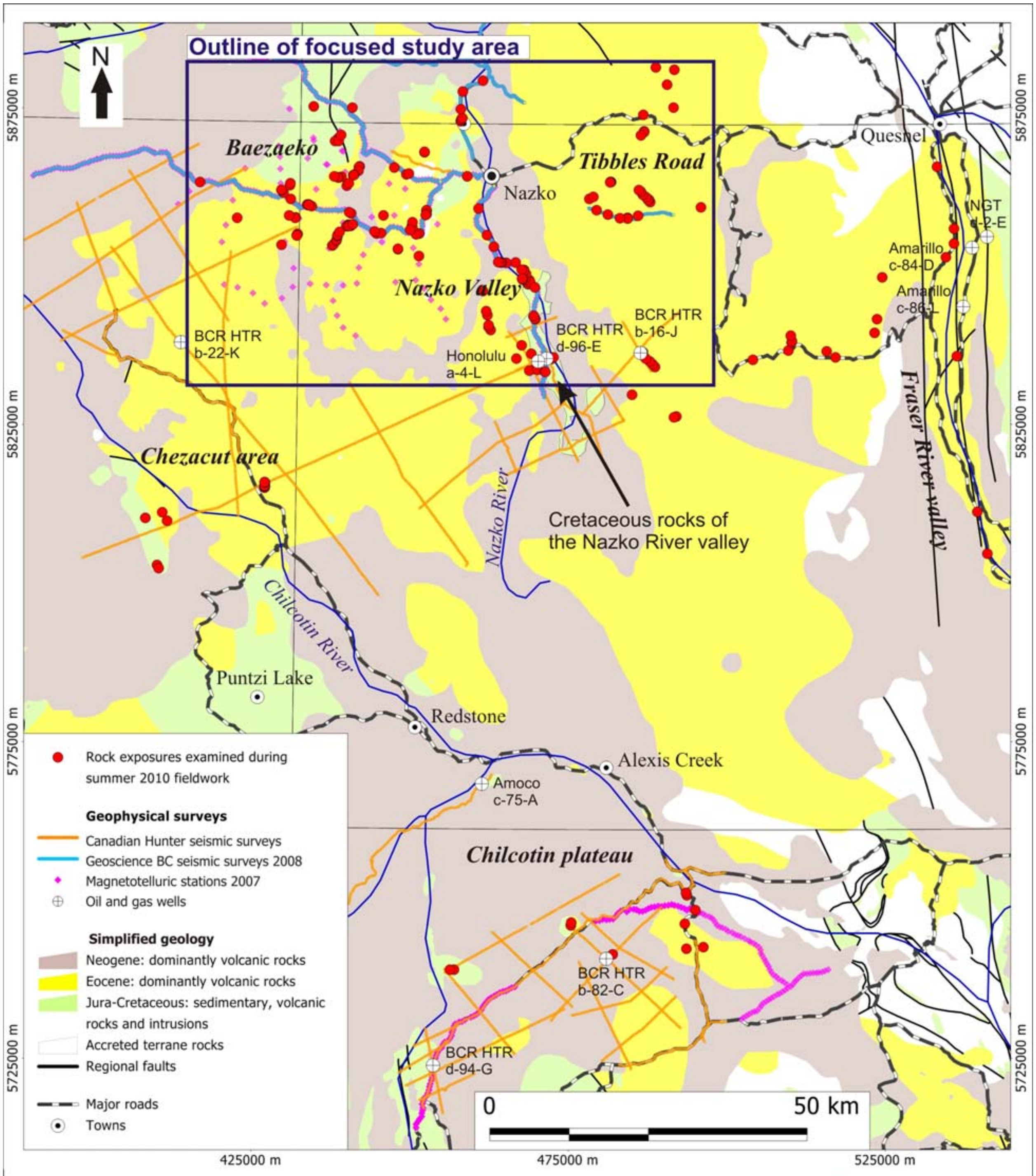

**Figure 1-2: Distribution map of summer 2010 documented outcrops over a simplified geology layout of the Nechako region, central British Columbia (based on Massey et al., 2005; UTM Zone 10N, NAD 83). Black rectangle outlines focused study area and the three main traverses referred to in this report. Map also displays oil and gas wells (Ferri and Riddell, 2006), seismic lines (Calvert et al., 2009; Hayward and Calvert, 2009) and magnetotelluric stations (Spratt and Craven, 2009, 2010).**

For the purpose of this report, a focused study area of about 80 x 50 km was selected around the community of Nazko (Figure 1.2). It comprises the most detailed and relatively continuous lithological and structural dataset collected during the field work and contains numerous previously undocumented rock exposures. Additionally, this part of the Nechako region has been extensively surveyed by seismic, gravity and MT surveys, and the integration of these previous surveys with recently mapped outcrops is especially relevant.

## 1.2 Physiography and Glacial History

The Nechako region is part of the Interior Plateau of central British Columbia. It is characterized by an area of subdued topography between the Coast Mountains to the west and the Cariboo Mountains to the east. Subdued topographic relief in the Nechako region results from several Pleistocene glaciations and resultant thick accumulations of glacial materials. The last major glaciation recorded in the Canadian Cordillera took place during Early and Late Wisconsinian times and achieved its maximum extent around 15000-14000 years BP (Clague, 1991; Clague and James, 2001). At this time, the ice sheet covered all of southern British Columbia to depths up to 2 km beneath the center of the ice sheet in the Interior of BC (Clague and James, 2001).

Growth and decay of the Cordilleran Ice Sheet triggered isostatic adjustments in the crust and mantle of the Canadian Cordillera. Sedimentological records and paleo-shorelines indicate that isostatic rebound resulting from the most recent decay of the Cordilleran Ice Sheet occurred very rapidly and was complete within a period of 4000 years (Clague, 1991; Clague and James, 2001).

The present-day topography and physiography of the Nechako region results from combined erosional-depositional processes generated by successive growth and decay cycles of the Cordilleran Ice Sheet, and associated isostatic uplift. The region is almost entirely below tree line. Bedrock is exposed along ridges and small buttes, in drainages and rivers, and along the numerous logging roads.

## 1.3 Previous Work and Summary of Existing Data

### 1.3.1 Geological Datasets and Maps

Regional geological maps of the Nechako region include the geological compilations by Massey et al. (2005), the Nechako NATMAP project (Struik et al., 2007), QUEST, QUEST West and QUEST South projects led by Geoscience BC from 2007 to 2010 (see Geoscience BC website for more details). The NATMAP and QUEST surveys do not cover the study area part of this project. Riddell (2006) completed a geological compilation for the Nechako region since it had potential for oil and gas exploration. This compilation has been used as a reference map for most geophysical projects taking place in this area.

Bedrock geology maps for the Nechako region (Tipper, 1959 and 1969; Mihalynuk et al., 2008a and 2009; Diakow and Levson, 1997) are available at a 1:50,000 or 1:250,000 scale and cover NTS map sheets 093F, part of 093G, B and C, part of 092N and most of 092O. Surficial Quaternary geology maps are also available in these areas.

Radiometric age dates for British Columbia are compiled in the CordAge database (Breitsprecher and Mortensen, 2004) and include several dates for the project area (see Chapter 3 for more details). Geochemical analyses of lithological units were conducted as part of this and various past projects in the Nechako region. This data and interpretations for Neogene and Holocene volcanic rocks are compiled and compared to Eocene signatures (see Chapter 3 of this report for more details).

#### 1.3.2 Geophysical Surveys and Datasets

Results from several aeromagnetic and gravity surveys are available for the Nechako region and many are available from the Geological Survey of Canada's Geoscience Data Repository website (http://gdr.nrcan.gc.ca). In particular, the Geological Survey of Canada conducted a high-resolution regional aeromagnetic survey in the Interior Plateau of British Columbia in 1993-1994 (GSC, 1994; Teskey et al., 1997; see Chapter 5 of this report for more details).

#### 1.3.3 Physical Properties Datasets

Physical properties measurements from surface samples have been conducted as part of several past studies in the Nechako region (Andrews et al., 2008; Enkin et al., 2008; Quane et al., 2010). The latest BC Rock Property database integrates all of the data collected in previous studies. Data pertaining to the focused study area have been used in this report. They include density, magnetic susceptibility, resistivity measurements on Chilcotin Group basalts, Cheslatta Lake basalts, Eocene volcanic rocks, and Jurassic and Cretaceous volcanic rocks and sediments.

Additionally, Mwenifumbo and Mwenifumbo (2010) conducted physical property measurements and well logs interpretations on several oil and gas wells of the Nechako region.

#### 1.3.4 Oil and Gas Exploration Data

Exploration efforts in the Nechako region between 1931 and 1986 have resulted in over 1100 km of seismic profiles, 5000 km of gravity surveys, and the drilling of 12 wells. Recent surveys and interpretive efforts facilitated by Geoscience BC (i.e., Calvert et al., 2009; Hayward and Calvert, 2009; Spratt and Craven, 2009, 2010) include approximately 330 km of seismic reflection data and new magnetotelluric surveys. More details on the wells and surveys are provided in Chapter 6.

Well logs and reports are available from the Ministry of Energy and Mines website (http://www.empr.gov.bc.ca) . Recent seismic surveys conducted by Geoscience BC in 2008 can be found on the Geoscience BC website (http://www.geosciencebc.com/s/2009-09.asp). In addition, a 2D joint inversion of seismic, magnetotelluric and gravity data was recently completed (WesternGeco MDIC, 2010).

#### 1.3.5 Mineral Exploration Data

The Nechako region has seen limited exploration and mapping compared to the rest of British Columbia, because of the extensive glacial till and forest cover and limited rock exposures. Additionally, Chilcotin Group basalts cover the region and have long been a barrier to exploration, but recent studies show that their distribution and thickness are not as extensive as initially thought (Andrews and Russell, 2007 and 2008; Mihalynuk, 2007; Dohaney et al., 2010a). Recent work in the Nechako region has been focused on the development of exploration activities in the context of the Pine Beetle infestation in central British Columbia and its devastating effects on the economic sustainability (Westfall, 2004).

The MINFILE Mineral Inventory (http://minfile.gov.bc.ca/) contains a number of mineral deposits, prospects and showings for the Nechako region. Several technical reports and thesis work provide information about the mineral occurrences hosted in the Jura-Cretaceous and Eocene sequence. This information is included in a metallogenic summary for the Nechako region in Chapter 2.

### 1.4 Statement of the Problem

Central BC's Nechako region is partially underlain by Jura-Cretaceous successor basin clastic sedimentary rocks that have the potential to host petroleum (Ferri and Riddell, 2006; Riddell and Ferri, 2008). However, this Mesozoic stratigraphy and related structures have been subjected to widespread Eocene magmatic, thermal and structural overprinting, which have extensively modified and complicated the rocks of interest. Variable thicknesses of Eocene volcanic strata now extensively cover potential hydrocarbon host rocks. Masking of the hydrocarbon prospective strata is further exacerbated by the extensive cover of Late Cenozoic subaerial Chilcotin flood basalts, typically less than 50 m thick, and extensive glacial sediments, typically between 10 and 50m thick (Andrews and Russell, 2008).

As a result of this extensive, variably thick and heterogeneous post-Cretaceous cover, recent geophysical surveys (Calvert et al., 2009; Hayward and Calvert, 2009; Spratt and Craven, 2009, 2010) aimed at understanding the structure of the Jura-Cretaceous basin, but they are poorly constrained by geological observations.

Unravelling the effects of the Eocene volcanic stratigraphy and structure on the regional geology is further exacerbated because the stratigraphy of the Eocene volcanic rocks is controversial. Eocene volcanic rocks have been traditionally divided into the Ootsa Lake Group and the Endako Group (Souther, 1991; Anderson et al., 2000), but distinctions between the two groups based on age, composition or field criteria are unclear.

Understanding the stratigraphy of the Eocene volcanic rocks will benefit the regional tectonic evolution for central British Columbia. In fact, this part of the Cordillera likely experienced a range of tectonic settings from the Late Cretaceous to the Neogene and includes regional scale extensional features such as calderas or pull-apart basins. These features have important implications for explaining the structural architecture of the Nechako region.

### 1.5 Objectives and Implications

The objectives of this report are to:

- <u>Propose an improved stratigraphic model for the Eocene period</u> in the Nechako region based on field characteristics of Eocene volcanic rocks including: lithologies and facies variations, geochemical signature, age, field relationships and lithologic characteristics. To develop this model, existing geological and geophysical data will be combined with new field observations and data.

- Assess the physical properties of Eocene volcanic rocks in the context of mapped lithologies and textures. Physical properties constitute a direct link between the geology and geophysical models.
- Constrain the variable thicknesses and structural framework of Eocene volcanic rocks in order to quantify the depth of underlying Cretaceous rocks, provide insights into the Jura-Cretaceous basin architecture, and improve understanding of the tectonic evolution of this part of British Columbia.

Characterization of the nature, thickness and structural framework of Eocene volcanic rocks in the Nechako region will provide new insights into the area's Early Cenozoic history, contribute to improved interpretations and add value to existing geophysical, particularly seismic and magnetotelluric, data sets. Such information, integration and interpretations will provide a stronger geological foundation to facilitate future exploration efforts for natural resources, including oil and gas and mineral deposits.

### 1.6 Methods

A number of methods were utilized in this project, including:

- Field investigations: mapping, description of lithologies and volcanic facies, structural measurements, systematic magnetic susceptibility measurements, rock sampling (Figures 1.2 and 1.3; Appendices 1 and 5)

- Petrography: microscopic observation of selected samples to constrain mineral assemblages and abundance in the different mappable units (Figure 1.3)

- Geochemistry: whole rock geochemical analysis of selected samples to characterize the geochemical signature of Eocene volcanic rocks and confirm composition of identified mappable units (Figure 1.3; Appendix 2)

- Geochronology: U-Pb isotopic dating of selected samples to constrain ages of magmatism and constrain age relationships between mappable units (Figure 1.3)

- Physical property measurements: in addition to systematic magnetic susceptibility measurements in the field, wet-dry density measurements were conducted on a continuous suite of samples (Appendices 3 and 4)

- Structural interpretations: a preliminary stratigraphic and structural framework based on lineament interpretation was produced from aeromagnetic maps.

- Thickness model: variable thicknesses of the Eocene package were assessed using a combination of field observations, well logs, and a computed GIS model.

- Gravity and magnetic inversions: gravity and magnetic inversions were carried out for selected areas using the Grav3D and Mag3D codes from the University of British Columbia- Geophysical Inversion Facility (UBC-GIF)

Integration of the different datasets and results in a detailed and comprehensive final product aimed at representing the different aspect of Eocene volcanic rocks in the Nechako region.

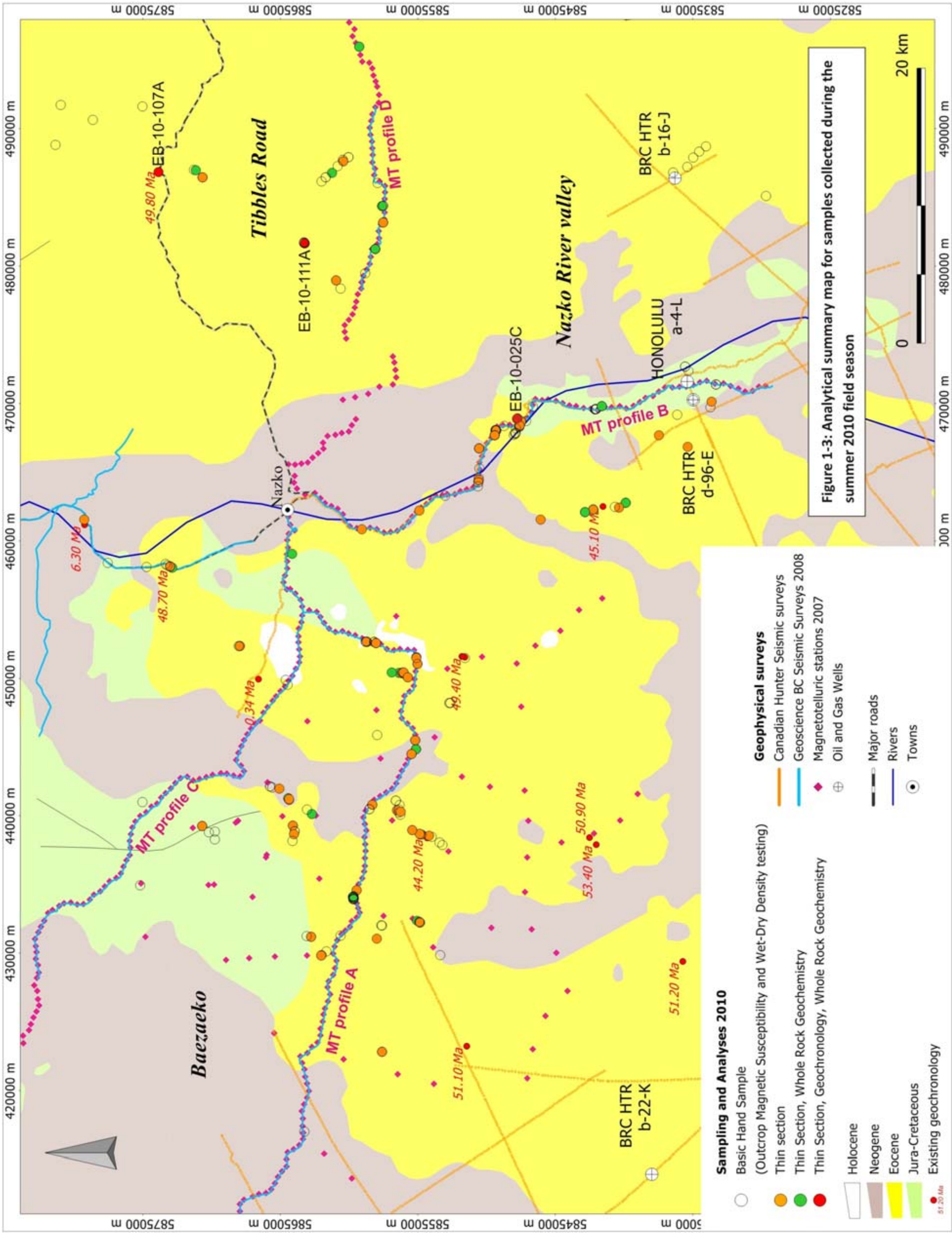


**Figure 1-3: Analytical summary map for samples collected during the summer 2010 field season**

# 2 Regional Geology

## 2.1 Tectonic Setting

The Nechako region is underlain by the accreted Paleozoic and Mesozoic terranes of the western Canadian Cordillera, including the Stikine (island arc), Cache Creek (subduction-related accretionary-complex) and Quesnel (island arc) terranes (Figure 1.1; Monger and Price, 2002; Gabrielse and Yorath, 1991).

Late Cretaceous and Eocene volcanic rocks were emplaced in a post-accretionary setting during a regional, crustal-scale extensional event, associated with movement along major fault systems (Struik, 1993). These structures include Late Cretaceous to Early Eocene northwest-trending extensional and dextral faults such as the Yalakom fault (Struik, 1993). Coeval normal to strike-slip northeast-trending faults are associated with Eocene dikes (Lowe et al., 2001). From the Early Eocene to the Early Oligocene, northwest-directed extension generated north-trending en echelon fault systems such as the regional dextral Fraser fault. The Nechako region is bounded by the Yalakom and Fraser faults to the west and east, respectively (Figure 1.1).

## 2.2 Regional Geology & Magmatic evolution

Magmatic evolution of the Nechako region of central British Columbia is associated with the geomorphic evolution of the Canadian Cordillera from the Middle-Late Jurassic and the accretion of terranes to the ancestral western margin of North America. Two metamorphic and plutonic complexes formed as a result of successive phases of accretion, the Omineca Belt to the east and the Coast Belt to the west (Mathews, 1991).

In the Early Cretaceous, magmatic activity was minimal throughout the Canadian Cordillera, but contemporaneous with uplift and volcanism in the western Cordillera (Mathews, 1991). Mid-Cretaceous calc-alkaline magmatism in southern BC produced the Spences Bridge-Kingvale volcanic suite, near the southern margin of the Tyaughton Trough, and the Kasalka Group volcanics further north in the central Intermontane Belt (Souther, 1991). These volcanic rocks comprise mainly felsic pyroclastic rocks of the Kasalka Group, overlain by basaltic, andesitic and rhyolitic flows, welded and non-welded ignimbrites of the Spences Bridge and Kingvale groups. These rocks may represent a chain of stratovolcanoes associated with subsiding, fault-bounded basins. They unconformably overlie late Early Cretaceous clastic marine sediments of the Skeena Group (Souther, 1991).

Late Cretaceous and Paleocene times were dominated by transcurrent faulting and arc magmatism (Mathews, 1991). Upper Cretaceous volcanic rocks of the Brian Boru and Tip Top formations (70-72 Ma, K-Ar; Souther, 1991) are documented in the northern part of the province. These isolated centres of volcanism produced sequences of andesite to dacitic flows and breccias and interlayered volcaniclastic and pyroclastic rocks, with associated dikes and plutons. The Late Cretaceous Bulkley suite (88-70 Ma; Souther, 1991; Friedman et al., 2001) comprises high-level intermediate composition intrusive bodies.

During the Early and Middle Eocene, widespread calc-alkaline and alkaline volcanism occurred in the interior of the Canadian Cordillera, associated with a change from dominantly compressional deformation to rotation and extension (Mathews, 1991). High heat flow was accompanied by extension and followed by rapid uplift and denudation. Sedimentary and volcanic rocks accumulated in local structural depressions such as grabens and basins, and are preserved in present-day topographic lows. In particular, locally thick, discontinuous subaerial calc-alkaline Eocene volcanic sequences of the Ootsa Lake and Endako groups (53-45 Ma; Grainger et al., 2001) unconformably overlie deformed Mesozoic rocks and have been mapped as part of this study. Flow-banded to massive intermediate volcanic flows and associated breccias dominate. Widespread units of welded rhyolitic ash deposits are locally interbedded with basaltic and andesitic flows. The wide distribution and lateral variations of these sequences suggest multiple volcanic events taking place at several discrete volcanic centres.

A period of magmatic quiescence followed the Middle Eocene and led to the development of subdued topography (Mathews, 1991), later covered by extensive flood basalts of the Neogene Chilcotin Group.

## 2.3 Stratigraphy

Thick, discontinuous sequences of Eocene volcanic rocks cover over 15,000 km$^2$ of the Nechako region, central British Columbia. They unconformably overlie Jura-Cretaceous basin clastic sedimentary rocks and are extensively masked by Neogene subaerial Chilcotin flood basalts and Quaternary glacial sediments.

### 2.3.1 Jura–Cretaceous Basin Stratigraphy

Jurassic strata (Figure 2.1) are poorly exposed in the region. Basalt and andesitic lava flows, sedimentary rocks, lapilli tuff and rhyolite ash flows of the Early and Middle Jurassic Hazelton Group are exposed in the Tsacha Lake area (NTS 093F; Diakow and Levson, 1997). Similar units ascribed to the Hazelton Group are also identified in the western part of the Quesnel 1:250 000 map sheet (NTS 093B; Tipper, 1959). Middle to Upper Jurassic strata consist of sandstone, conglomerate, shale and minor calcareous sediments, andesitic, rhyolitic and basaltic flows associated with tuff, breccias and volcaniclastic sandstone and conglomerate (Riddell, 2006; Riddell and Ferri, 2008). In the Chilanko Forks (Mihalynuk et al., 2009) and Chezacut areas (Mihalynuk et al., 2008a), undated occurrences of volcaniclastic rocks, basalts, dacite tuff and breccias occur, which may be Jurassic in age as inferred by Tipper (1969).

Cretaceous rocks are sparsely exposed in the region. Thick beds of Cretaceous conglomerate and sandstone are locally exposed along the Nazko River valley (Figure 1.2) as a result of tectonic deformation and tilting, but their extent outside of this narrow belt in unknown. These clastic sedimentary rocks are rich in chert clasts, but contain a variety of clasts types in variable proportions, including quartzite and volcanic rock pebbles (Figure 2.1). Feldspar crystals and muscovite flakes are locally abundant.

### 2.3.2 Eocene Volcanic Rocks

Locally thick, subaerial Eocene volcanic sequences unconformably overlie the deformed Mesozoic rocks. Eocene magmatic rocks erupted during a period of regional northwest-directed extension (Struik and MacIntyre, 2001) associated with movement along major north-northwest-trending structures, such as the Yalakom and Fraser dextral strike-slip faults. Dextral transtensional events were accompanied by extensive volcanism, which probably exploited the major extensional structures as conduits towards the surface.

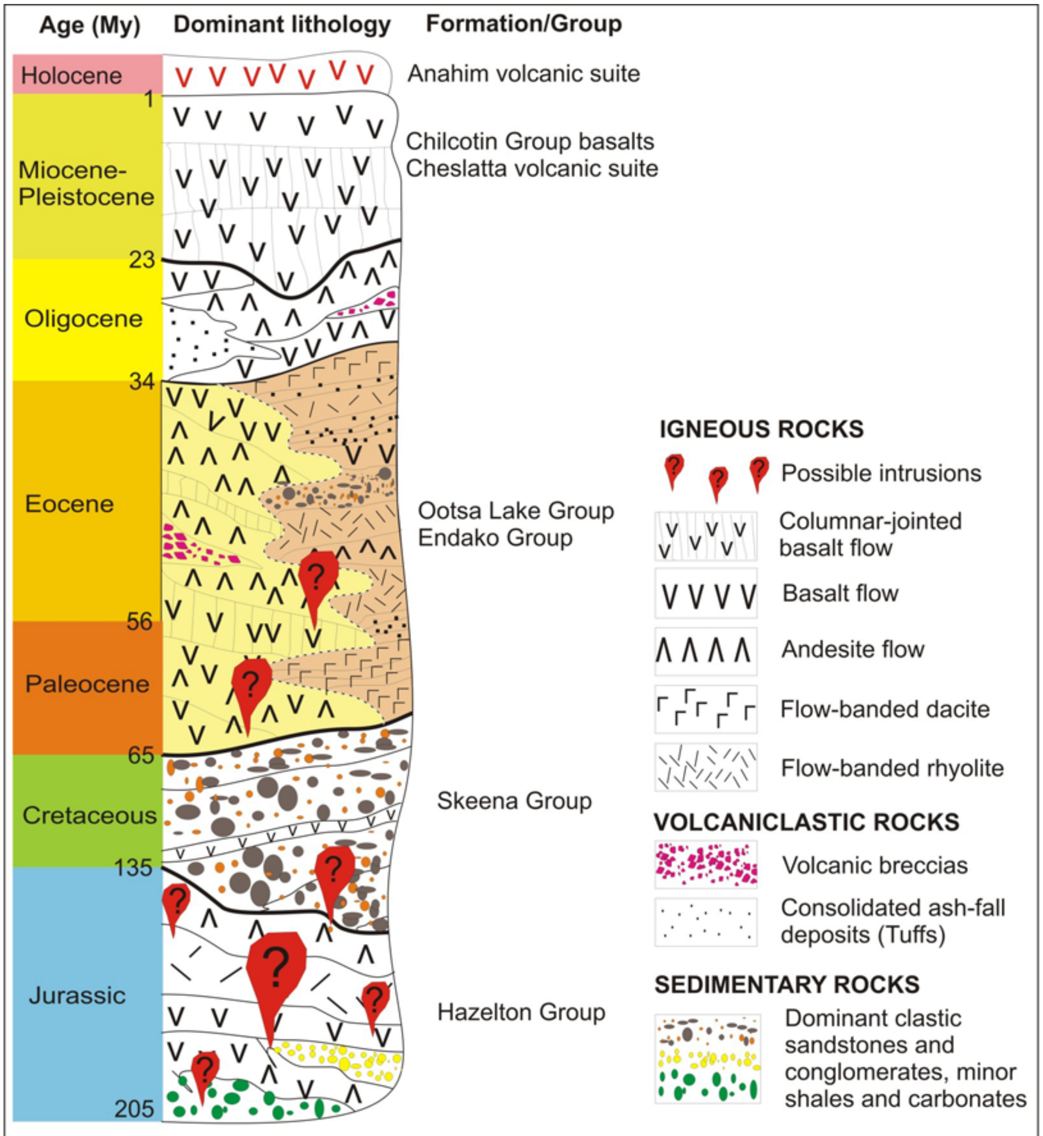

**Figure 2-1: Simplified regional stratigraphy for the Nechako region, central British Columbia**

Eocene volcanic rocks have been traditionally divided into the Ootsa Lake Group and the Endako Group (Figure 2.1; Souther, 1991; Anderson et al., 2000). The Ootsa Lake Group comprises flow-banded rhyolite, dacite, amygdaloidal basalt flows and minor andesite flows and tuff units (Diakow and Mihalynuk, 1986; Wetherup, 1997; Grainger et al., 2001; Riddell, 2006), locally interbedded with alternating sandstone and coarse pebble- to cobble-conglomerate beds (Diakow and Mihalynuk, 1986; Wetherup, 1997). Regional lithological variations are observed between the northern and southern part of the Nechako region. To the north, on the Whitesail Lake map sheet (NTS 093E), diorite sills and dikes, andesitic and basaltic flows, and augite-phyric basalt flows are intermixed with dacitic tuff at the base, air-fall tuff, ash-flow tuff, debris flow deposits and conglomerate (Grainger et al., 2001). On the Nechako

River and Fort Fraser map sheets (NTS 093F and 093K respectively), rhyolitic flows and domes, tuff, pyroclastic and autoclastic breccias and minor dacitic and andesitic flows dominate (Grainger et al., 2001). The age of the Ootsa Lake Group in the Vanderhoof area has been constrained between 53–47 Ma by U-Pb and Ar-Ar dating techniques (Grainger et al., 2001).

The Endako Group consists of andesitic basalts and basalt flows (Grainger et al., 2001). They are distinguished from the younger Chilcotin Group basalts by the presence of significant amounts (5–30%) of elongate to acicular plagioclase phenocrysts and limonite-, chlorite-, calcite- or quartz-filled amygdules (Wetherup, 1997). Whereas the Chilcotin basalts are normally flat-lying, the Endako Group basalts occur as beds 1 to 3 m thick consisting of rarely columnar-jointed, moderately to highly vesicular lava and dipping moderately from 20 to 30° (Wetherup, 1997). West of the Fraser River, south of Quesnel, an Eocene assemblage of pyroclastic rocks, lava flows and minor sedimentary rocks has been assigned to the Endako Group (Logan and Moynihan, 2009). This assemblage includes autobreccias, monomictic and diamictic debris deposits that predominate over coherent flows, tuffs and sedimentary rocks. East of the Fraser River, locally columnar-jointed, flat-lying vesicular basalt or basaltic andesite flows interlayered with clastic units yielded a K-Ar age of 50–44 Ma (Logan and Moynihan, 2009), which is similar to the 51–45 Ma (Ar-Ar) age previously obtained for the Endako Group (Grainger et al., 2001).

### 2.3.3 Eocene and/or Oligocene Rocks

Tipper (1959) recognized a distinct mappable unit in the northern part of the Quesnel 1:250 000 map sheet, east of the Nazko River. This unit consists of basalt, andesite, related tuff and breccias, as well as minor conglomerate, sandstone and shale (Figure 2.1). From the field relationships, these rocks were inferred by Tipper to be younger than and distinct from the Ootsa and Endako groups, but younger than the Chilcotin basalts.

### 2.3.4 Neogene and Quaternary Volcanic Rocks

Unconformably overlying the Eocene volcanic sequences are the Neogene (28–1 Ma) Chilcotin Group flood basalts (Figure 2.1; Andrews and Russell, 2008). These are generally flat-lying to shallow-dipping, massive to columnar-jointed, olivine-phyric basalt lavas with minor pillow basalts and hyaloclastite (Bevier, 1983). They cover an area possibly as large as 30 000 $km^2$ in central BC and have been demonstrated to be thinner than 50 m, except in paleodrainage areas where they can be over 50 m thick (Andrews and Russell, 2007; Andrews and Russell, 2008).

The Cheslatta Lake volcanic suite has recently been recognized as a distinct magmatic event that took place during the Miocene in central British Columbia (Anderson et al., 2001). Volcanic rocks of the Cheslatta Lake suite are mafic, alkaline rocks characterized by columnar-jointed, olivine-phyric basalt and diabase volcanic rocks. The suite is distinct from other units by the abundance of ultramafic, mantle derived xenocrysts and phenocrysts and by its outcrop characteristics and structural setting (Anderson et al., 2001).

The Anahim Volcanic Belt is an east-trending chain of Miocene to Holocene (Bevier, 1989) shield volcanoes and intrusions in central BC. The Nazko Cone is located in the study area and is characterized by red-brown oxidized subaerial basalt flows and brecciated basalts, a pyroclastic cone and tephra deposits (Figure 2.1; Tipper, 1959). The volcanic package consists of basal subaerial flows and subglacial hyaloclastite, overlain by pyroclastic cone deposits and lava flows (Souther et al., 1997). Basalts of the Anahim Belt are typically alkaline and peralkaline basalts with isotopic and chemical composition similar to Chilcotin Group basalts (Bevier, 1989).

#### 2.3.5 Mesozoic and Cenozoic Intrusions

Post accretionary plutonic suites of the Late Triassic, Middle Jurassic, Late Jurassic–Early Cretaceous, Late Cretaceous and Eocene intrude older sequences (Figure 2.1; Struik and MacIntyre, 2001; Riddell, 2006), but few have been mapped in the central part of the Nechako region. These intrusions display a range of compositions from granite, through diorite, granodiorite, monzonite and tonalite to syenite (Massey et al., 2005). They are not included in the present study as they were not investigated.

### 2.4 Deformation events

Three major fault systems, north-, northwest- and northeast-trending, are recognized in the Nechako region (Struik, 1993). North-trending dextral faults form an en échelon fault system and include the Pinchi and Fraser regional faults (Struik, 1993). Their last movements are inferred to be Late Eocene to Early Oligocene in age and are coeval with the northwest-directed extension that exposed the Vanderhoof Metamorphic Complex between 55–45 Ma (Struik, 1993; Wetherup and Stuik, 1996; Wetherup, 1997).

Early Eocene northwest-trending faults, such as the regional Yalakom and Casey faults, are attributed to extension and dextral-translation processes (Struik, 1993). In the Endako region, the Casey fault presents a minimum of 4 km of horizontal dextral displacement (Lowe et al., 2001). These faults are inferred to be older than the north-trending strike-slip faults, and have accompanied the development of Early Cenozoic pull-apart basins (Struik, 1993).

Northeast-trending faults show dip-slip extensional motion (Struik, 1993) and, in the Endako region, are associated with northwest-trending faults. They show normal or strike-slip displacement and are often filled with Eocene mafic dikes (Lowe et al., 2001). Extensional deformation is confined to the Late Cretaceous, Paleocene or Early Eocene, and has the same age constraints as the northwest-trending strike-slip faults (Struik, 1993).

Considerable evidence for deformation is found within the Mesozoic to Cenozoic rocks of the Nechako region. Widespread block faulting and extension is inferred to have taken place during Eocene magmatic events (Struik and MacIntyre, 2001). In the Chezacut map area, large-scale folding rather than block faulting and rotation is proposed to explain the variable dips of Ootsa Lake Group strata, as well as penetrative, closely spaced shear fabrics (Mihalynuk et al., 2008b).

### 2.5 Metallogeny

Several styles of mineralization occur in the Nechako region including porphyry, epithermal, polymetallic veins and subvolcanic epigenetic mineral occurrences (Figure 2.2; Lane and Schroeter, 1997; Bordet and

Hart, 2010). A limited number of mineral exploration prospects have been discovered in this region, despite the recognized economic potential of volcanic and plutonic rocks from the Jurassic to the Eocene in adjacent areas. Late Cretaceous and Eocene volcanic rocks have the most potential to host epithermal gold and silver mineralization.

A unique style of Au-Ag mineralization associated with Late Cretaceous rhyolitic fragmental rocks and associated high-level intrusions previously variably ascribed as epithermal or porphyry deposits are newly recognized as a distinct class. These include the Capoose deposit (53.4 Mt of 0.41 g/t Au, 24 g/t Ag; Andrew, 1988; Awmack et al., 2010), the Blackwater deposit (historic 6 Mt of 37g/t Ag, 0.05g/t Au, recent drill intersection of 206 m at 1.56 g/t Au; Tempelman-Kluit, 2011), and the Newton prospect (recent drill intersection of 189 metres at 1.56 g/t gold) (Figure 2.2). This style of disseminated Au-Ag mineralization can form large tonnage low grade deposits and is associated with elevated but non-economic values of zinc or copper. Capoose and Blackwater may be related to Late Cretaceous high-level intrusions and coeval volcanism of the Bulkley suite (Friedman et al., 2001) and show a similar non-systematic association of Ag and Au grades. Structural controls are not consistent between these three deposits; however the location of the Newton prospect between two regional dextral faults suggests the influence large scale faults can have on the localization of mineralization. These deposits were formed from low temperature, neutral pH fluids and are likely epithermal in nature, but lack veining and other traditional features of the low suphidation model.

Another type of deposit attracting exploration interest is low sulfidation epithermal Au-Ag mineralization associated with Eocene rhyolitic and intermediate flows and breccias, such as the past-producing Blackdome mine (145 kt of 50 g/t Ag, 11.3 g/t Au; Faulkner, 1986), and the Wolf and Clisbako prospects (Figure 2.2). The Blackdome deposit was emplaced in the Eocene in a similar structural setting as the Newton Late Cretaceous prospect, and shows strong correlation between the style and orientation of mineralized zones with the fault zones. At the Wolf and Clisbako prospects, mineralization is associated with Eocene fragmental felsic volcanic rocks affected by multi-stage veining and brecciation (Andrew, 1988; Chapman and Kushner, 2009).

In the two deposit styles reviewed here, host rocks show textural and compositional similarities but are associated with different magmatic events. Distinction between the different suites based on field criteria is challenging, and radiometric dating is necessary to clarify temporal relationships. These distinct styles of Au-Ag mineralization throughout the Nechako region record an evolution of magmatic, volcanic, and metallogenic conditions from the end of the Cretaceous through the Eocene. This evolution is associated with episodic but widespread magmatic and hydrothermal activity in a post-accretionary, dominantly extensional setting. The numerous volcanic centers relative to major structures bounding the region are considered to be key features in deposit localization.

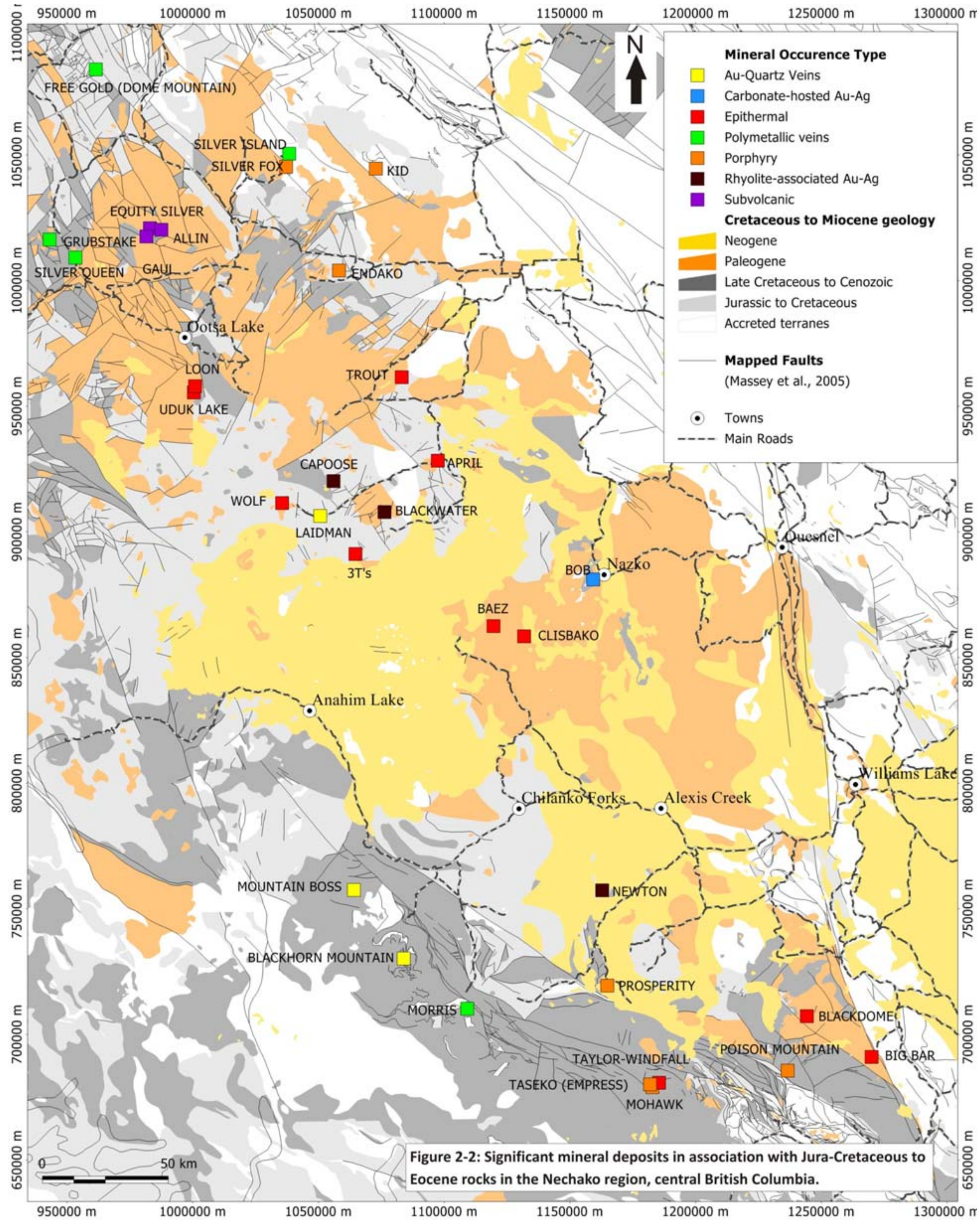


**Figure 2-2: Significant mineral deposits in association with Jura-Cretaceous to Eocene rocks in the Nechako region, central British Columbia.**

# 3 <u>Geology of the Eocene Volcanic Rocks</u>

## 3.1 Summary of Field Investigations

Field surveys conducted in 2010 covered a large portion of the Nechako region (Figure 1.2; Table 3.1), with emphasis in the area near Nazko and along existing seismic, gravity and magnetotelluric (MT) surveys (Figure 1.3). Over 200 rock exposures were mapped, many new outcrops were documented, and about 300 rock samples were collected (Appendix 1). Magnetic susceptibility data were also collected at each outcrop (Appendix 4).

Numerous previously undocumented rock exposures have been identified in the Nazko–Clisbako, Baezaeko and Tibbles Road areas, which allowed the collection of a detailed and relatively continuous lithological and structural dataset (Figure 1.3; Appendices 1 and 5). This dataset constitutes the basis of deliverables presented in this report. These three main traverses will be reviewed in detail and referred to as Nazko, Baezaeko and Tibbles traverses. Other surveyed areas include the Chilcotin plateau, the Chezacut area, and the Fraser River valley between Quesnel and Williams Lake (Table 3.1); they were reviewed in Bordet and Hart (2011).

The following points regarding mapping and interpretation of field data should be considered:

- Exposure is limited in the Nechako region, therefore establishing the continuity of units mapped in one outcrop or a series of outcrops is very challenging. In addition, lateral variations of volcanic facies due to the nature of volcanic processes and has to be taken into consideration;

- Few contacts are exposed and mappable between the different units. Some outcrops showed differing volcanic facies, allowing for the grouping of facies within similar or distinct units;

- A preliminary stratigraphic model was developed following the summer 2010 field season. This model is still being developed and needs to be tested and improved with further work.

**Table 3-1: Summary of traverses and corresponding geophysical surveys carried out in the Nechako region of central British Columbia**

| Traverse name | 50K NTS sheet | Traverse description | Approximate length | # of outcrops | Seismic lines [1 to 3] | MT surveys [4] | Oil and gas wells [5] |
|---|---|---|---|---|---|---|---|
| Nazko-Clisbako | 093B; 093G | NS traverse along the Nazko River and Clisbako River valleys, from 15km north of Nazko south to the Honolulu well | 46 km | 66 | GBC 2008-05 and GBC 2008-12; Canadian Hunter | Profile B | HONOLULU a-4-L; BRC-HTR d-96-E |
| Baezaeko | 093B; 093C | EW traverse along the Baezaeko forestry road and secondary branches | 36 km | 70 | GBC 2008-10 ; Canadian Hunter | Profiles A, E | |
| | | NW traverse along the Old Baezaeko Road and secondary branches | 18 km | 21 | GBC 2008-06 ; Canadian Hunter | Profile C | |
| Tibbles Road / Highway 59 | 093B; 093G | EW traverse along the Tibbles FSR and secondary branches; continuity of units assessed along Hwy 59 to the north | 18 km | 24 | GBC 2008-15 ; Canadian Hunter | Profile D | |
| Chezacut | 093C | Review of several outcrops previously mapped by Mihalynuk et al. (2008) | 50 km | 17 | Canadian Hunter | | BCR-HTR b-22-K |
| Chilcotin plateau | 092O; 092N | Several traverses in various directions, mainly following the old CH seismic lines | 20 km by 10 km | 11 | Canadian Hunter | Profiles F, G, H | BCR-HTR d-94-G; BCR-HTR b-82-C |
| Batholith transect | 093B | EW traverse along the 3400 FSR | 50 km | 22 | Batholith transect | | BCR-HTR b-16-J |
| Fraser River valley | 093B | Review of several outcrops along the Fraser River valley between Quesnel and Williams Lake | 100 km | 11 | | | NGT d-2-E; AMARILLO c-86-L; AMARILLO c-84-D |

***Source references for geophysical data:***

| | |
|---|---|
| *1- Geoscience BC (GBC) seismic lines* | Calvert et al., 2009<br>http://www.geosciencebc.com/s/Fileaccess_OilGas.asp |
| *2- Canadian Hunter seismic lines* | Hayward and Calvert, 2009 |
| *3- Batholith seismic transect* | Wang et al., 2010 |
| *4- Magnetotelluric surveys* | Spratt and Craven, 2009<br>Spratt and Craven, 2010 |
| *5- Oil and gas wells* | Ferri and Riddell, 2006 |

### 3.2 Lithological Descriptions

Lithological units mapped and sampled during the 2010 field season are detailed in Table 3.2. Units are listed according to their inferred stratigraphic position from oldest to youngest. Mappable units are defined based on volcanic facies using primary lithologies, textures, field occurrences, and relationships with other units. Descriptions of the rock types are supported by macroscopic and microscopic sample observations.

A total of 101 samples were selected for petrographic analysis as part of this project (Figure 1.3; Appendix 1). Covered thin sections (30 microns, 26*46 mm) were done by Vancouver Petrographics in Vancouver between August 2010 and March 2011. Petrographic descriptions were used to characterize the mineralogy and texture of the different units and distinguish Eocene volcanic rocks from younger volcanic sequences. Additionally, thin sections of brecciated volcanic units provide indications on the fragmentation mechanisms.

For each unit, the following information is compiled in Table 3.2:

- Stratigraphic position and mappable unit name
- Dominant and subordinate lithologies and volcanic facies part of the unit based on hand samples and thin section descriptions
- Location/Distribution of the unit
- Field occurrence, with an estimation of the thickness or volume of the unit
- Relationship to other units (observed and inferred)
- Age of the Unit (existing or new geochronology, correlation with other units or lithologies)

Pre-Eocene units are divided into two: a Lower to Middle Jurassic package, equivalent to the Hazelton Group, and a Cretaceous package, equivalent to the Skeena Group (Table 3.2). These rocks have not been mapped in detail as part of this study and no distinctions are made between the units in each package. However, Cretaceous clastic sedimentary rocks stratigraphically beneath the Eocene sequence have been observed and described at several locations along the Nazko River valley. Similarly, Jurassic sedimentary rocks and andesitic flows previously mapped in the northwestern part of the focused study area were evaluated. Contacts were not seen between the Jurassic and Eocene packages.

At least six distinct mappable Eocene units are recognized. Each unit includes up to several volcanic facies (Table 3.2). The most common lithology is dacite lava, both coherent and breccias facies. Some units have a large spatial distribution and are recognized along several traverses whereas other units were observed at only one or two localities.

Vitreous dacite coherent lava and breccias, are recognized at multiple locations especially along the Baezaeko traverse. Coherent lavas are commonly blocky to columnar-jointed, and flow tops are highly vesicular. Brecciated parts commonly display a highly weathered white to red matrix, with massive to vesicular blocks of vitreous dacite. This unit displays at least two subunits: a plagioclase-phyric dacitic lava, and an aphanitic to finely pyroxene-phyric lava. The pyroxene dacite was recognized previously in the Chezacut and Chilanko Forks map areas (Mihalynuk et al., 2008a & 2009).

Flow-banded, platy-weathered hornblende-phyric dacite is also widespread in the Baezaeko area. This lithology was also recognized in the Chezacut and Chilanko Forks map areas (Mihalynuk et al., 2008a & 2009). All these dacitic flows have both coherent and associated fragmental facies which locally have a very distinctive intense silicification, blocky shapes, or weathering of the matrix.

In the Tibbles Road area, two distinct groups of white flow-banded rhyolite flows are recognized. To the north along the highway, a biotite-K-feldspar-phyric flow-banded rhyolite has been previously mapped by Tipper (1959) and dated at 49.8 Ma (Rouse and Matthews, 1988). This rhyolitic lava commonly contains magnetite crystals. Further south, rock exposures of white-flow banded rhyolite are also found but contain quartz, biotite and no magnetite. The stratigraphic and age relationship between these two distinct units is not clear and should be clarified by additional fieldwork and radiometric dating.

Andesitic flows have been mapped in the Baezaeko, Nazko and Tibbles areas. They are inferred to be younger that other Eocene dacitic and rhyolitic lavas (this study). However stratigraphic relationships need to be clarified in several locations.

Basaltic and andesitic flows distinct from the Chilcotin Group are also mapped. Local volcaniclastic or epiclastic deposits have been identified, but their relationships with the other units is uncertain.

Table 3 2: Description of the main mappable units and corresponding volcanic facies based on field observations

| Lithology | Location/Distribution | Field occurrence/Thickness | Relationship to other units | Age | Interpretation |
|---|---|---|---|---|---|
| ***Anahim volcanic suite basalt flows and breccias*** | | | | | |
| Basalt flows and breccias: Subaerial flow (base), subglacial hyaloclastite, pyroclastic cone and lava flows (top) (Souther et al., 1997). | Nazko Cone (UTM 449337, 5864344) and other localized patches throughout the area (Massey et al., 2005). Recent seismic activity in of the Nazko Cone in 2007. | Red-brown oxidized subaerial basalt flows and brecciated basalts, pyroclastic cone and tephra plume (Tipper, 1959). Total volume < 0,1 km$^3$ (Souther et al., 1987) | Unconformable contact with all other units (inferred) | Pleistocene: 0.34 ą 0.03 Ma (K-Ar; Souther et al., 1987). Last erruption 7200 yrs BP (C; Souther et al., 1987) | |
| ***Chilcotin Group basalts*** | | | | | |
| Olivine-phyric basalt: Dark brown-grey flat to shallowly dipping massive to columnar-jointed, sparsely to highly vesicular, olivine-phyric basalt. Varying amount of vesicles from base to top flow. Minor associated pyroclastic and volcaniclastic sedimentary rocks (Bevier, 1983; Mathews, 1989) | Mapped at several locations throughout the field area. Distribution controlled by location of paleochannels (Gordee et al., 2007) | Thickness controlled by Miocene paleotopography and paleochannels location. Ranges between ≤20 m to ≤150 m (Andrews and Russell, 2008). Estimated area covered ~36500 km$^2$ (Gordee et al., 2007). Estimated volume of lava erupted 33000 km$^3$ (Bevier, 1983) | Unconformable contact with all other units (inferred) | Neogene: whole rock K-Ar dating identified three pulses at 15-13 Ma, 9-6 Ma, 3-1 Ma (Bevier, 1983; Matthews, 1989) | |
| ***Cheslatta Volcanic Suite basalts*** | | | | | |
| Xenocrystic olivine-phyric basalt: Basanite, transitionnal basalt and alkali olivine basalt (Anderson et al., 2001). Common ultramafic, mantle-derived xenoliths in a dark, dense, aphanitic non vesicular groundmass (Sample EB-10-141; Anderson et al., 2001). | One occurrence mapped west of the Baezaeko traverse (EB-10-141). Cospatial with Chilcotin basalts in central British Columbia. Distinct topographic character: underlie points or buttes of 30-150 m relief (Anderson et al., 2001). | Scattered erosional remnants of volcanic and diabasic necks, lava flows, and dykes. Typically columnar-jointed, undeformed and flat-lying (Anderson et al., 2001). High magnetic susceptibility (average 44.10-3 S.I. as measured at field station EB-10-141).<br><br>Extent from 200 m$^2$ to 3 km$^2$ extent for individual volcanic plugs. 10-15 m thicknesses observed at individual localities (Anderson et al., 2001). | Unconformable contact with all other units (inferred) | Early to Middle Miocene: 21-11 Ma whole rock K-Ar and Ar-Ar ages (Anderson et al., 2001) | |
| ***Polymictic volcaniclastic and epiclastic deposits*** | | | | | |
| Polymictic volcanic conglomerate: Pale yellow weathered matrix contrains mm-size fragments of volcanic rock. Subrounded blocks include chlorite altered, banded, glassy rhyolite / pale pink bt- plag-qz-Kpar rich rhyolitic tuff / banded rhyolite and red/dark grey basalt or andesite. | Along the Bazaeko forestry road, field station EB-10-125 (UTM 452582, 5858030) | 20 m thick exposure of pale yellow, bedded, polymictic volcaniclastic debris flow(?) contains blocks volcanic rocks of various sizes. Intrabed layering, but variable block size at different levels. Syndepositional faults. | Based on topographic relationships, this unit lies above coherent and brecciated Eocene volcanic units described at field stations EB-10-120 to EB-10-124 | Eocene(?) Or Holocene(?): Inferred younger than underlying Eocene coherent flows and breccias. Could also be Eocene or Miocene. | Epiclastic volcanic conglomerate: alluvial fan deposit? |
| Polymictic breccias and crystal-rich polymictic tuff. Subangular to subrounded large (up to 1m) clasts of basalt, rhyolite (or rhyolitic tuff?), andesite, some clasts are very oxidized; matrix contains ash to lapilli size fragments of various composition (bimodal). | Several occurrences of polymictic breccias in Baezaeko area along forestry roads | Bedded, unsorted, polymictic volcaniclastic deposits, with clasts ranging from ash-size to large blocks. Commonly oxidized. Up to 5 m thick outcrop exposures | Locally overlying flow-banded vesicular dacite (Figure 3.17) | Eocene (inferred). No available geochronology. | |
| ***Coherent and brecciated mafic lavas (distinct from Neogene Chilcotin basalts)*** | | | | | |
| Coherent basalt flow and autobreccia | Several occurrences recognized in other studies and assigned to the Eocene Endako Group (Haskin et al., 1998; Barnes and Anderson, 1999) | An approximately 150 m thick sequence of Eocene Endako Group mafic flows was mapped in the Kenney Dam area (NTS 093F) by Barnes and Anderson (1999). Could be misinterpreted as Chilcotin basalt. | | Possibly correspond to Eocene mafic flows | |
| ***Coherent and brecciated andesitic lavas*** | | | | | |
| Flow-banded to columnar-jointed, massive to vesicular light grey plagioclase-pyroxene-phyric andesitic lava. Associated breccia contains angular to subangular, massive to moderately vesicular blocks of red-altered plagioclase-pyroxene andesite. Quartz veining; locally chlorite altered. Minor layers of felsic volcanic sandstone locally interbedded with lava flows. | Nazko River valley (flow banded and columnar-jointed; EB-10-026, 22, 23, 25, 28, 34-35); Tibbles Road (mainly flow-banded; EB-10-98, 99, 103, 112-118, 208-211); Baezaeko (EB-10-124) | About 15-25 m thick (Nazko valley; Figures 3.7 & 3.8) | Observed at individual outcrops, this unit overlies Eocene dacitic flows. Mapped by Tipper (1959) as younger than rholitic and dacitic flows. | Eocene and/or Oligocene (Tipper, 1959). No available geochronology. | |
| Coherent amygdaloidal andesite flow: epidote (?) altered fine grained aphanitic andesite; Vesicles filled coated or filled with aggregates of white crystals including calcite and quartz. | Clisbako Mouth Forestry Service Road (EB-10-027) | Distinctive amygdaloidal green-altered andesite flow. Exposure only covers a few meters square, no apparent thickness could be measured | Observed above a coherent andesite-basalt flow along the Clisbako traverse | Eocene and/or Oligocene (Tipper, 1959). No available geochronology. | |
| ***Coherent and brecciated flow-banded dacite (undivided)*** | | | | | |
| Flow-banded sparsely vesicular to amygdaloidal dacite and flow-associated dacitic breccias. Flow-banded, light pink, thinly laminated, vesicular biotite-plagioclase-phyric dacite with devitrification textures (spherulites) associated with silicified hyaloclastite. Magnetic, relatively massive. Local hydrothermal alteration. | Nazko River valley, Clisbako River valley and vicinity of well B-16-J; Tibbles road (minor); Bazeaeko traverse (minor and possibly associated with other units) | Thick complex of dacitic domes, flows and associated facies across the Indian Head promonty, Nazko valley. Minimum thickness estimated from log (Nazko valley; Figure 3.7) about 170 m. | At outcrop EB-10-100 flow-folded, flow-banded dacite is underlying unit of platy flow-banded rhyo-dacite | Eocene: 45.10 Ma Ar/Ar age (Clisbako traverse area; Metcalfe et al., 1998) | Coherent dacite flows and domes; Eo_Brecciated dacite flow; Eo_Coherent dacite flow; Eo_Coherent flow-banded dacite; Eo_Coherent flow-banded dacite and breccia; Eo_Coherent flow-banded vesicular dacite |
| ***Coherent and brecciated vitreous dacite*** | | | | | |
| Coherent columnar jointed pyroxene-phyric vitreous dacite. Spherulitic fractures common.<br>Coherent flow-banded blocky to columnar jointed vitreous plagioclase-phyric dacite and breccia. Euhedral elongated plagioclase phenocrysts. Devitrivication textures commonly observed in matrix. Commonly associated with yellow-orange weathered breccia containing blocks of glassy dacite; fragmental facies is usually found at the base below the coherent glassy dacite. | Widespread in the Bazaeko area. Some occurrences mapped in the Tibbles road area could be part of the same unit. Pyroxene dacite previously described at Mount Sheringham (Mihalynuk et al., 2009). | Blocky to columnar-jointed, yellow weathered exposures, but fresh rock is dark grey-black. Best outcrops along in the southern Nazko River valley: thick columnar-jointed dacite flows in the Clisbako area (EB-10-031 and EB-10-033). Minimum thickness estimated from cross-sections: From about 40 m to over 100 m or 200 m. | Locally underlying Eocene andesitic and mafic flows. Mount Sheringham pyroxene dacite unit sits atop light pink flow-banded dacite (Mihalynuk et al., 2009) | Eocene: 49.4 Ma (Ar/Ar, Metcalfe et al., 1998); 45.7 Ma (K/Ar; Rouse and Mathhews, 1988) | |
| ***Pyroclastic deposits*** | | | | | |
| Accretionary lapilli-stone and layered tuff: Light grey, layered tuff displays rhytmic layering at the cm-scale probably resulting from deposition in water (maybe lacustrine environment). Accretionary lapilli-stone overlain by chaotic fragmental unit formed of a white-grey tuffaceous matrix containing plagioclase-phyric vitreous dacite blocks. | Large road-side quarry along Baezaeko-Michelle forestry road (outcrop EB-10-130) | Large open quarry of chaotic volcaniclastic deposit, with clasts ranging from ash-size to large blocks. Characteristic pale white-yellow matrix containing large dark glassy blocks of volcanic rock. Minimum thickness estimated from field observations: about 20 m. | Underlying chaotic fragmental facies at the base of vitreous dacite unit | Eocene (inferred). No available geochronology. | Deposition of tuff in a lacustrine environment indicated by rythmic layering. Followed by subaerial deposition of accretionary lapilli. |
| ***Coherent and brecciated platy-weathered flow-banded dacite and rhyodacite*** | | | | | |
| Grey flow-banded and brecciated rhyo-dacite: acicular hornblende, anhedral to subhedral plagioclase phenocrysts, green colored quartz phenocrysts. Locally silicified. Locally flat and elongated vesicles, coated or filled with silica. Highly silicified distinctive red colored breccia. | Widespread in the Bazaeko area and Tibbles road area. Recognized in Chilanko Forks and Chezacut maps areas (Mihalynuk et al, 2008a and 2009) | Platy-weathered, grey-brown flow-banded dacitic to rhyodacitic flows. Distinctive silicified red-altered breccia inferred to be spatially and genetically associated with the coherent flow-banded rhyodacite facies.<br>Minimum thickness estimated from cross-sections and logs: 24 m (Figure 3.8); about 40 m (Figure 3.11); about 50 m (Figure 3.17) | Locally underlying glassy dacite flows | Eocene: 44.2 (Ar/Ar, Metcalfe et al., 1998); 48.7 Ma (K/Ar; Rouse and Mathhews, 1988) | |
| ***Coherent and brecciated flow-banded rhyolite*** | | | | | |
| K-feldspar-Biotite-phyric flow-banded rhyolite, also rich in magnetite. Some aligned flattened vesicles. | Tibbles Road (Outcrops EB-10-104 to to 107) | Roadside outcrops and quarries, large exposure of white, flow-banded rhyolitic volcanic rock. Minimum thickness of 30 m. | No contact directly observed with overlying andesitic flows unit. Mapped by Tipper (1959) as older than andesitic and basaltic flows. | Paleocene and/or Eocene (Tipper, 1959). Existing K/Ar age at 49.8 Ma (Rouse and Mathews, 1988). New U-Pb age at 51,1 Ma (this study). | |
| Biotite-Quartz-phyric flow-banded rhyolite | Tibbles Road (Outcrops EB-10-108 to 111) | Roadside outcrops and quarries. large exposure of white, flow-banded rhyolitic volcanic rock. | No contact directly observed with overlying andesitic flows unit or K-feldspar-biotite phyric rhyolite. | Upcoming Ar-Ar ages (this study) | |
| ***Conglomerate and Sandstone of the Skeena Group (or equivalent)*** | | | | | |
| Yellow-orange chert pebble conglomerate and sandstone. Clasts are dominantly chert but also quartzite and volcanic rock pebbles. Feldspar crystals and muscovite flakes are locally abundant. Also some shale, greywacke (Massey et al., 2005; Riddell, 2006). Minor andesite, breccia and tuff (Massey et al., 2005). | South of the Nazko River valley (Indian Head promontory, vicinity of wells a-4-L and d-96-E); North of the Nazko River valley. Several field stations as part of this study. | Cliffs of interbedded clastic conglomerate and sandstone. Up to 130 m thick (Indian Head promontory); about 2400 m in well a-4-L (Riddell et al., 2007); about 3000 m in well d-96-E (Riddell et al., 2007); at least 1200 m in well c-75-A, about 1700 m in well b-82-C and about 2000 m in well d-94-G (no basal contact with Jurassic rocks; Riddell et al., 2007) | Unconformably overlies Jurassic sequence; unconformably underlies Paleocene-Eocene sequence | Lower Cretaceous (Skeena Group); U-Pb radiometric ages in oil and gas wells (Riddell, 2010) from about 93 to 107 Ma | |
| ***Andesitic lavas and fragmental rocks of the Hazelton Group (or equivalent)*** | | | | | |
| Andesite, basalt and related tuff and breccia; conglomerate, greywacke, shale; argillite, tuffaceous argillite, limy argillite; limestone; minor dacitic to rhyolitic tuffs, breccias and flows (Massey et al., 2005). Intensely veined and faulted. | North of the Baezaeko traverse. Several field stations as part of this study (Outcrops EB-10-187 tp EB-10-193, NTS 093B & G). | Roadside quarries, cliffs, small road side outcrops. Based on topography contours, minimum thickness is about 200 m (Figure 3.15). At least 324 m in well d-96-E (Riddell et al., 2007); about 500 m in well b-16-J (Riddell et al., 2007 | Stratigraphic base of the sequence. Possibly in fault contact with Eocene volcanic rocks. | Lower Jurassic to Middle Jurassic (Hazelton Group); U-Pb radiometric ages in oil and gas wells (Riddell, 2010) from about 140 to 170 Ma | |

### 3.3 Geochemistry

#### 3.3.1 Method

A total of 29 samples were selected for whole rock geochemical analysis to characterize the geochemical signature of Eocene volcanic rocks (Figure 1.3; Appendix 2). The selected rocks represent the suite of coherent volcanic lithologies identified during the 2010 field season, including three samples identified in the field as Chilcotin basalts. The samples are distributed across the focused study area to illustrate possible spatial variations in chemical compositions. The samples selected for geochemical analysis were previously characterized by a petrographic analysis and are listed in Appendix 1.

Sample preparation prior to analysis included cleaning of the samples and cutting off fresh blocks with the rock saw. Three blind duplicate samples were randomly selected and included in the selection. Three MDRU standards pulps of andesitic (MBX-1), rhyolitic (P1) and dacitic (WP-1) composition were selected based on expected range of composition of tested samples.

The 35 samples including blinds and duplicates were shipped to the ACME Laboratories in Vancouver. The analytical suite used was 4A4B and includes:

- Whole rock by ICP (21 elements): Total abundances of the major oxides and several minor elements are reported on a 0.2g sample analysed by ICP-emission spectrometry following a Lithium metaborate/ tetraborate fusion and dilute nitric digestion. Loss on ignition (LOI) is by weight difference after ignition at 1000°C.
- Total trace elements by ICP-MS (45 elements): Rare earth and refractory elements are determined by ICP mass spectrometry following a Lithium metaborate / tetraborate fusion and nitric acid digestion of a 0.2g sample (same decomposition as Group 4A). In addition a separate 0.5g split is digested in Aqua Regia and analysed by ICP Mass Spectrometry to report the precious and base metals.

#### 3.3.2 Results

Analysis of geochemical results was conducted using the IoGas software. Results are presented in Appendix 2 of this report. Samples analyses were generally of good quality, with little deviation observed between original samples, duplicates and lab duplicates values.

The loss of ignition (LOI) for the resulting analyses range between 0.3% and 8.5%, but is commonly between 1.0 and 2.5 % which is reasonable for volcanic rocks. Major element concentrations have been recalculated based on the anhydrous sum of major elements.

$SiO_2$ contents amongst the analysed samples ranges from 49.4 and 75.3wt%. For the Eocene sequence, the lowest $SiO_2$ concentration is 54 wt%. MgO concentrations range between 0.15 and 3.67 wt% for the Eocene volcanic rocks, and are higher for the three Chilcotin samples (~ 5-7 wt%). $Fe_2O_3$ is between about 1 and 8 wt% for Eocene rocks, and significantly higher for Chilcotin samples (11-12 wt%). $Al_2O_3$ is generally high in all samples analysed, between 13-18 wt%.

General whole rock classification diagrams for the selected Eocene volcanic rocks are shown in Figure 3.1. Major elements only are interpreted in this report, but future work will include interpretation of the trace elements. Samples are represented according to their location (symbol shape) and unit category (symbol color). Eocene and Miocene volcanic rocks plotted on the AFM diagram (Figure 3.1a) show a clear calc-alkaline affinity. On the Alkaline/Subalkaline classification diagram (Figure 3.1b), these same rocks form a subalkaline trend; importantly none of them show alkaline affinities. The Total-Alkali-Silica (TAS) diagram (Figure 3.1c) shows that analyzed Eocene rocks plot along a trend from the basaltic trachyandesite to rhyolite fields. Most samples plot between the dacite and trachydacite fields. Finally, the Peccerillo-Taylor $K_2O$ vs $SiO_2$ diagram (Figure 3.1d) displays a trend of Eocene volcanic rocks within the high potassium calc-alkaline field.

Figure 3.2 shows major element trends for Eocene volcanic rocks analyzed in this project. Linear trends are observed for several major elements, including $Fe_2O_3$, MgO, CaO, $TiO_2$, $P_2O_5$, MnO (negative slope) and $K_2O$ (positive slope). Andesitic flows of the Tibbles Road area show a consistent distinctive signature characterized by a low silica content (~53-58 wt.%), and a systematic position at the extremity of linear trends for the elements listed above. It is interesting to note that the opposite extremity of these trends is formed by samples of the flow-banded rhyolite mapped in the Tibbles Road area; this unit was inferred to be older than the andesitic flows by Tipper (1959). Dacitic units usually show consistent trends, but are not easily distinguishable based on major elements concentrations.

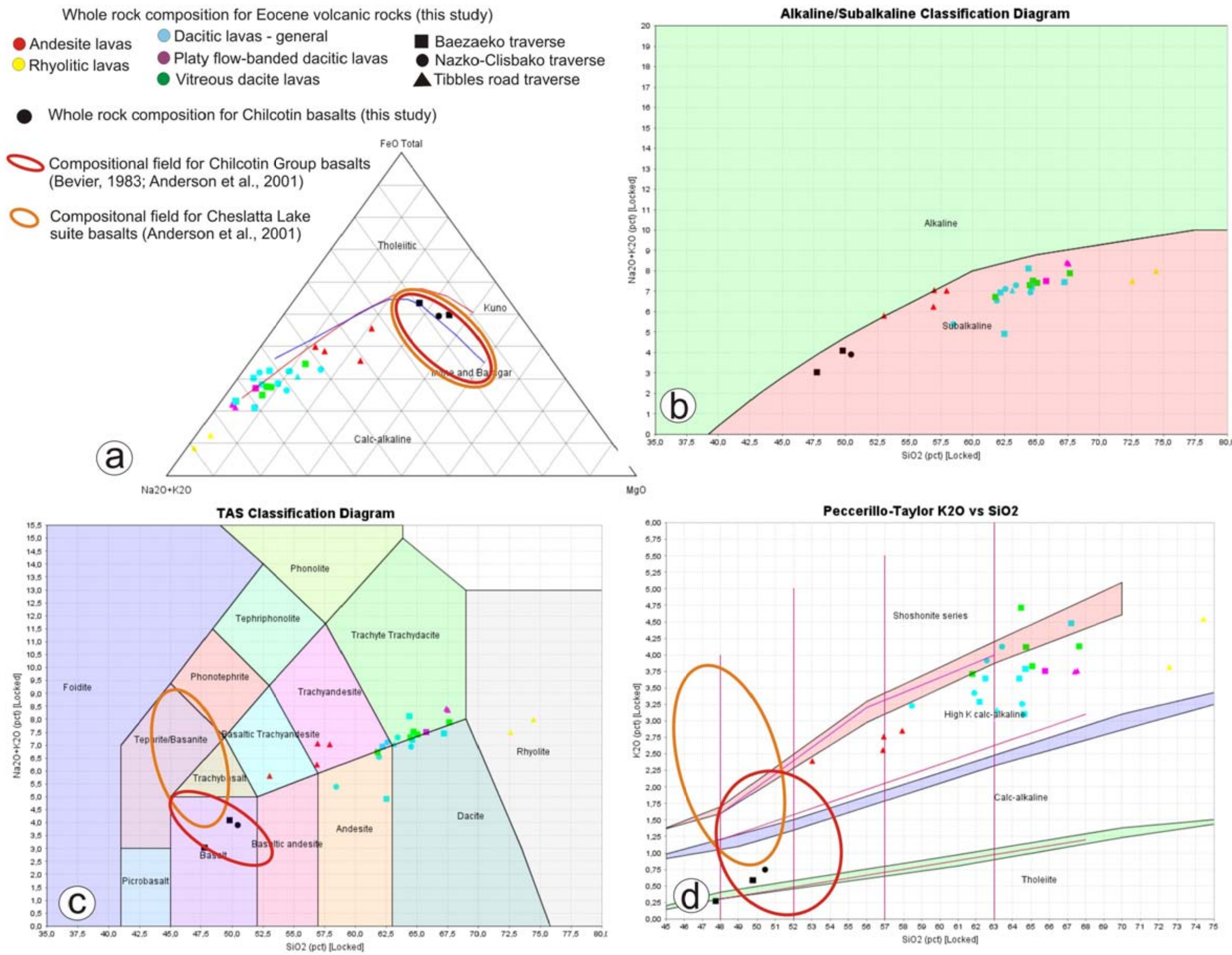


**Figure 3-1: Whole rock composition of Eocene volcanic rocks analyzed in this study and compositional field for Chilcotin Group basalts and Cheslatta Lake basalts: a) AFM diagram, after Irvine and Baragar (1971); b) Alkaline/Subalkaline classification diagram, after Irvine and Baragar (1971); c) TAS Classification Diagram, after Le Maitre et al. (1989); d) K2O vs SiO2 diagram, after Peccerillo and Taylor (1976).**

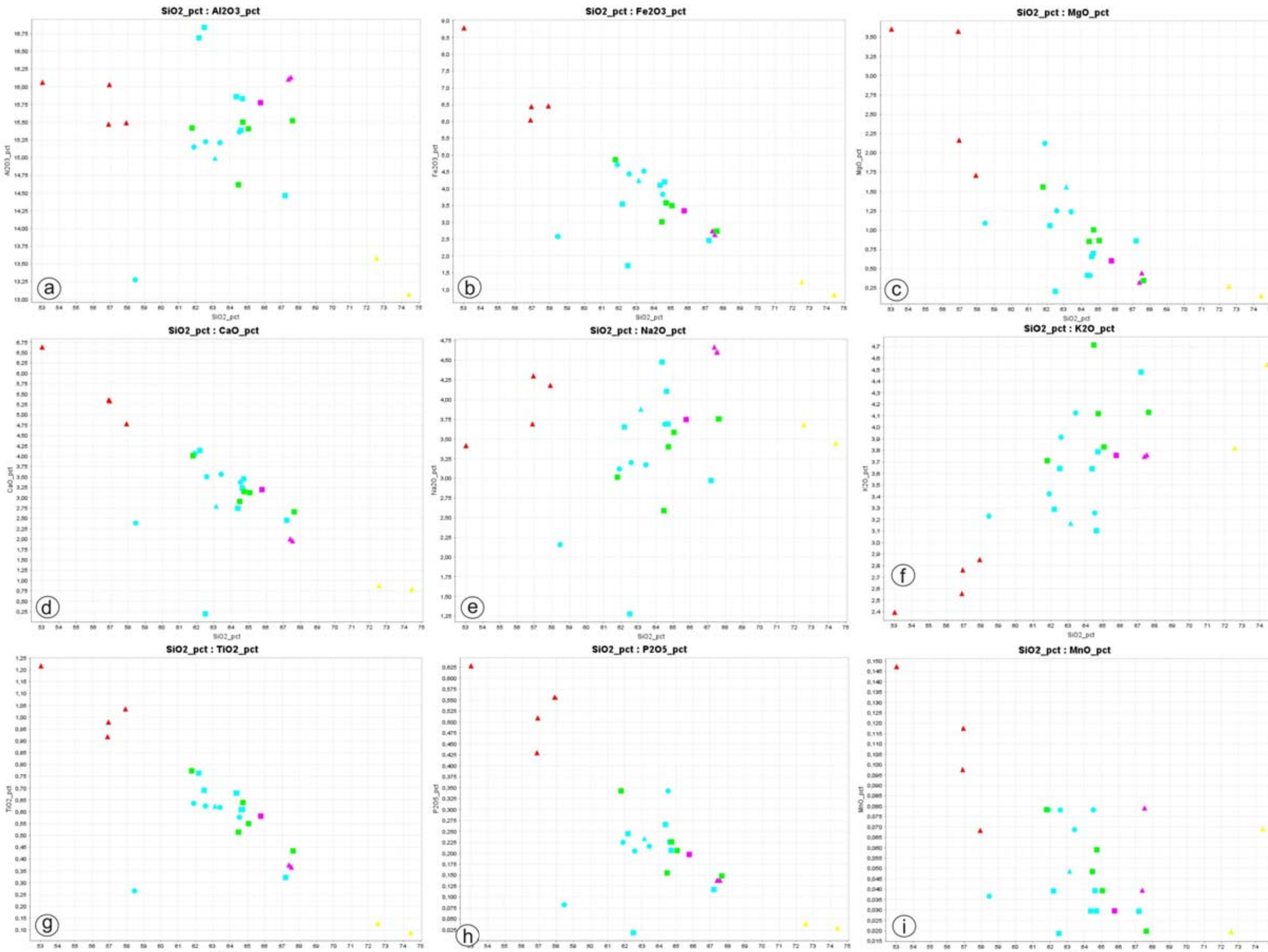


**Figure 3-2: Geochemical Harker diagrams for Eocene volcanic rocks. Major elements (%) relative to SiO2 content: a) Al2O3; b) Fe2O3; c) MgO; d) CaO; e) Na2O; f) K2O; g) TiO2; h) P2O5; i) MnO.**

### 3.3.3 Existing Geochemistry Data

Previous geochemical analyses for Eocene Ootsa Lake and Endako volcanic rocks are compiled in the Data Repository of Breitsprecher et al. (2003).

Compositional fields for the Chilcotin Group basalts and Cheslatta Lake suite basalts are compiled from Bevier (1983), Anderson et al. (2001) (Figure 3.1). These Neogene volcanic rocks show significantly different geochemical signatures than the Eocene volcanic rocks part of this study.

More details on the geochemistry of Neogene mafic lavas of the Chicoltin Group and Anahim volcanic belt are provided in Larocque and Mihalynuk (2009). Their work was conducted in an area that encompasses the limits of the study area for this project.

## 3.4 Geochronology

### 3.4.1 Methods

Six samples collected during the summer 2010 were selected for zircon U-Pb laser-ablation ICP-MS dating, based on the distribution of samples through the study area. Dominantly felsic lithologies were chosen since they are more likely to yield zircons. The samples are from pyroclastic deposits and rhyolitic lavas that are interpreted to result from primary volcanic processes.

Sample processing was conducted at the PCIGR Laboratory at the University of British Columbia. The different steps of sample processing include: 1) Crushing and grinding; 2) Density separation using the Wifley table; 3) Heavy liquid separation of heavy minerals; 4) Zircon identification and picking; 5) Zircon mounting in epoxy resin; 6) Laser ablation and analysis on ICP-MS; 7) Data reduction and data interpretation. Raw data were reduced and processed by Jim Mortensen.

### 3.4.2 Results

A sample of white to light pink, flow-banded, biotite-K-feldspar-phyric rhyolitic lava from the Tibbles Road traverse was selected for dating. Twenty-three small and large zircon grains were picked from sample EB-10-107A (Figure 1.3). The resulting age is **50.5 ± 2.0 Ma**, which is Early Eocene. This is consistent with the previous K-Ar age of 49.8 ± 3.4 Ma obtained at the same location (Rouse and Mathews, 1988). In the geologic compilation by Massey et al. (2005), this unit is part of the Eocene to Oligocene Endako Group. However, the sample's characteristics would better match Tipper's Paleocene and/or Eocene unit which is interpreted as an equivalent to the Ootsa Lake Group. Sample EB-10-107A also contained four xenocrystic zircon grains which yielded Late Jurassic ages between 137.4 and 150.7 Ma. This rhyolitic flow is likely contaminated by older basement units. Biotite was also retrieved from sample EB-10-107A and will be used to conduct Ar-Ar dating.

A white lithic-rich volcanic sandstone, probably a tuff, overlying a coherent andesite flow and associated breccias from the Nazko Valley was also dated. This sample belongs to a package previously ascribed to the Ootsa Lake Group (Massey et al., 2005) and constrained to the Paleocene and/or Eocene by Tipper

(1959). Only one grain of zircon was retrieved from this lithology (sample EB-10-025C; Figure 1.3), and it returned a U-Pb age of 51.1 ± 4.4 Ma, which of course has a low degree of confidence.

Other samples initially selected for U-Pb dating from the Early Eocene quartz-biotite-phyric rhyolite lava from Tibbles Road did not contain zircons. However a significant amount of biotite could be retrieved from samples EB-10-111A (Figure 1.3) and will be dated using the Ar-Ar technique.

### 3.4.3 Previous Geochronology

Previously-determined isotopic age dates acquired in the Nechako region are mostly compiled in the CordAge database (Breitsprecher and Mortensen, 2004). Ar/Ar dating on biotite or whole rock (Metcalfe et al., 1998), and K/Ar on biotite or whole rock (Rouse and Mathews, 1988) returned several Early Eocene ages, from about 53.4 Ma to 44.2 Ma. Grainger et al. (2001) determined several U/Pb and Ar/Ar ages between 47 and 53 Ma for Eocene andesitic, dacitic and rhyolitic flows ascribed to the Early Eocene Ootsa Lake Group.

Recent fieldwork in the Nechako region also led to the collection and additional dating of Eocene volcanic rocks. Mihalynuk et al. (2008c) published an Ar/Ar age of 51.65 +/-0.58 Ma from an ignimbritic lapilli tuff-breccia composed of acicular hornblende, biotite, quartz and feldspar in a fine-grained matrix, from the Riske Creek area. Recent isotopic dating was conducted on rock chips from several oil and gas wells, and returned Early Eocene ages ranging from 60.3 +/- 2.2 Ma to 48.51 +/- 0.99 Ma (Riddell, 2010; Chapter 5 of this report).

The Chilcotin Interactive Database (Dohaney et al., 2010b) contains several Miocene, Pliocene and Pleistocene ages. Farrell (2010) conducted Ar/Ar dating of 12 samples in the Chasm Provincial Park and constrained emplacement events for Chilcotin basalts between 10 +/- 0.48 Ma and 8.72 +/- 0.37 Ma. Anderson et al. (2001) constrained the Chelslatta Lake volcanism from the middle Miocene to late Oligocene but provided no detailed age dates. Mathews (1989) obtained an age of 6.3 ± 0.6 Ma for the Chilcotin basalts. Souther et al. (1987) obtained a Holocene age of 0.34 ± 0.06 Ma at the Nazko cone.

## 3.5 Eocene Stratigraphy

A general 1:100000 scale map of the focused study area (Figure 3.3) was produced based on road side traverses realized during the summer 2010. It shows the variety of lithologies and volcanic facies encountered along the MT and seismic surveys, and also the extent of Chilcotin basalts and Cretaceous and Jurassic units. Contacts for these units are from Massey et al. (2005), but have been locally updated based on recent mapping done as part of this study. A series cross-sections and stratigraphic logs were produced in order to illustrate the different mappable units and volcanic facies described in the previous sections of this chapter (Table 3.2).


Figure 3-3: Preliminary 1:100,000 scale field map of the Nechako region based on road side traverses, showing the location of cross-sections AA', BB', CC' and DD'. Location of figures 3.4 to 3.12 indicated by black rectangles. Inset map shows map location in British Columbia. Map compiled by Esther Bordet based on 2010 field season mapping. Original contacts for Chilcotin Group, Hazelton Group and Skeena Group from Massey et al. (2005) have been locally modified.

Deformed Cretaceous clastic sedimentary rocks (Table 3.2) are exposed along the Nazko River valley (Figure 3.4), and tilting of these strata may be syn- or post-Cretaceous. They are unconformably overlain by coherent and brecciated andesitic and dacitic lavas inferred to be Eocene in age (Figures 3.4 & 3.5; Tipper, 1959; Massey et al., 2005). Chilcotin basalt flows locally overlain unconformably the Eocene sequence (Figure 3.3; Tipper, 1959).

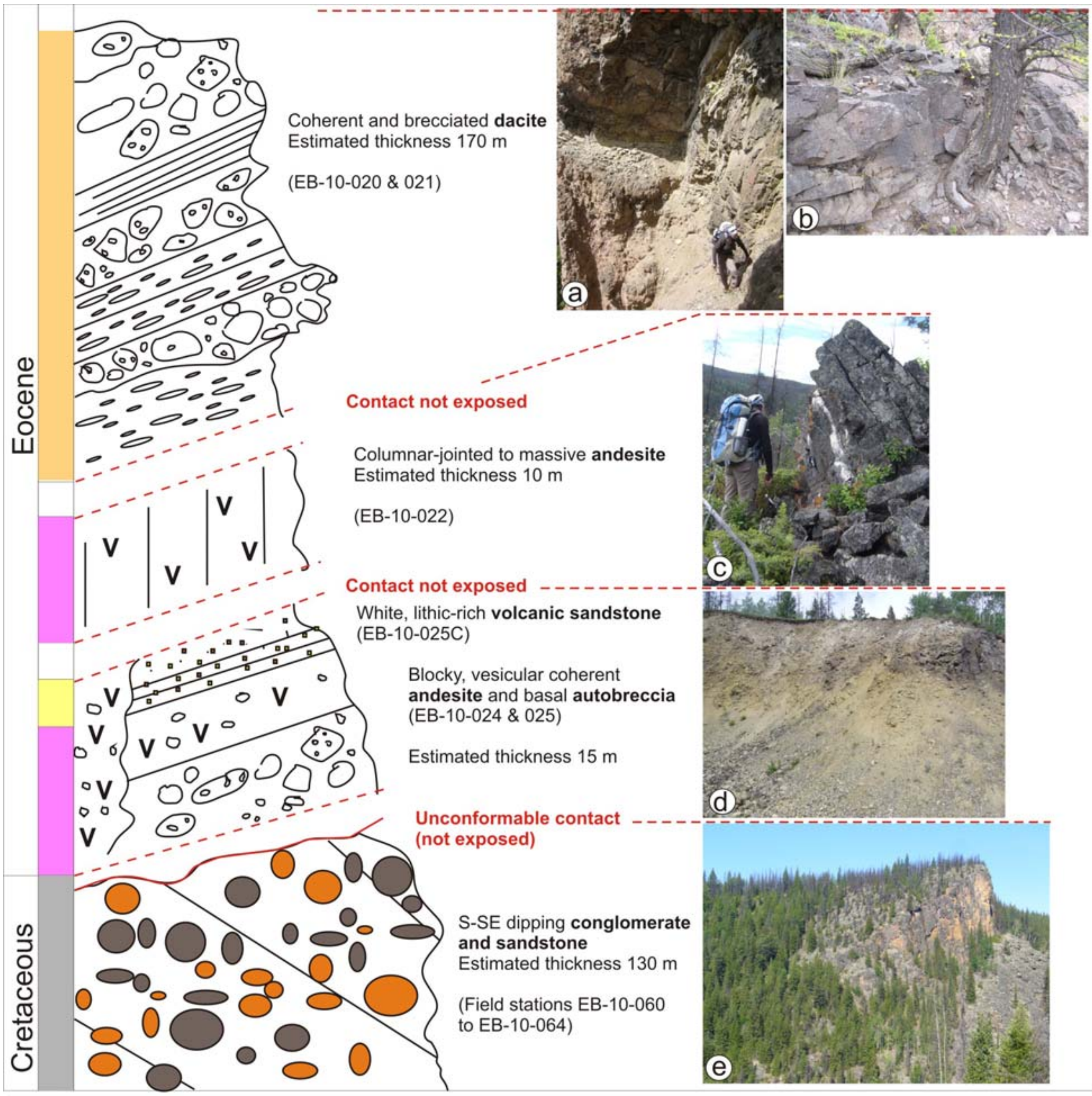


**Figure 3-4: Stratigraphic log (UTM 468325, 5847605) and characteristic lithologies for Indian Head, southern Nazko River valley, illustrated by field photographs. a-b) Thick coherent and brecciated dacitic lava which is probably part of a lava dome complex; c) Columnar-jointed andesite; d) White, lithic-rich volcanic sandstone overlying coherent and brecciated andesitic lava; e) southeast-dipping Cretaceous conglomerates at the Indian Head promontory.**

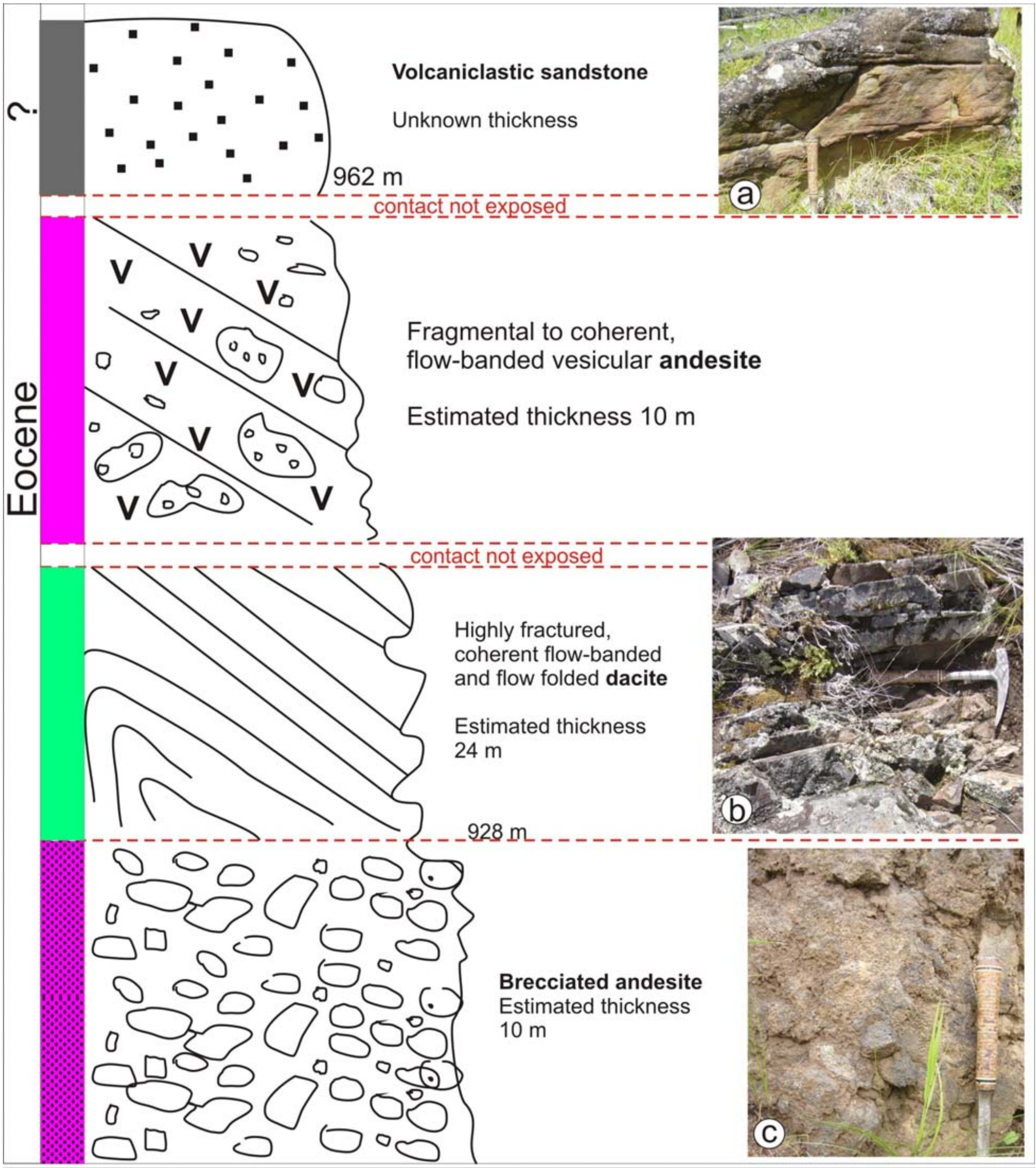


**Figure 3-5: Stratigraphic log (UTM 468054, 5849305) and field photographs of characteristic lithologies for field station EB-10-035, southern Nazko River valley. a) Volcaniclastic (?) sandstone with medium grained quartz, feldspar, and mafic crystals at the top of the succession; b) Flow-banded, brittle fractured, dark grey, microcrystalline plagioclase-hornblende-pyroxene dacite; c) Fragmental flow-associated andesitic breccia at the base of the succession.**

Eocene volcanic rocks are also exposed to the east, along the Clisbako River (Figure 3.6). The Clisbako valley traverse displays in particular a massive exposure of columnar-jointed dacitic lava.

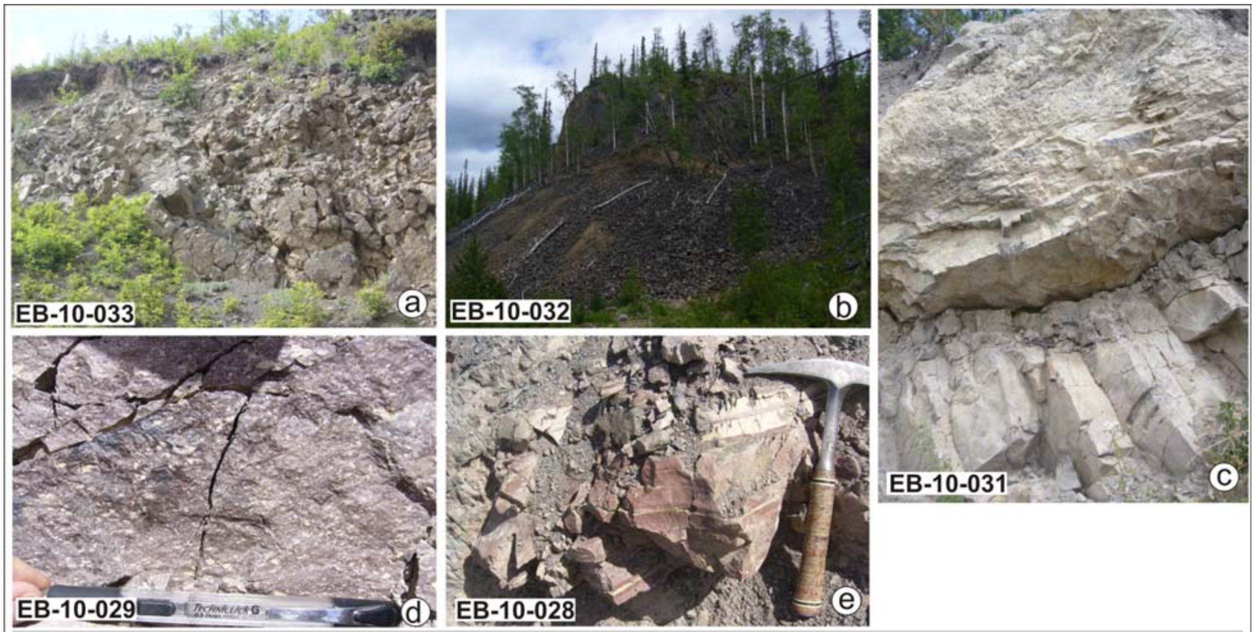


**Figure 3-6: Characteristic lithologies for the Clisbako traverse, southern Nazko River valley. a) Columnar-jointed plagioclase-pyroxene-phyric dacite flow. Columns are subhorizontal; b) Thick flow of columnar jointed plagioclase-pyroxene-phyric dacite. Columns are subvertical. At the base of the outcrop, dacitic lava is interbedded with layered volcanic sandstone; c) Coherent, columnar jointed plagioclase-hornblende dacite and associated flow top breccia; d) Vesicular pink/beige fractured K-feldspar-phyric flow-banded dacite; e) Flow-banded red/beige dacite forming the base of the outcrop. Overlain by massive to vesicular, flow-banded dark grey, plagioclase-phyric andesite and associated autobreccia.**

Characteristic lithologies observed in the region east of the Baezaeko traverse are illustrated by field photographs and a cross-section AA' (Figure 3.7). Flow-banded dacite, rhyodacite and vitreous dacite flows dominate this area. These lithologies are likely Eocene in age. In the valley, thick beds of Chilcotin basalt are exposed.

Further west along the Baezaeko traverse, dacitic flows and breccias units dominate (Figure 3.8). On cross-section B-B' (Figure 3.8), a distinctive unit formed of accretionary lapilli-stone and layered tuff is indicated. This pyroclastic deposit is overlain by a chaotic deposit involving blocks of black vitreous dacite (Table 3.2). Along cross-section C-C' (Figure 3.9), blocky columnar-jointed plagioclase-phyric vitreous dacite overlays flow-banded aphanitic to finely hornblende-phyric dacite flows and breccias. Locally, exposures of Chicotin basalt are observed. They are commonly found in topographic lows (Figures 3.8 and 3.9).

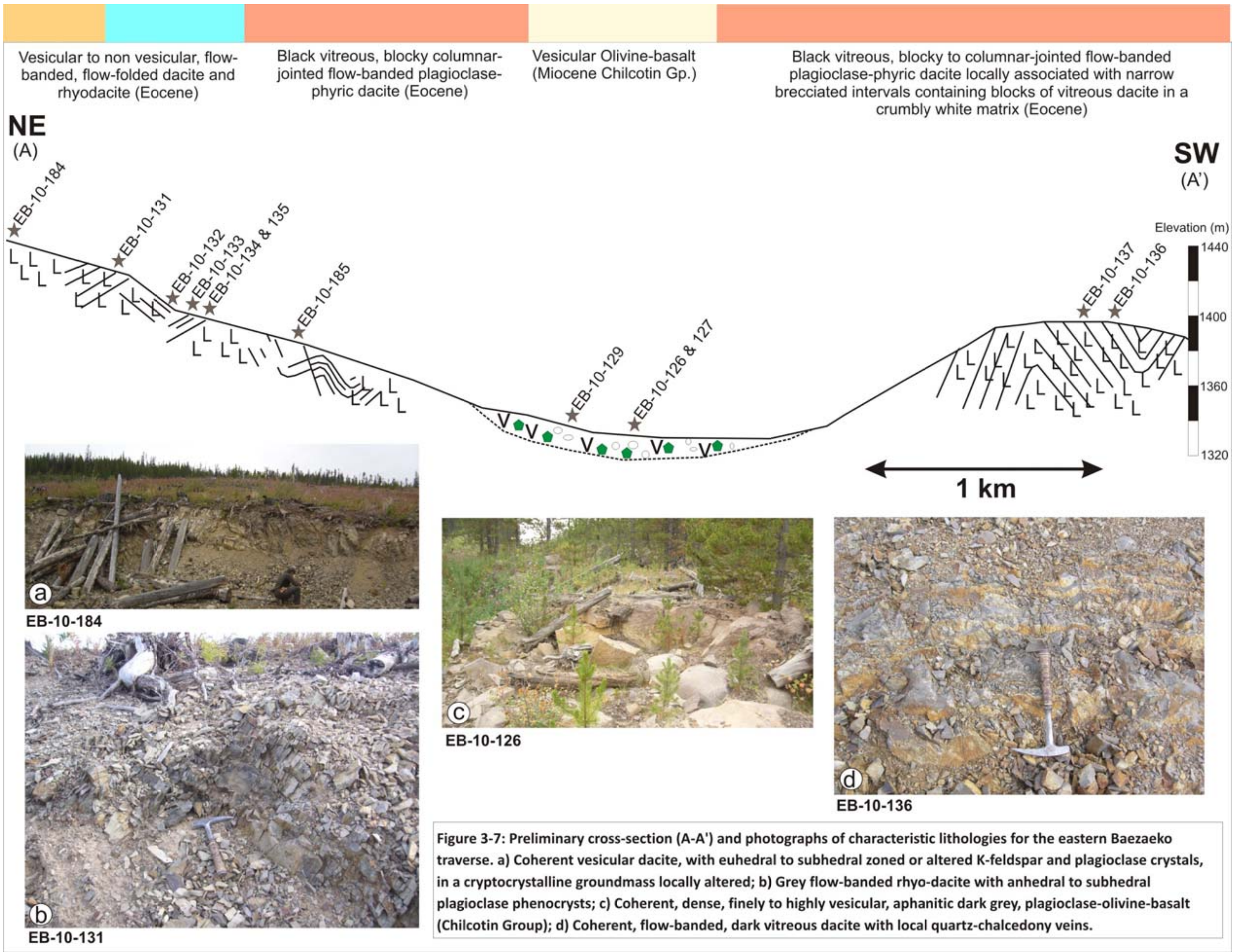


**Figure 3-7: Preliminary cross-section (A-A') and photographs of characteristic lithologies for the eastern Baezaeko traverse. a) Coherent vesicular dacite, with euhedral to subhedral zoned or altered K-feldspar and plagioclase crystals, in a cryptocrystalline groundmass locally altered; b) Grey flow-banded rhyo-dacite with anhedral to subhedral plagioclase phenocrysts; c) Coherent, dense, finely to highly vesicular, aphanitic dark grey, plagioclase-olivine-basalt (Chilcotin Group); d) Coherent, flow-banded, dark vitreous dacite with local quartz-chalcedony veins.**

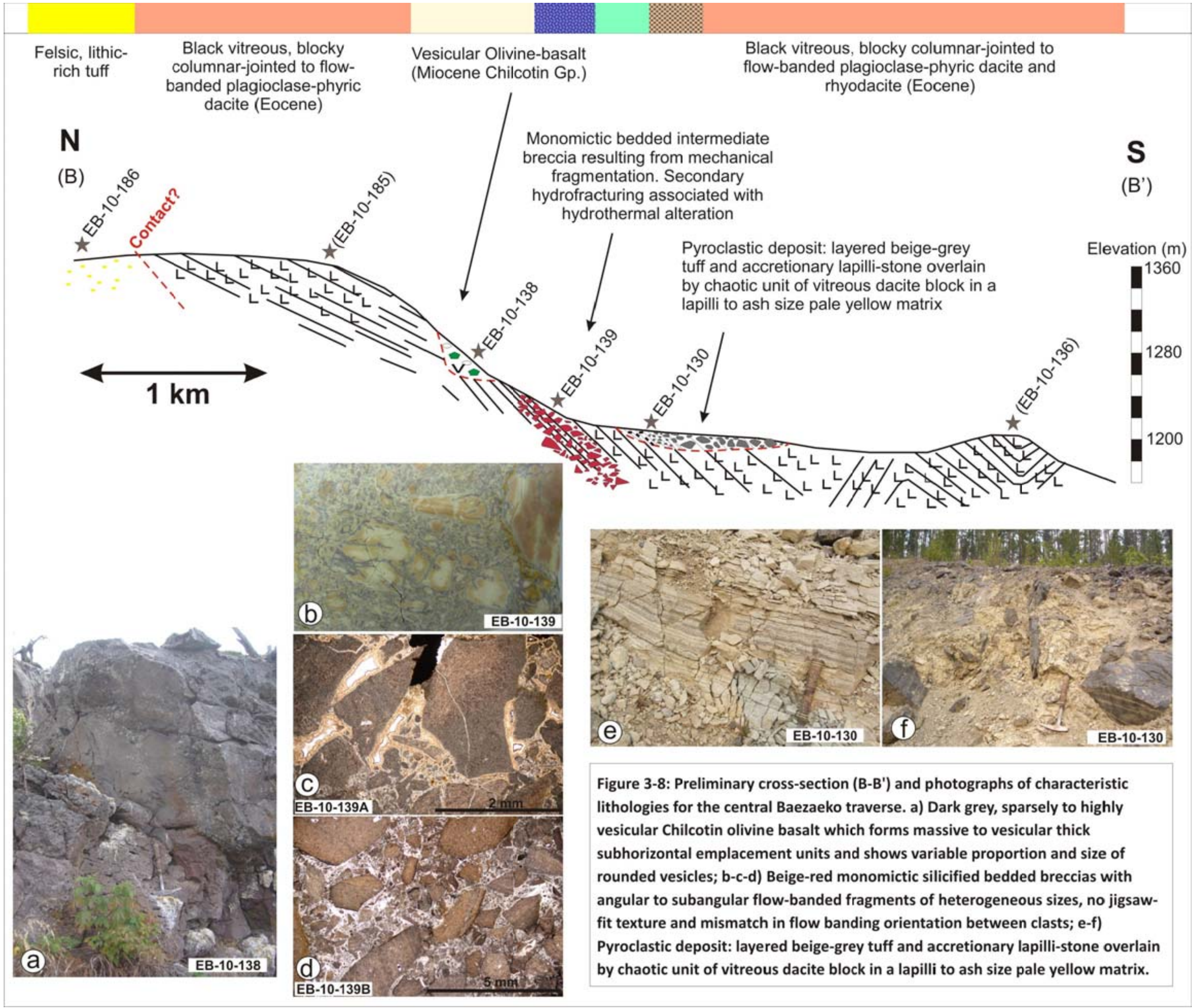


**Figure 3-8: Preliminary cross-section (B-B') and photographs of characteristic lithologies for the central Baezaeko traverse. a) Dark grey, sparsely to highly vesicular Chilcotin olivine basalt which forms massive to vesicular thick subhorizontal emplacement units and shows variable proportion and size of rounded vesicles; b-c-d) Beige-red monomictic silicified bedded breccias with angular to subangular flow-banded fragments of heterogeneous sizes, no jigsaw-fit texture and mismatch in flow banding orientation between clasts; e-f) Pyroclastic deposit: layered beige-grey tuff and accretionary lapilli-stone overlain by chaotic unit of vitreous dacite block in a lapilli to ash size pale yellow matrix.**

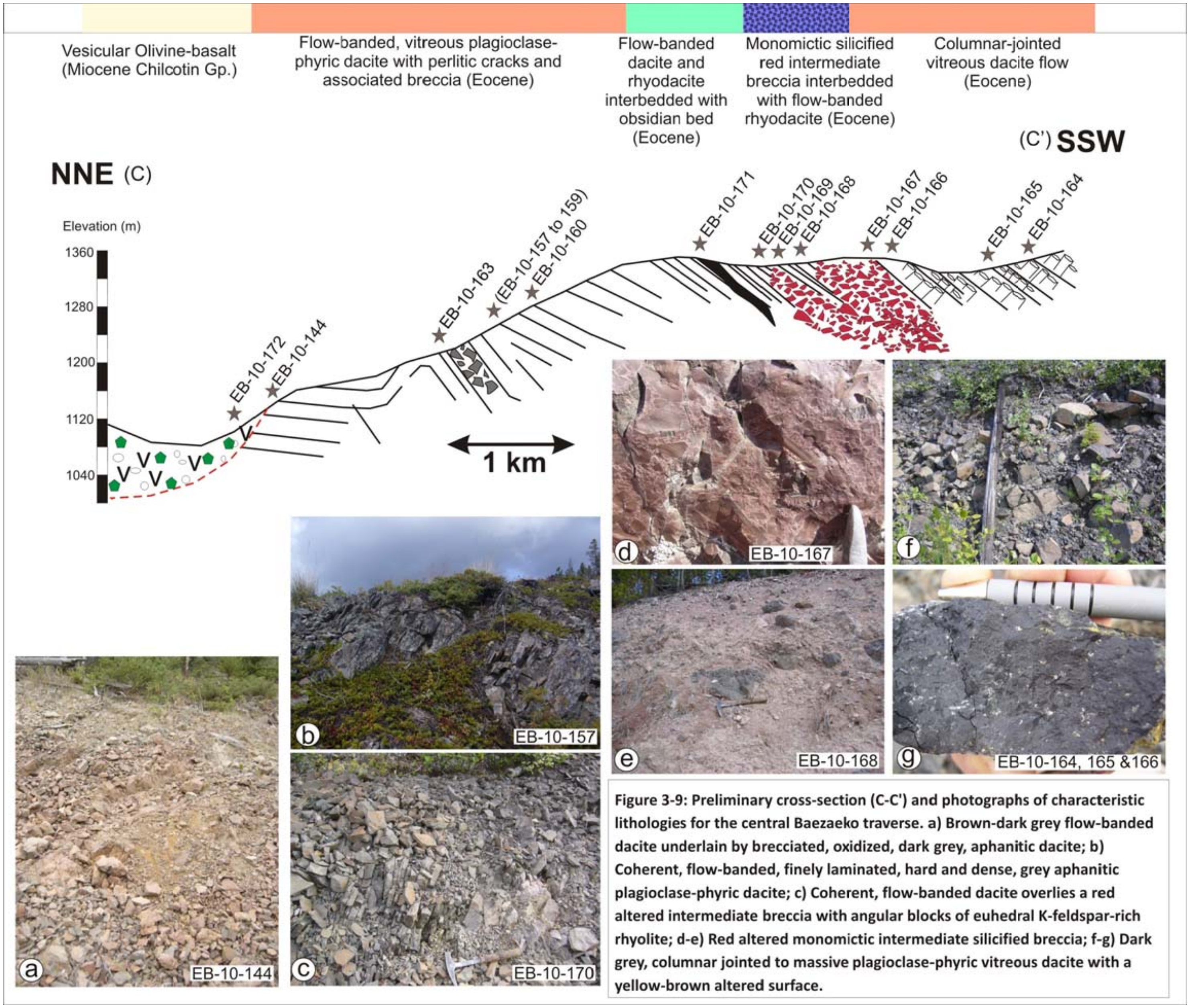


**Figure 3-9: Preliminary cross-section (C-C') and photographs of characteristic lithologies for the central Baezaeko traverse. a) Brown-dark grey flow-banded dacite underlain by brecciated, oxidized, dark grey, aphanitic dacite; b) Coherent, flow-banded, finely laminated, hard and dense, grey aphanitic plagioclase-phyric dacite; c) Coherent, flow-banded dacite overlies a red altered intermediate breccia with angular blocks of euhedral K-feldspar-rich rhyolite; d-e) Red altered monomictic intermediate silicified breccia; f-g) Dark grey, columnar jointed to massive plagioclase-phyric vitreous dacite with a yellow-brown altered surface.**

In the northern part of the Baezaeko traverse, the contact between Eocene volcanic rocks and Jurassic andesitic flows has not been mapped, but is likely to be a fault contact as illustrated on cross-section D-D’(Figure 3.10). Flow-banded dacite and brecciated dacite are common lithologies (Figures 3.10 and 3.11). Several exposures of polymictic volcanic breccia in contact with volcanic sandstones occur (Figure 3.10). As seen in  previous locations, exposures of Chilcotin basalts occur in topographic lows (Figure 3.10) or unconformably overlying Eocene strata (Figure 3.11). Finally, in the western of the Baezaeko traverse, an exposure of xenocrystic basalt is mapped and is assigned to the Cheslatta Lake volcanic suite (Figure 3.3; outcrop EB-10-141).

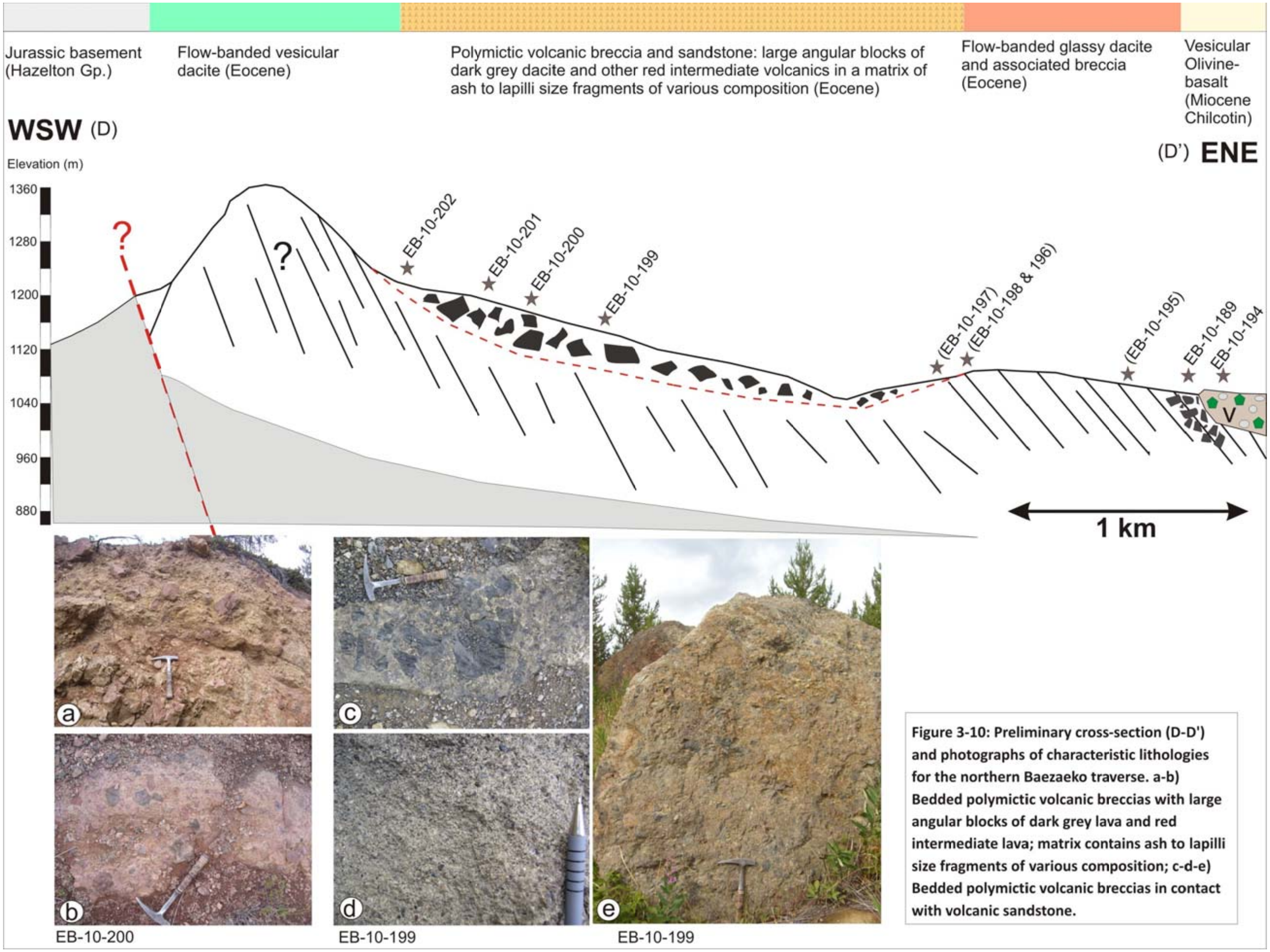


**Figure 3-10: Preliminary cross-section (D-D') and photographs of characteristic lithologies for the northern Baezaeko traverse. a-b) Bedded polymictic volcanic breccias with large angular blocks of dark grey lava and red intermediate lava; matrix contains ash to lapilli size fragments of various composition; c-d-e) Bedded polymictic volcanic breccias in contact with volcanic sandstone.**

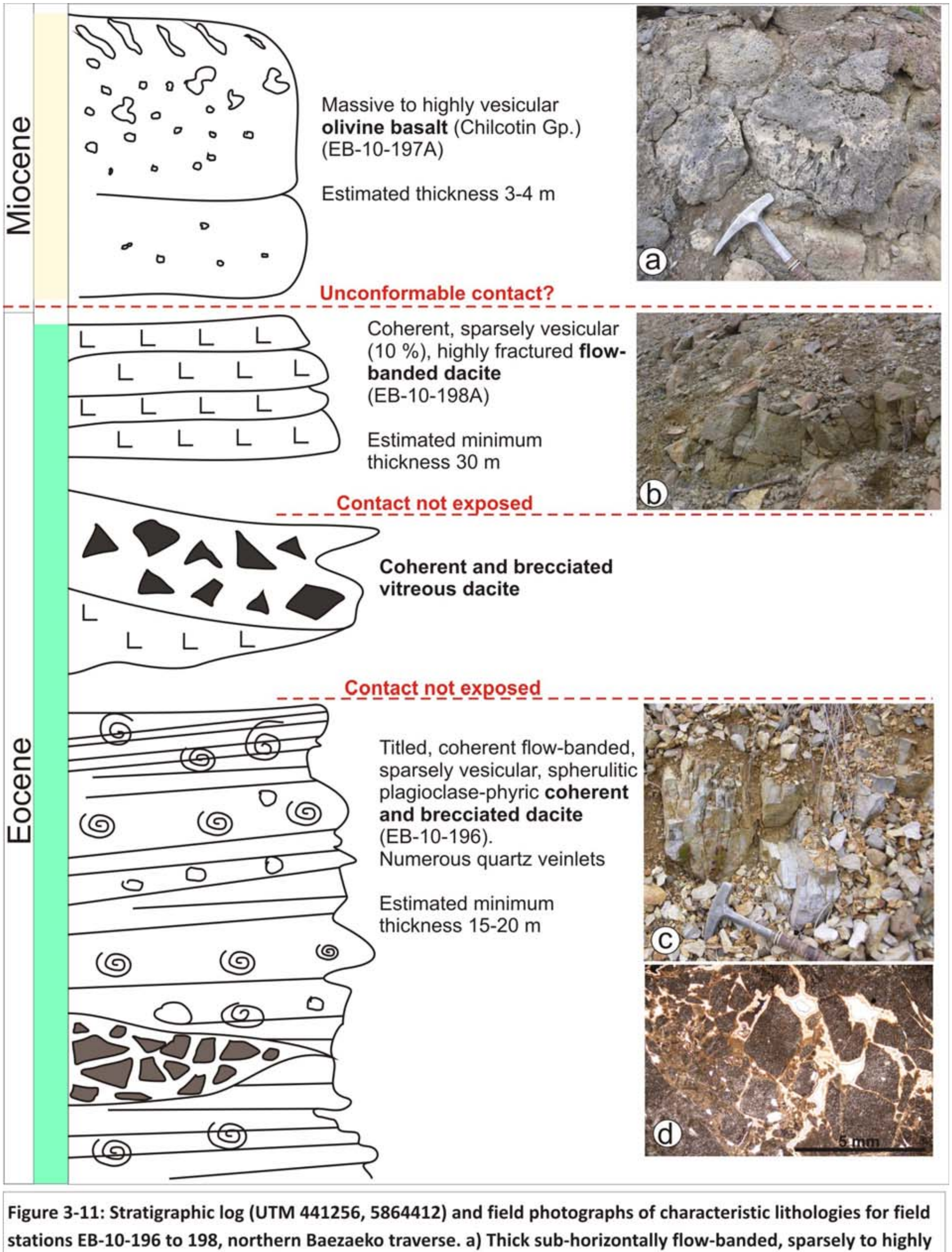


**Figure 3-11: Stratigraphic log (UTM 441256, 5864412) and field photographs of characteristic lithologies for field stations EB-10-196 to 198, northern Baezaeko traverse. a) Thick sub-horizontally flow-banded, sparsely to highly vesicular dark grey aphanitic olivine-basalt; b) Flow-banded, light pink, thinly laminated, vesicular spherulitic dacite; c) Outcrop of flow-banded, light pink, thinly laminated, vesicular dacite with devitrification textures (spherulites) and silicified breccia (d).**

In the Tibbles Road area, widespread Early Eocene rhyolitic flows (Table 3.2; Figure 3.12) are overlain by Late Eocene andesitic flows (Tipper, 1959; this study). Flow-banded and brecciated dacite lava also represent a common lithology in this area (Table 3.2; Figure 3.12).

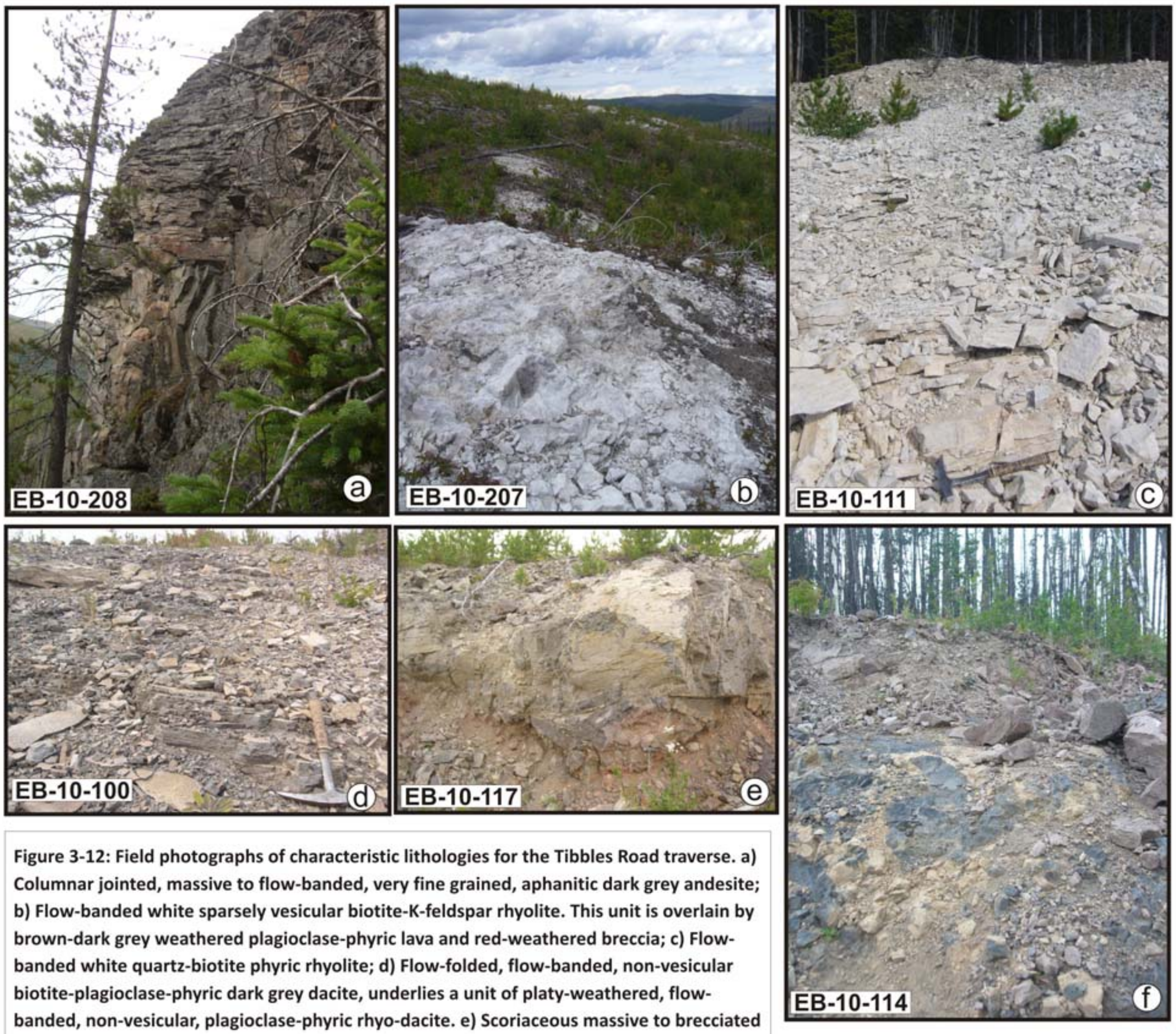


**Figure 3-12: Field photographs of characteristic lithologies for the Tibbles Road traverse. a) Columnar jointed, massive to flow-banded, very fine grained, aphanitic dark grey andesite; b) Flow-banded white sparsely vesicular biotite-K-feldspar rhyolite. This unit is overlain by brown-dark grey weathered plagioclase-phyric lava and red-weathered breccia; c) Flow-banded white quartz-biotite phyric rhyolite; d) Flow-folded, flow-banded, non-vesicular biotite-plagioclase-phyric dark grey dacite, underlies a unit of platy-weathered, flow-banded, non-vesicular, plagioclase-phyric rhyo-dacite. e) Scoriaceous massive to brecciated red-purple oxidized intermediate lava overlain by highly fractured and faulted, vesicular, flow-banded dark grey-brown aphanitic andesite; f) Red to dark grey vesicular andesite with common chalcedony along fractures, overlying yellow-weathered intermediate volcanic breccia.**

# 4 <u>Physical Rock Properties</u>

## 4.1 Introduction

Physical rock property measurements were conducted as part of this study to provide data that can be utilized as a link between the observed geology and the geophysical surveys. This data will allow for the development of more robust interpretations and models.

## 4.2 Density

### 4.2.1 Method

The bulk densities of all samples collected within the focused study area were measured using the wet-dry density method. Measurements were conducted at the Volcanology and Petrology Laboratory / Centre for Experimental Studies of the Lithosphere at UBC, under the supervision of Kelly Russell and Betsy Friedlander. Results are presented in Appendix 3 of this report. The wet/dry experimental method is summarized as follows from Friedlander and Russell (2011):

"The wet/dry method for determining density is also known as the Hydrostatic Weighing (Displacement method) and is derived from the Buoyancy law. Bulk density of the sample ($\rho_S$) is determined using the follow relationship:

$$\boldsymbol{\rho_S = m_D * \rho H_2O / (m_D - m_W)}$$

where:

- $\rho H_2O$ is the density (g $cc^{-1}$)of the water (dependent on temperature)
- $m_D$ is the mass (g) of the sample dry
- $m_W$ is the mass (g) of the sample submerged in $H_2O$

Each sample measurement is replicated 3 times. After the dry mass is determined, all samples are soaked for 24 hours to allow water to fill any pore spaces within the sample.

Calibration experiments are performed on standard Pyrex glass having a known ρ (2.23 g $cc^{-1}$) for every 15 unknown samples. The results of the replicate analyses on the known standard are reported on a separate data sheet and provide a quantitative measure of our experimental uncertainty.

Density is reported to the 4$^{th}$ decimal although the measurement uncertainty lies within the 3$^{rd}$ decimal. Error is propagated to determine the uncertainty ($\sigma\rho_S$) with the following equation:

$$\boldsymbol{\sigma\rho_S = \rho H_2O/(m_D - m_W)^2 * [( m_D{}^2 * \sigma\, m_W{}^2)+(m_W{}^2 * \sigma m_D{}^2)]^{(1/2)}}$$

where $\sigma m_D$ and $\sigma m_W$ are the uncertainties in measurement of dry and wet masses, respectively."

### 4.2.2 Results

The average density of samples collected during the project range from 1.4 to 2.9 g/cc. For the entire sample run, the average standard error on measured densities is +/- 0.0025 g/cc (e.g., 0.102%). The variability on individual samples in indicated in Appendix 3; samples with more pore spaces have slightly higher errors.

The distribution of average density values over the focused study area is presented in Figure 4.1. Samples collected during the summer 2010 field season and samples from part of the BC Physical Property database (Enkin et al., 2008) are plotted. This map shows a predominance of density values between 2.3 and 2.7 g/cc over all the area dominated by Eocene volcanic rocks. Higher values (>2.7 g/cc) are locally observed, in particular in Jurassic or Neogene volcanic rocks. Bulk density values lower than 2.3 g/cc are typically concentrated in the Cretaceous clastic sedimentary rocks.

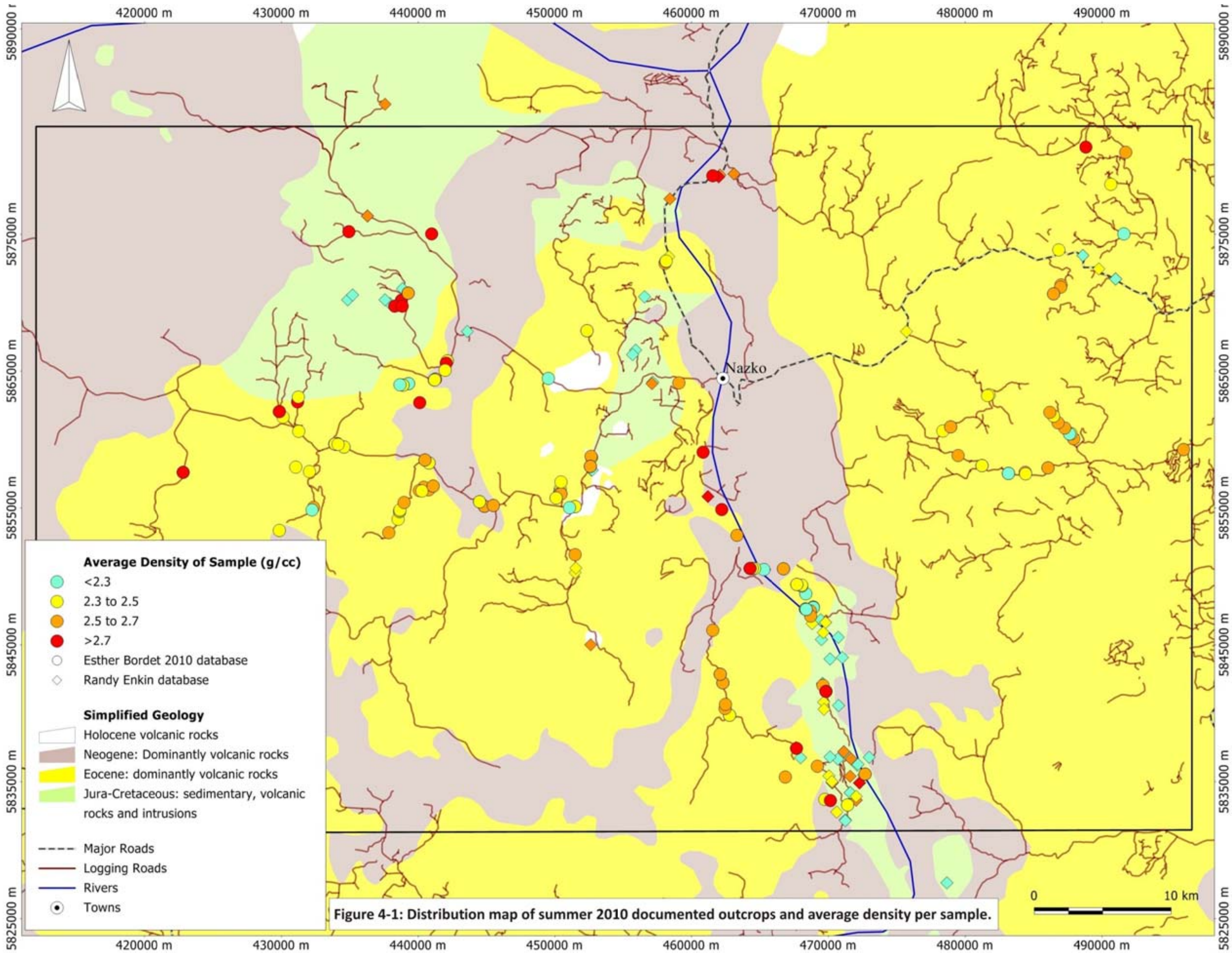


**Figure 4-1: Distribution map of summer 2010 documented outcrops and average density per sample.**

Whisker plots (Figure 4.2), were designed using IoGas software to represent the variability of bulk densities depending on the rock composition, rock texture, or stratigraphic position. Eocene volcanic rocks cover the entire range of bulk density values. Andesitic and dacitic lava flows and intermediate composition volcanic breccias represent the majority of samples collected and show the higher density values (approx. 2.4-2.8 g/cc). On the contrary, epiclastic and volcaniclastic deposits, and weathered and oxidized volcanic breccias display densities with the lower range of measured values.

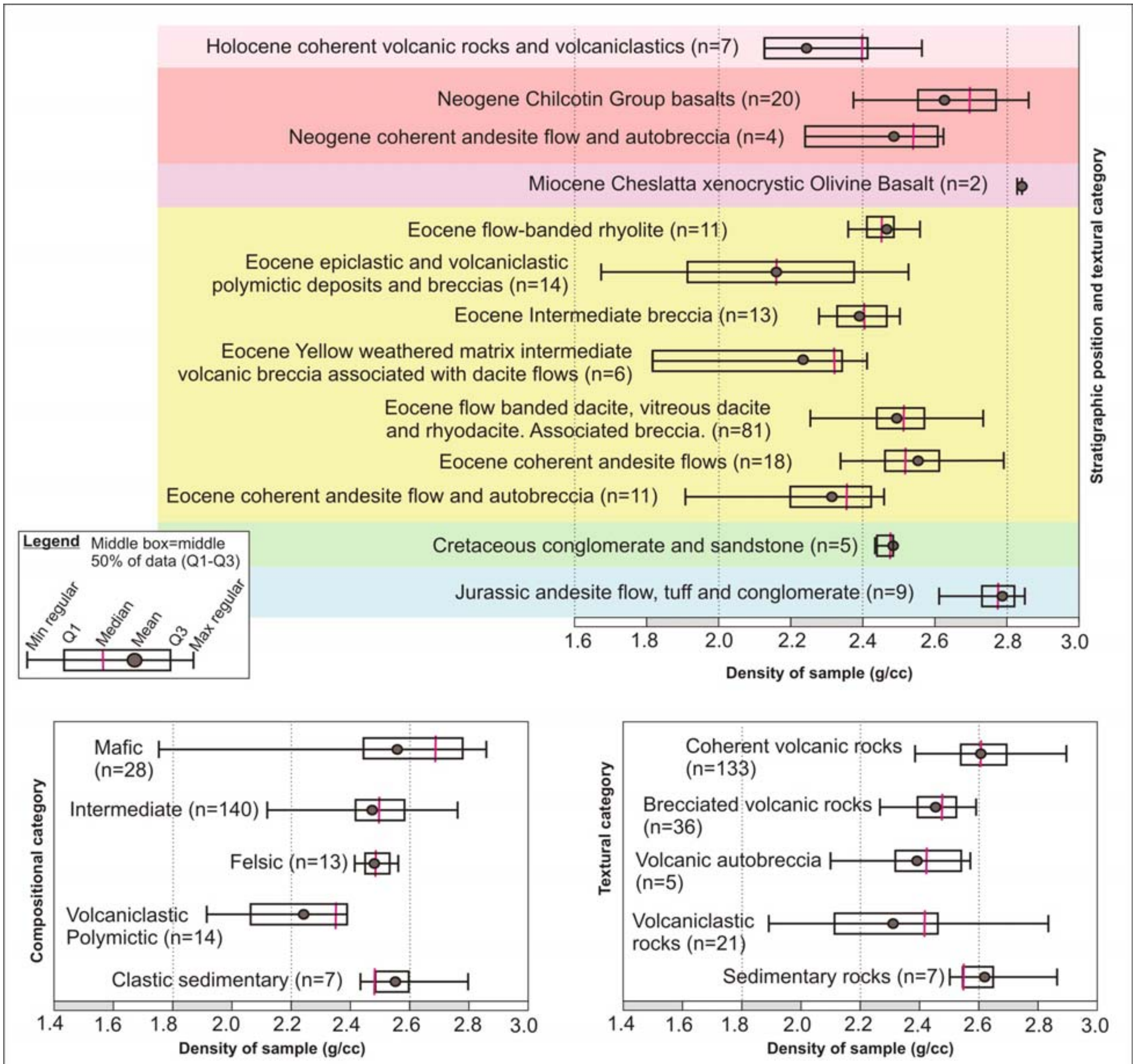


**Figure 4-2: Whisker plots of average densities by: a) Mappable unit or volcanic facies; b) Compositional category; c) Textural category.**

## 4.3 Magnetic Susceptibility

### 4.3.1 Method

Magnetic susceptibility was measured systematically at each outcrop using a KT-10 Magnetic Susceptibility Meter throughout the field program. A minimum of ten readings were recorded at each outcrop, and more readings were conducted if several lithologies were identified. Minimum, maximum and average magnetic susceptibility per outcrop are compiled in Appendix 4. The average magnetic susceptibility value per outcrop was used to compile the maps and plots presented below. Data are presented in dimensionless $10^{-3}$ S.I. unit format.

Individual outcrops typically recorded a wide range of magnetic susceptibility values. Possible discrepancies in measurements result from the variability in the rocks, but lower results were due to surface oxidation of many outcrops. To increase the internal consistency of the dataset, multiple measurements on individual samples could be conducted.

### 4.3.2 Results

Average magnetic susceptibility values for all samples range between $0.033 \times 10^{-3}$ and $43 \times 10^{-3}$ (S.I). Most of the data are within the $1\text{-}20 \times 10^{-3}$ range, and only xenocrystic basaltic rocks assigned to the Cheslatta Lake suite display very high magnetic values.

The distribution of average magnetic susceptibility values per outcrop over the focused study area is presented in Figure 4.3. Samples collected during the summer 2010 field season are combined with samples from the BC Physical Property database (Enkin et al., 2008). They are plotted over the TMI (total magnetic intensity) image for the region (Geological Survey of Canada, 1994; Teskey et al., 1997). The lowest magnetic susceptibility values correspond with exposures of the Cretaceous clastic sedimentary rocks, in the Nazko River valley in particular. At these locations, magnetic susceptibility values are typically between 0-0.001 (Figure 4.4). In areas dominated by Eocene volcanic rocks, magnetic susceptibility values commonly range between 4 and 10. The highest values are associated with the Cheslatta Lake suite basalts, and andesitic flows and breccias of the Tibbles Road traverse. In general, volcanic rocks from the different units present a great variability of magnetic values from 0 to 20 (Figure 4.4).

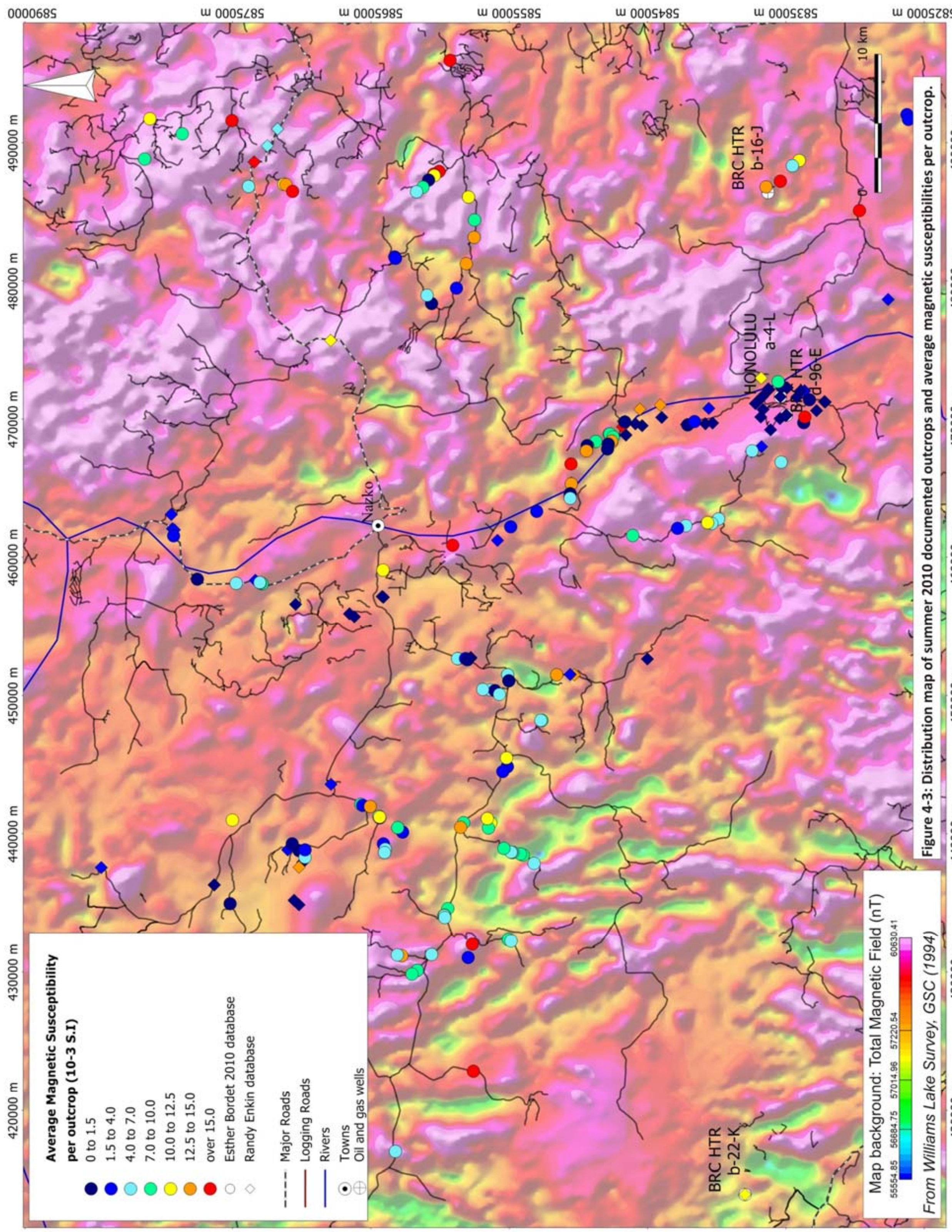


**Figure 4-3: Distribution map of summer 2010 documented outcrops and average magnetic susceptibilities per outcrop.**

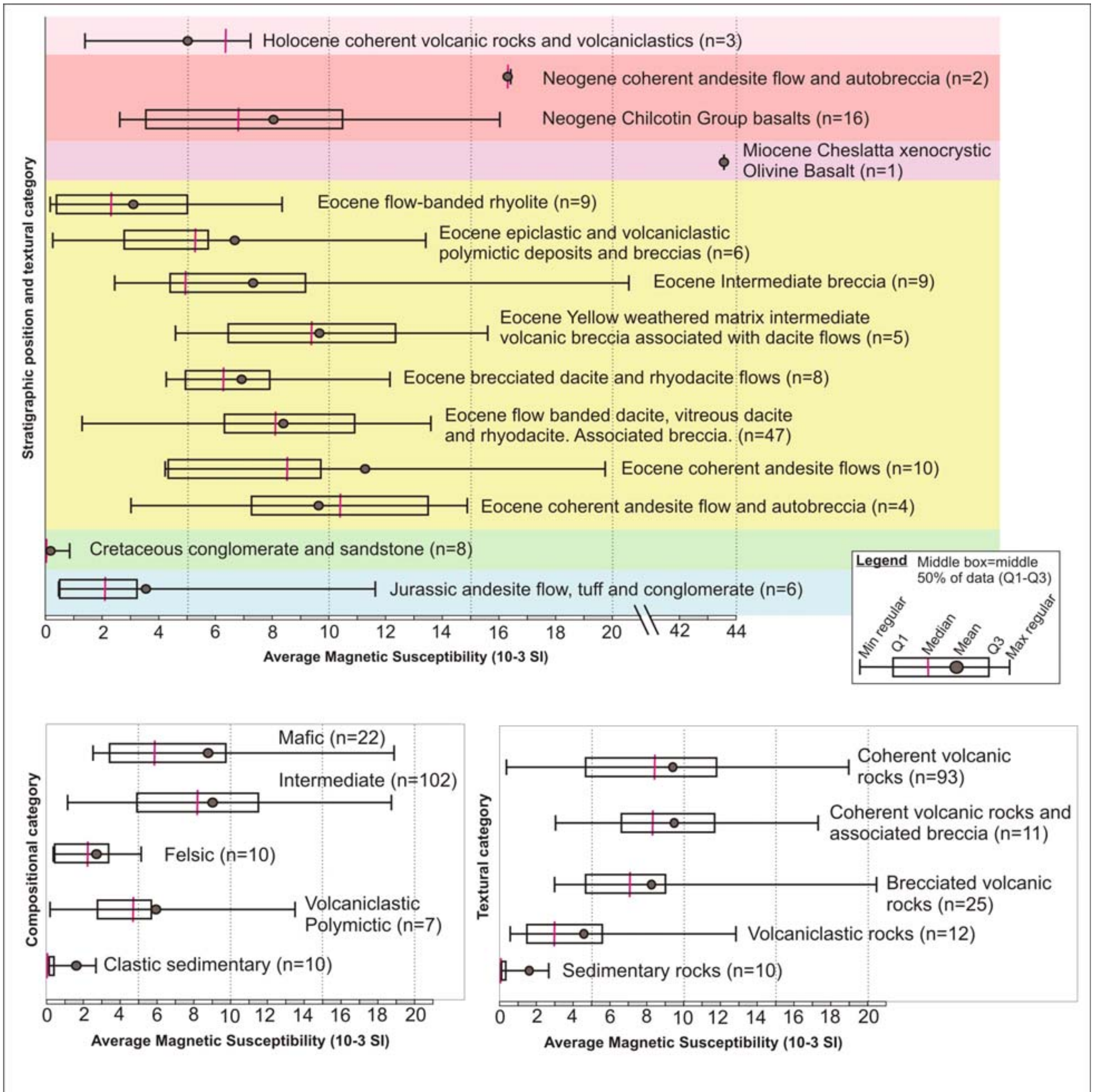


**Figure 4-4: Whisker plots of average magnetic susceptibilities by: a) Mappable unit or volcanic facies; b) Compositional category; c) Textural category.**

## 4.4 Comparison with Previous Datasets

The BC Physical Property database (Enkin et al., 2008) contains a complete range of physical property measurements (density, magnetic susceptibility, resistivity, remanent magnetisation, Koenigsberger ratio) for a series of rock samples collected in British Columbia. In this report, only samples from the Nechako region were selected. Spatial variability in the magnetic susceptibility and average density for these samples are displayed on maps of Figures 4.1 and 4.3.

Additional whisker plots (Figure 4.5) were generated for these samples in order to establish comparisons with the samples collected as part of this study. Overall, the range of density and magnetic susceptibility values measured in the present study are consistent with previous datasets collected in the Nechako region.

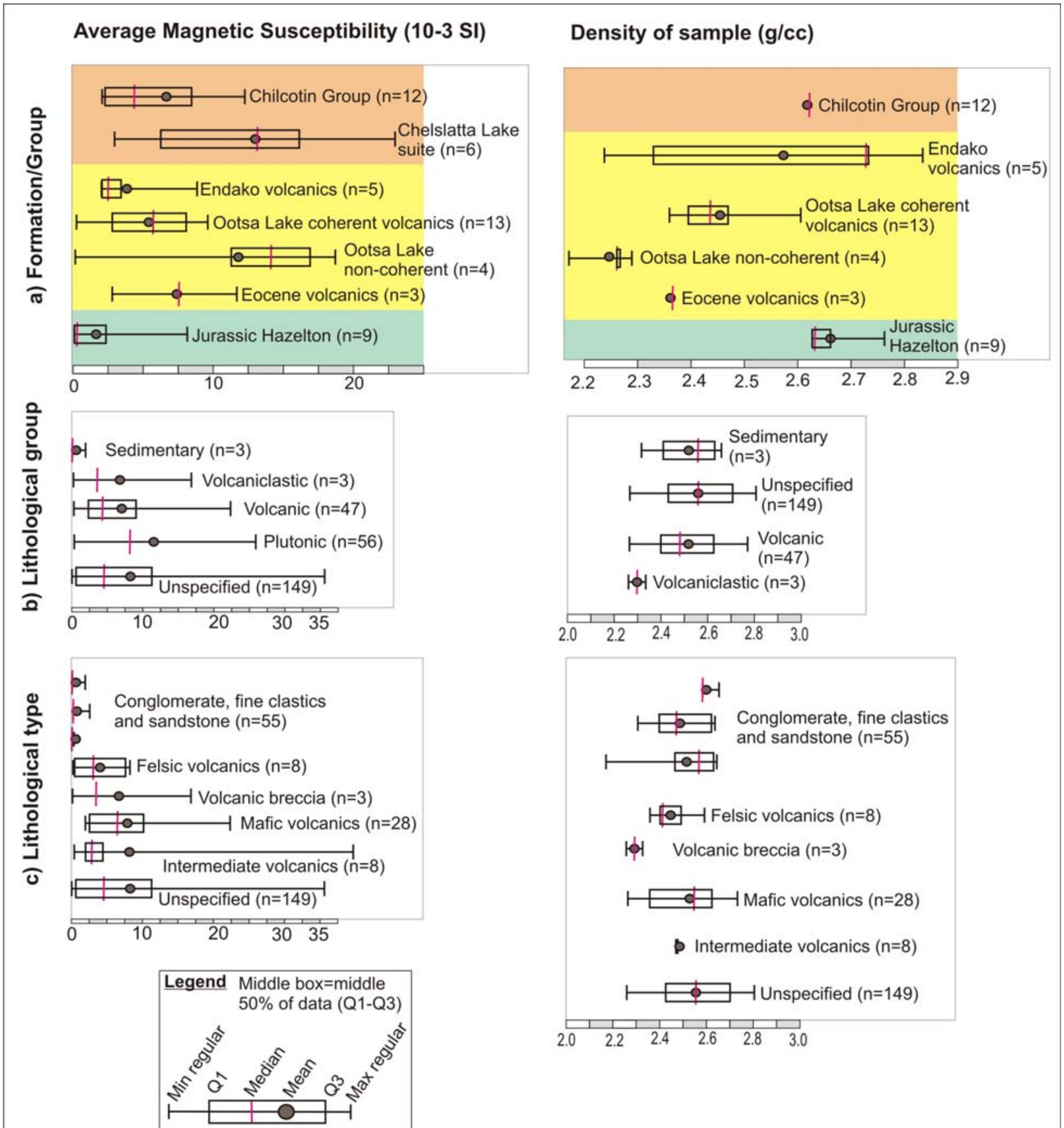


**Figure 4-5: Whisker plots of average densities and magnetic susceptibilities from the BC Physical Property database by: a) Formation/Group; b) Lithological group; c) Lithological type.**

# 5 Thickness and Structural Framework of Eocene Volcanic Rocks

## 5.1 Introduction

Understanding the structural framework of the Eocene volcanic package in the Nechako region has critical implications for unravelling the underlying Jura-Cretaceous basin evolution, and for the tectonic evolution of central BC during the Eocene. This in turn has implications for development of oil and gas and mineral exploration strategies. Abrupt variations in the thickness of Eocene volcanic rocks for example, can indicate the location of structural highs and depressions, and help guid interpretation of fault trends.

Different data sources representing variable scales of observation have been integrated to evaluate the thickness, as well as the stratigraphic and structural patterns of Eocene volcanic rocks in the Nechako region. These are described in the following sections. However, the following limiting factors should be considered:

- Extensive glacial drift covers and limits the extent of outcrop exposures and prevents assessment of the lateral continuity of the mapped units
- Chilcotin Group basalt cover Eocene rocks in several localities
- The basal contact of Eocene rocks is only exposed at a few locations
- The number of oil and gas wells that intersect the Eocene rock packages is limited. These wells provide local constraints for depth but do little to explain lateral variations in the thickness of Eocene volcanic rocks.

## 5.2 Thickness and Structural Constraints from Field Datasets

### 5.2.1 Field Observations and Topography

Based on field observations, a minimum thickness of individual units can be evaluated in well-exposed areas. Many outcrops occur in topographic highs, which help in assessing the thickness of associated units. Average minimum thicknesses of units mapped during the summer 2010 are indicated in Table 3.2. These thicknesses are estimated from elevations measured with a GPS, which concur with the NTS elevations along the mapped sections. The scale of observation is limited to one outcrop or to a series of outcrops. However, these observations can be projected to a topographic surface to assess the lateral extent and equivalent apparent thicknesses of mapped units.

A Digital Elevation Model (DEM) for the Nechako region (Centre for Topographic Information, 1997) was used to constrain the thicknesses of the different units mapped. The selected DEM surface is larger than the focused study area used for mapping. It includes NTS sheets 093B, 093C, 093F, 093G and parts of 092 and 092N (Figure 1.2) and shows an elevation range between 252 m and 3412 m. This area includes all of the 2008 seismic and MT surveys, and all of the oil and gas wells.

Structural measurements collected from outcrops during the 2010 field season are compiled in Appendix 5. They include the following features: 1) Planar structures: bedding, flow-banding, fractures, veins, faults; 2) Linear features: joint intersections in columnar-jointed lavas, flow lineations indicated by elongated vesicles.

Most of these measurements have been compiled on Schmidt equal area stereographic projections on the lower hemisphere. Structural measurements were used in the construction of the cross-sections and maps presented in this report. Most measurements represent flow-banding surfaces and cannot be used to constrain the structural framework of studied rocks.

### 5.2.2 Oil and Gas Wells

Several oil and gas wells were drilled in the Nechako region from 1960 to 1985 (Figure 1.2). Well log reports are available for most of these wells, and some of them provide high-quality lithological descriptions by the well site geologists. In such cases, the ages of the different lithological packages can be interpreted. In some reports, lithological descriptions are poor and are more difficult to use to constrain the ages of the units.

A summary of oil and gas wells information is provided in Table 5.1. For each well, general information is compiled including location, UTM coordinates, collar elevation, Kelly Bushing (KB) elevation and total well depth. In addition, elevations of the base of the Neogene (Chilcotin Group basalts, Anahim Belt basalts and glacial drift) and the base of the Paleogene (mostly volcanic rocks of the Paleocene, Eocene and Oligocene) have been compiled from different bibliographic sources.

The wells B-22-K and B-16-J are particularly relevant to the study of Eocene volcanic rocks. Detailed field logs for these two wells (Cosgrove, 1981 and 1982) were compiled and summarized to evaluate the thickness of the Eocene volcanic package and its lithologic and textural characteristics. East of the Nazko River, the exploration well B-16-J intersected about 1800m of Paleocene-Eocene interbedded conglomerate, sandstone and tuff that were overlain by Eocene mafic volcanic (Cosgrove, 1981; Figure 5.1). West of the Nazko River, well B-22-K intersected 3500m of Early Eocene to Oligocene volcanic rocks, including plagioclase-phyric andesite and breccias, interbedded volcanic flows and volcaniclastic rocks (Cosgrove 1982; Figure 5.2). Radiometric ages exist for these two wells and provide constraints to the ages and thicknesses of the different rock packages (Riddell et al., 2010).

Other wells that intersect the Chilcotin basalts and/or Eocene volcanic rocks include C-30-J and B-82-C (Table 5.1). Wells D-96-E and A-4-L were drilled in the Nazko River valley and intersected only the clastic Cretaceous succession (Ferri and Riddell, 2006; Riddell et al., 2007; Riddell, 2010).

**Table 5-1: Compiled Neogene and Paleogene volcanic rocks thickness information from oil and gas wells. a) General wells information; b) Compiled elevations for reference geological units**

**a. General wells information**

| Well ID | Well name | General location | Date | UTM Easting (Zone 10) | UTM Northing (Zone 10) | Elevation collar (m) | KB (m) | Total Depth (m) |
|---|---|---|---|---|---|---|---|---|
| c-75-A 93B/4 | HB Redstone | Chilcotin Plateau | 1960 | 461398.00 | 5768336.00 | 792.61 | 795.65 | 1303.30 |
| b-82-C 92O/14 | Redstone | Chilcotin Plateau | 1981 | 480980.00 | 5740701.00 | 1227.20 | 1234.30 | 1720.00 |
| d-94-G 92O/12 | CanHunter Redstone | Chilcotin Plateau | 1985 | 453711.00 | 5723900.00 | 1333.20 | 1337.90 | 2165.00 |
| b-16-J 93B/11 | Esso Nazko | East of Nazko Valley | 1980 | 486398.00 | 5836290.00 | 1411.26 | 1418.36 | 2700.00 |
| a-4-L 93B/11 | Honolulu Nazko | Nazko Valley | 1960 | 471599.00 | 5835406.00 | 922.03 | 926.29 | 3300.48 |
| d-96-E 93B/11 | CanHunter Nazko | Nazko Valley | 1980 | 470283.00 | 5834950.00 | 1208.20 | 1214.60 | 3324.00 |
| c-38-J/93-G-6 | Vieco Texacal | SE of Prince George | 1972 | 485378.00 | 5922112.00 | 701.00 | 704.70 | 1277.72 |
| b-22-K 93C/9 | CanHunter Chilcotin | SW Baezaeko area | 1981 | 413936.00 | 5837969.00 | 1384.20 | 1391.30 | 3778.00 |

**b. Compiled elevations for reference geological units**

| Well ID | Elevation collar (m) | Elevation Base Miocene (m) | Elevation Base Eocene (m) | Comment | Reference |
|---|---|---|---|---|---|
| c-75-A 93B/4 | 792.61 | n/a | n/a | | Riddell et al. (2007); Rouse (1992) |
| b-82-C 92O/14 | 1227.20 | n/a | **1007.2** | | Riddell et al. (2007); Rouse (1992) |
| d-94-G 92O/12 | 1333.20 | n/a | n/a | | Riddell et al. (2007) |
| b-16-J 93B/11 | 1411.26 | n/a | **-308.74** | Depth Paleocene | Cosgrove (1981); Riddell et al. (2007); also see Figure 6.1 of this report |
| a-4-L 93B/11 | 922.03 | n/a | n/a | | Riddell et al. (2007); Rouse (1992) |
| d-96-E 93B/11 | 1208.20 | n/a | n/a | | Riddell et al. (2007); Rouse (1992) |
| c-38-J/93-G-6 | 701.00 | **518.16** | **259.08** | No age constraints for descriptions of lithologies in well log report, elevation base Miocene and Eocene (Paleocene in this case) are inferred | Steiner (1972) |
| b-22-K 93C/9 | 1384.20 | **1154.2** | **-2393.8** | Contradictory age results between Rouse (1992) and Riddell et al. (2007): palynology ages from Rouse place the base of Eocene at 720 m depth, recent U-Pb dates from Riddell et al. return Eocene ages for the entire well. | Cosgrove (1982); Rouse (1992); Riddell et al. (2007); also see Figure 6.2 of this report |

Notes:
Elevation base of Miocene is the boundary between Miocene+Younger units (including glacial drift) with older rocks
Elevation base of Eocene is the boundary between Eocene+Miocene+Younger units (including glacial drift) with older rocks

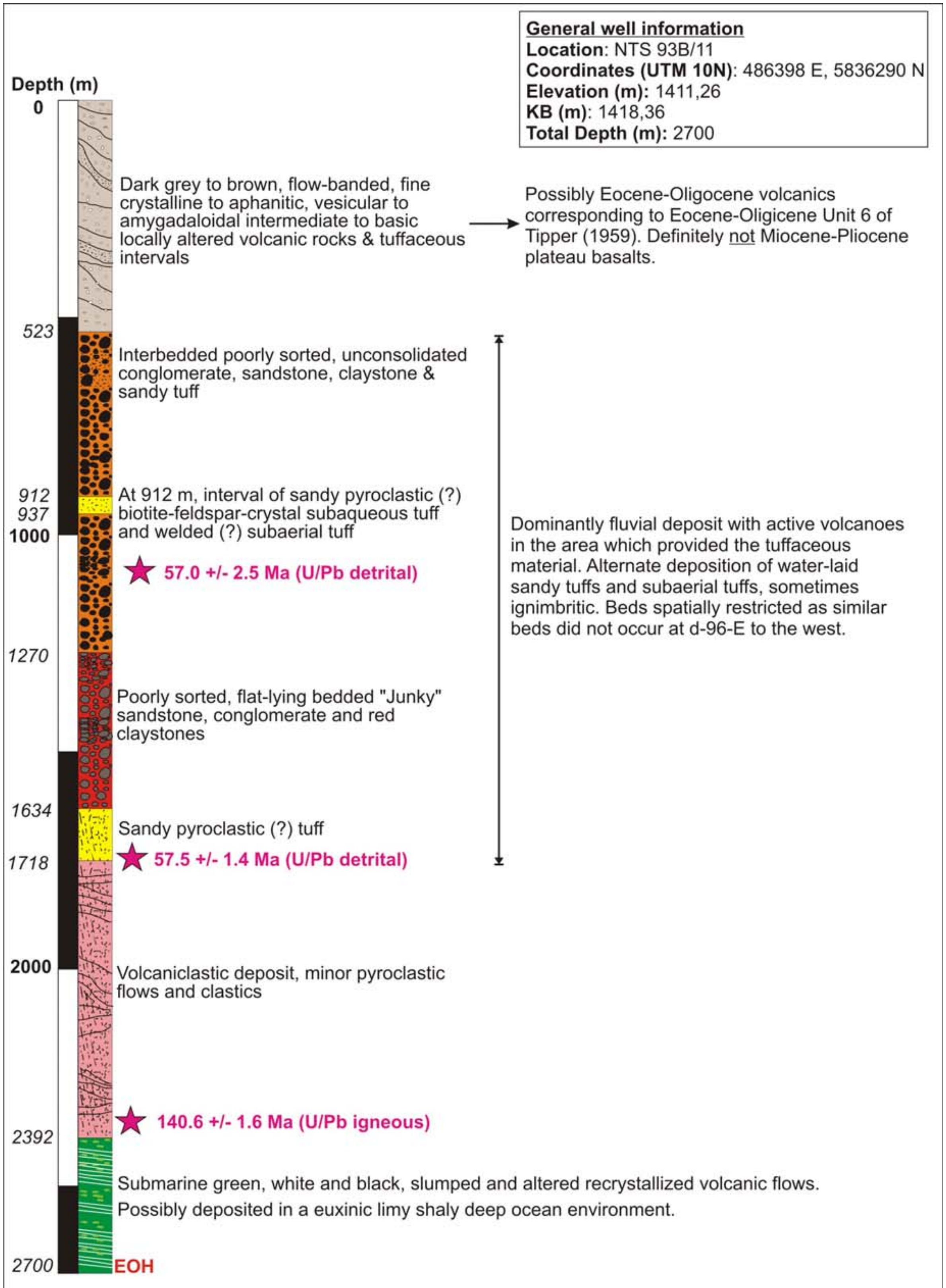


**Figure 5-1: Simplified well log for well B-16-J (1980). Adapted from original log and descriptions by Cosgrove (1981). U-Pb ages (★ )from Riddell (2010).**

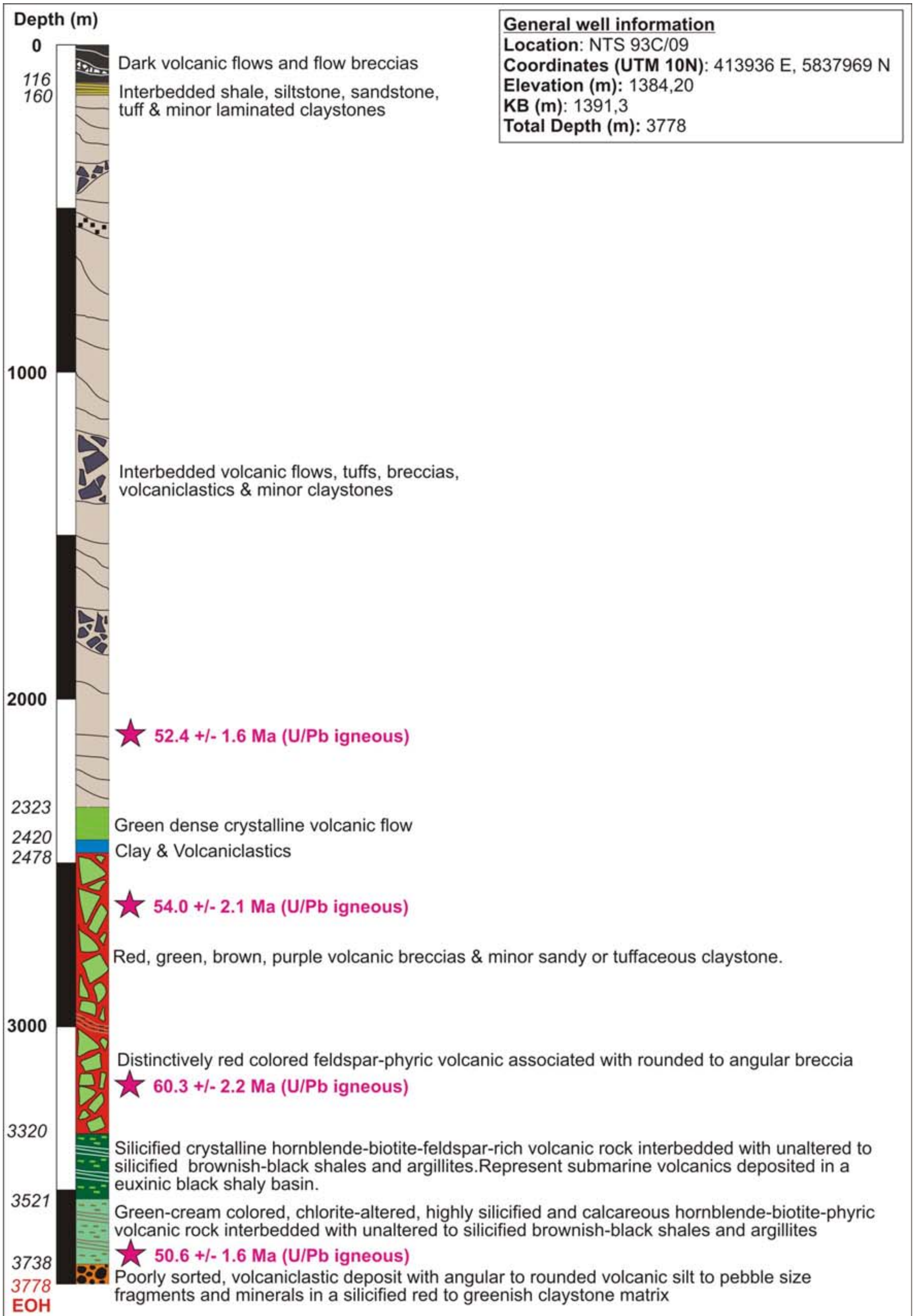


**Figure 5-2: Simplified well log for well B-22-k (1981). Adapted from original log and descriptions by Cosgrove (1982). U-Pb ages from Riddell (2010).**

### 5.2.3 Water Wells

The Chilcotin Interactive Database (Dohaney et al., 2010b) contains lithological thickness information for more than 1000 well logs across central British Columbia. This well log information was used by Andrews and Russell (2008) to constrain cover thickness across the Nechako region; logged "Basalt" intervals are attributed to the Chilcotin Group basalts.

In the present study, "Basalt" thicknesses from water wells have been used to generate an updated thickness model for the Chilcotin Group basalts, and to constrain surface elevations of underlying Eocene volcanic rocks. This process is described in more detail further in this chapter.

## 5.3 Thickness and Structural Constraints from Geophysical Datasets

### 5.3.1 Seismic and MT Surveys Lines

Magnetotelluric data were acquired by the Geoscience BC and the GSC in the fall of 2007. High-frequency audio-magnetotelluric and broadband data were collected at 734 site locations along 7 main profiles throughout the Nechako region (Figure 1.2; Spratt and Craven, 2009). Magnetotelluric sections by Spratt and Craven (in press) show a thin resistive unit ranging in depth from 0 to 200 m that correlates with mapped Chilcotin basalts, and a shallow conductive layer ranging in depth from 0 to 2000 m that is regionally correlated with the surface-mapped Eocene volcaniclastic rocks. Cretaceous sedimentary rocks show a resistivity signature comparable to the Eocene volcaniclastic rocks but show strong lateral variations. Their thickness can be up to 4000 m. Observations from the field and wells corroborate these interpretations from magnetotelluric datasets.

Seismic reflection surveys in the Nechako region were first aquired by Canadian Hunter Exploration Limited in the early 1980s (Figure 1.2). Data acquisition details are provided in Hayward and Calvert (in press) and are as follows: "The data were recorded using a vibroseis source with a 15 second sweep over a frequency range of 10 to 70 Hz. The shot interval was 100 m, except for [specific lines], which had an interval of 50 m. (...). Geophone receiver groups composed of L-15 geophones (with a natural frequency of 8Hz) were 100 m long. (...) Four seconds of data were recorded at a sample interval of 4 ms." These data were reprocessed by Arcis Corporation in 2006 which produced improved structure stack and time migrated sections, and constitute the base of interpretations proposed in Hayward and Calvert (2009), and Hayward and Calvert (in press).

In 2008, Geoscience BC designed a new seismic reflection program in the area near Nazko (Figure 1.2; Clavert et al., 2009), and acquired a number of lines coincident with the 2007 magnetotelluric surveys. Design of this new survey was directed towards maximizing the signal-to-noise ratio compared to the general poor quality of Canadian Hunter surveys. In particular, sweep was reduced to lower frequencies to improve transmission through near-surface volcanic rocks, and recording offset was increased to increase constraints on the thickness and depth of the volcanic layer (Calvert et al., 2009).

Seismic interpretations (Smithyman and Clowes, 2011; Hayward and Calvert, in press) suggest the development of fault-bounded pull-apart basins during the Eocene infilled with the products of extensive volcanism. Interpretations are constrained by oil and gas well logs and sonic logs, and by proposed velocity models.

### 5.3.2 Gravity and Magnetic Inversions

Preliminary unconstrained gravity inversion modeling was carried out as part of this project for three areas, Nazko Valley, Baezaeko, and Tibbles Road (Figures 5.3a and 5.3b). The source of the gravity data is the Nechako Basin airborne gravity survey completed in 2008 (Natural Resources Canada, 2008). A preliminary magnetic inversion was completed for the Nazko Valley study area only, using Natural Resources Canada residual total field aeromagnetic data (Geological Survey of Canada, 1994). The University of British Columbia - Geophysical Inversion Facility (UBC-GIF) Grav3D and Mag3D inversion codes were used (Li and Oldenburg, 1996, 1998), and the workflow outlined by Williams (2008) was followed for setting up and running unconstrained inversions. Regional removal was not completed prior to the gravity or magnetic inversions.

*Gravity Inversion Set-up*

The 2008 Nechako Basin airborne gravity data is gridded at 400 m, and the inversion mesh for each of the three study areas were designed to match this data spacing with 400 m cells at the core. Padding cells of increasing size were added to the mesh to a distance that is required to explain any features that might occur in the dataset but not directly within the volume of interest. The Bouger gravity data (2.67) was upward continued to 400 m (depth of gravity inversion core cells), to avoid high frequency effects in surface cells. The data was then draped onto Satellite Radar Topography Mission (SRTM) topography (90 m resolution), and 105 m (flight height) + 400 m (upward continuing distance) was added to the elevation. Errors of 0.05 mGal are used. The gravity inversion was run using default UBC-GIF parameters.

*Magnetic Inversion Set-up (Nazko Valley area only)*

Residual magnetic data is gridded at 275 m. The mesh core was designed with 275 m x 275 m x 250 m cells. Magnetic data was upward continued to 200 m. Data was draped on SRTM topography, and elevation was increased by 305 m (average flight height) + 200 m (upward continuing distance). Errors of 2 % (nT) are used on top of a minimum error representing 2% of the data range. The magnetic inversion was run using default UBC-GIF parameters. Caution should be used in interpretation of magnetic inversions using magnetic data collected over the Nechako Basin area. The default UBC-GIF magnetic inversion code assumes magnetic remanence is not present; however physical rock property studies from the Nechako Basin have indicated that remanent magnetization is present in Chilcotin basalts. This being said, the magnetic inversion results generally correlate well with magnetic susceptibility data collected on outcrop and from samples in the Nazko Valley, Baekaeko, and Tibbles Road areas. Susceptibility anomalies in the inversion also correlate well in places with gravity and MT inversion results.

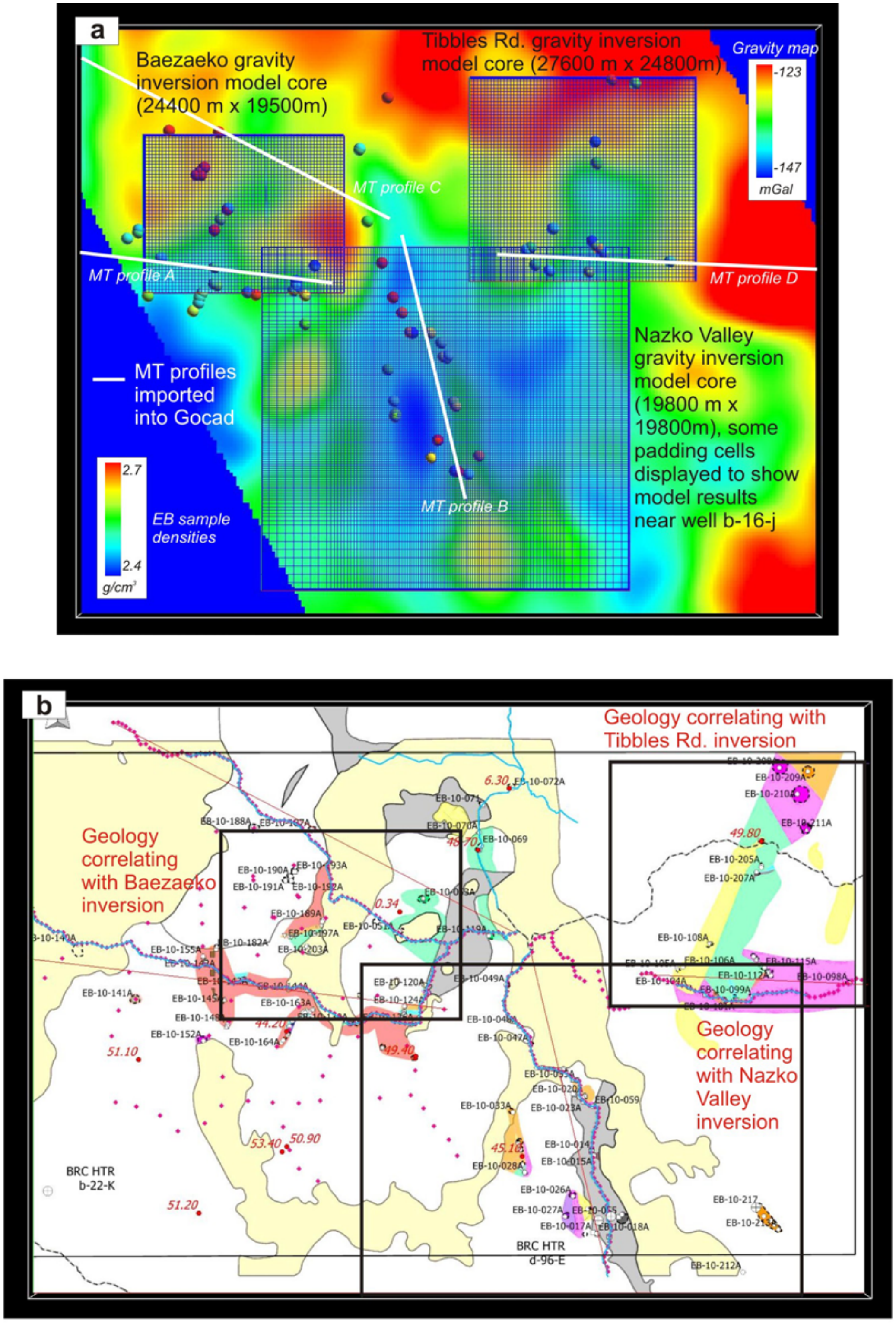


**Figure 5.3: Gravity data (a) and geology (b) for sites chosen for gravity and magnetic inversion modeling. See figure 3.3 for geological and symbol legends.**

Inversion results were imported into Gocad software, along with sample and outcrop magnetic susceptibility and density data, and raster images of recently mapped geology and MT inversion profiles (from Spratt and Craven, in press).

#### 5.3.2.1 *Physical Property Data Summary*

Before any interpretations on the results can be made, an understanding of expected physical property variations is required. Table 5.2 below summarizes the major susceptibility and density trends dictated from density and susceptibility measurements collected on the sample suite.

**Table 5-2: General density and magnetic susceptibility ranges for rocks sampled and mapped during this study.**

| | Density | Magnetic Susceptibility |
|---|---|---|
| ***Low*** | Mafic breccia, intermediate breccia, polymictic volcaniclastic | Cretaceous sedimentary rocks, intermediate volcaniclastic, felsic tuff |
| ***Medium*** | Dacite, intermediate volcaniclastic rocks, felsic tuff | Mafic breccia, polymictic volcaniclastic |
| ***High*** | Basalt, andesite, Cretaceous sedimentary rocks | Andesite, basalt, dacite, intermediate breccia |

#### 5.3.2.2 *Inversion Model Results*

The figures presented in this section show horizontal and vertical slices through the gravity and magnetic inversion models. Only the core cells of the Baezaeko and Tibbles Road inversions are shown, whereas for the Nazko Valley inversion, some padding cells are kept to show models results near the b-16-J well. Recent field mapping, samples (physical property data), oil and gas wells, and MT profiles are shown for comparison and to aid interpretations.

*Nazko Valley Gravity and Magnetic Inversions*

Figure 5.4a shows the geological map that corresponds to the core (plus inner padding cells) of the Nazko Valley gravity and magnetic inversions. Figure 5.4b shows a  horizontal slice at 200 m (above sea level) through the Nazko Valley gravity inversion. Figures 5.4a and 5.4b also show locations of MT inversion profiles and locations of cross-sections to be presented in subsequent figures.
Figure 5.4b shows a high density zone correlating with Cretaceous sedimentary rocks. This is consistent with the relatively moderate to high densities characterizing the Cretaceous sedimentary rock samples collected from this region. In areas where Eocene rocks have been mapped, densities vary. Lower density zones likely relate to accumulations of volcaniclastic or felsic rocks, and higher density zones likely reflect packages of coherent basaltic or andesitic rocks.

Density features of interest, corresponding with mapped geology and logged well lithology, are annotated on Figure 5.4c. They include:

i. A density high correlates with mapped Cretaceous sedimentary rocks and logged Cretaceous sedimentary units in wells a-4-L and d-96-E (beige colors along well length). This density high may be influenced by andesitic rocks mapped immediately to the west.
ii. Low to moderate density rocks occur east of the mapped Cretaceous rocks, which may indicate the presence of lower density brecciated or volcaniclastic rocks.
iii. A sharp gradient occurs between high density rocks (i) and low density rocks to the west. Low densities in the inversion result could reflect volcaniclastic rocks or brecciated units.
iv. Moderately dense rocks are suggested by the inversion result to occur near well b-16-J, where mafic rocks (green colors) and polylithic conglomerates have been recorded.
v. A moderate to high density zone aligns with mapped dacitic and andesitic rocks to the north.

An equivalent east-west cross-section through the magnetic inversion is shown in Figure 5.4d, and includes the following distinctive features:

i. Cretaceous sedimentary rocks correlate with a magnetic susceptibility low.
ii. To the west of mapped Cretaceous rocks, a high susceptibility anomaly dipping east correlates with mapped andesitic units.
iii. A low susceptibility zone near the center of the inversion cross-section overlaps with a density low in the gravity inversion.
iv. Andesitic rocks mapped west of the central susceptibility low (iii) are aligned with a narrow magnetic susceptibility anomaly.
v. At the western end of the cross-section, a high susceptibility zone correlates roughly with a high density zone from the gravity inversion result.

A cross-section through the gravity inversion result that is roughly aligned with MT profile B is compared to the MT inversion results in Figure 5.4e. The shallow localized high conductivity anomalies in the MT model are not imaged by the gravity inversion. At depth, large scale changes in the density model are generally mirrored by changes in the conductivity model. The regions characterized by high densities and low conductivities could reflect basement rocks.

The equivalent magnetic inversion section is shown with the MT profile in Figure 5.4f. As with the density model, changes in the magnetic susceptibility model at depth echo changes in the MT conductivity model.

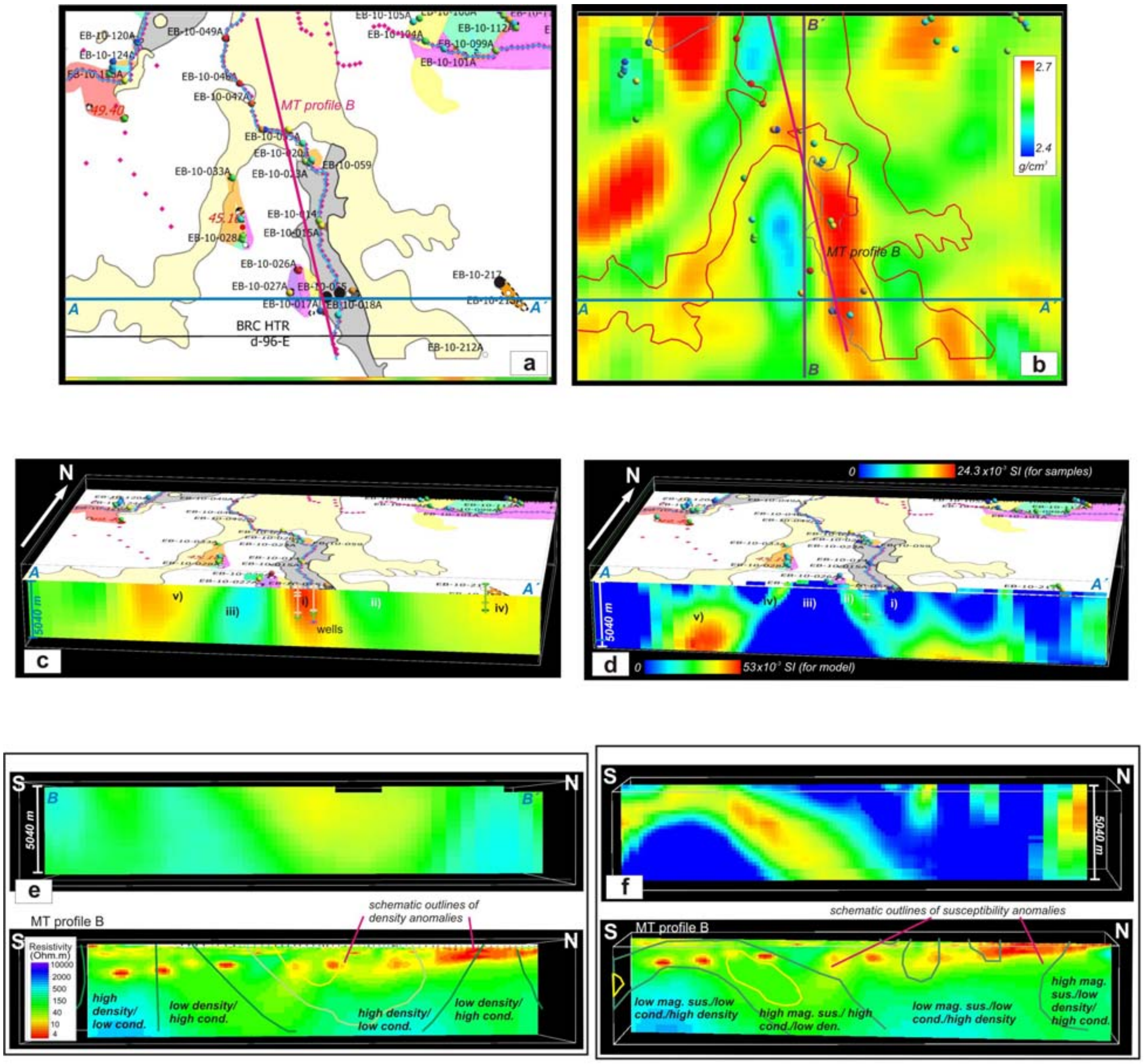


**Figure 5.4: Nazko Valley gravity and magnetic inversions. a) Geology of the Nazko area, with locations of MT profile B, and inversion cross-section A-A'. Spheres represent density measurements made during this study. See figure 3.3 for geological and symbol legends. b) Horizontal slice through gravity inversion at 200 m elevation, with locations of MT profile B and inversion cross-sections A-A' and B-B'. Spheres represent density measurements colored using the same scale as inversion results. c) A-A´cross-section at 5836600 m N through gravity inversion, north-facing; see text for explanation of numbered features. d) Cross-section at 5836600 m N through magnetic inversion, north-facing; see text for explanation of numbered features. Spheres on map represent magnetic susceptibility measurements. e) Cross-section through gravity inversion, west-facing; lower section shows MT profile B, roughly parallel to B-B' cross-section. f) Cross-section through magnetic inversion, west-facing; lower section shows MT profile B, roughly parallel to B-B' cross-section.**

*Baezaeko Gravity Inversion*

Geology from the Baezaeko area is shown in Figure 5.5a. A horizontal section through the gravity inversion model at 600 m for the same area is shown with locations of subsequent cross-sections and MT inversion profiles in Figure 5.5b. Mapped Cretaceous rocks to the east correspond with a density high. The Eocene rocks mapped here are predominantly dacitic, and both brecciated and coherent facies are represented. The density distribution near surface possibly maps out the local distribution of the varied dacite facies, with lower density areas representing more brecciated units. In general, densities measured on collected samples from this area correlate well with near-surface inversion results.

Figure 5.5c presents an east-west cross-section through the gravity inversion for the Baezaeko area. Density features of interest are annotated on the figure and commented below:

i. Cretaceous rocks are mapped above a density high. Some low density cells occur near surface. The western margin of the high density anomaly appears to dip to the west.
ii. Moderate to high densities potentially correlate with flow-banded to coherent dacitic units. High densities here do not appear to extend to depth.
iii. A low density zone toward the west may correlate with flow banded dacite, or polymictic units.
iv. A high density zone at the far western edge of the east-west section matches the location of mapped and sampled high density Hazelton Group andesitic basement rocks. The rocks dominate the north-western corner of the inversion area.

Figure 5.5d shows a northwest cross-section through the model with some anomalies noted:

i. Moderate to high density cells reflect Hazelton Group rocks.
ii. In the southwest corner of the inversion area, moderate density cells occur near surface, and correlate with mapped columnar jointed and vitreous dacite.
iii. Below these near-surface highs, is a lower density zone.
iv. A high density anomaly here has similar characteristics as feature ii from Figure 5.5c and suggests more coherent intermediate to mafic rocks extending to about 2500 m depth from the surface.

An East-West cross-section through the gravity inversion aligning with MT profile A is shown in Figure 5.5e. As in the Nazko Valley inversion, density variations at depth seem to correspond broadly with conductivity variations. Near surface, high conductivity zones vary in density, potentially reflecting brecciated units ranging from lower density dacitic to higher density andesitic rocks.

Figure 5.5f shows a correlation between depths of features predicted by the MT inversions and the gravity inversions.

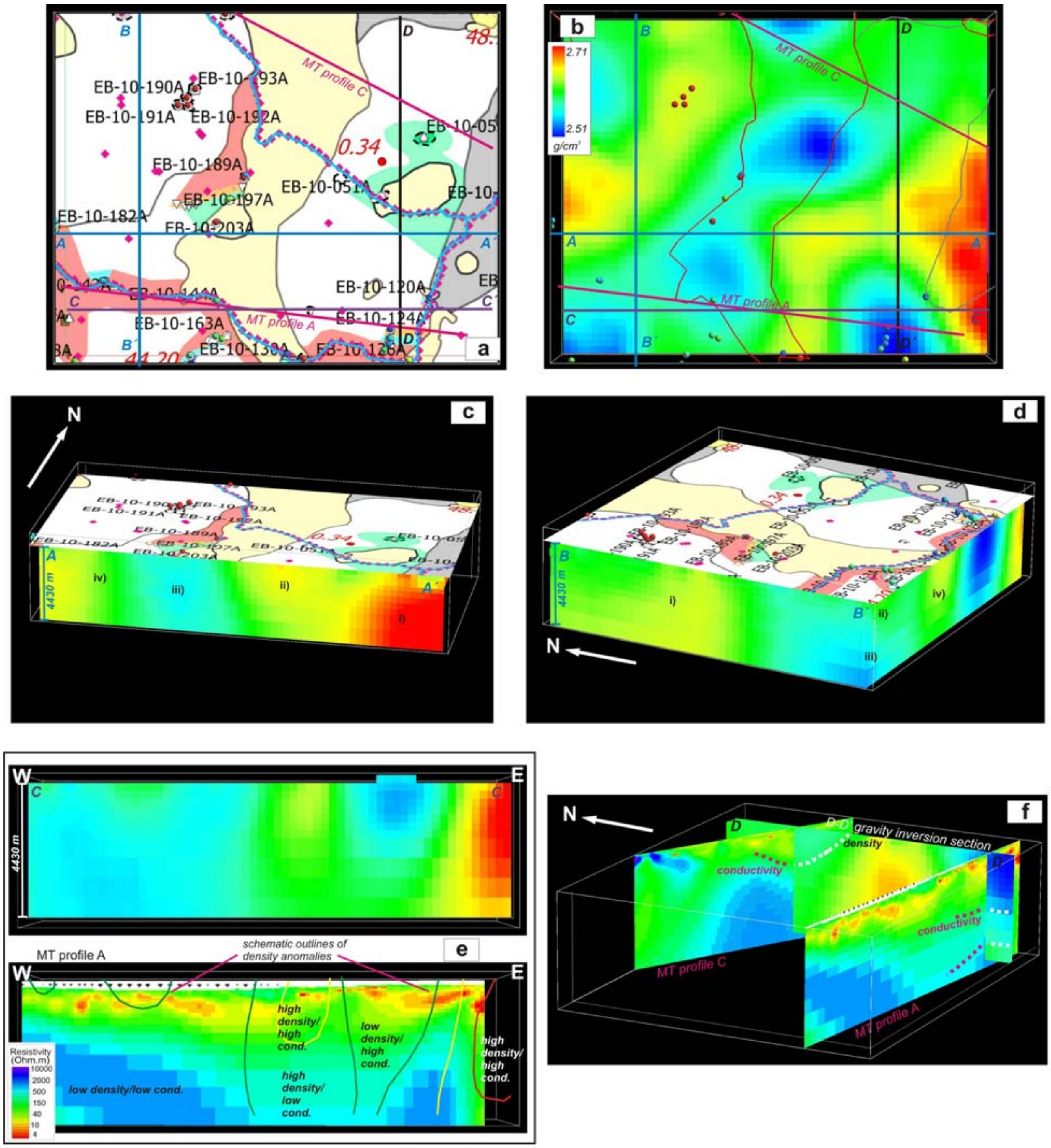


**Figure 5.5: Baezaeko gravity inversion model. a) Geology of the Baezaeko area, with locations of MT profiles A and C, and inversion cross-sections A-A', B-B', and C-C'. Spheres represent density measurements made during this study. See figure 3.3 for geological and symbol legends. b) Horizontal slice through gravity inversion at 600 m elevation, with locations of MT profiles A and C, and inversion cross-sections A-A', B-B', and C-C'. c) A - A' Cross-section at 5862360 m N through gravity inversion, north-facing; see text for explanation of numbered features. d) B-B' Cross-section through 456250 m E gravity inversion, east-facing; see text for explanation of numbered features. e) Cross-section through gravity inversion, north-facing; lower section shows MT profile A, roughly parallel to C-C' cross-section. f) Intersection of N-S density model slice with MT profiles C and A.**

*Tibbles Road Gravity Inversion*

Figure 5.6a presents Tibbles Road geology and 5.6b shows a horizontal gravity inversion slice for the same area at 600 m elevation. A prominent feature here is a high density ridge extending from the southern to northern edges of the model. The cause of this anomaly is not entirely clear from the mapped geology.

An east-west section through the gravity inversion is shown with density features highlighted in Figure 5.6c. Some of the prominent anomalies are described below:

i. A westerly dipping high density anomaly occurs in the western part of the cross-section. The anomaly may partly encompass a felsic tuff mapped here, but appears to reach a maximum slightly west of this unit.
ii. Densities are low to moderate west of the prominent high density ridge.
iii. To the east, moderate to high densities occur near-surface. Anomalies form basin-like shapes and dip off to the east. These highs potentially reflect coherent dacitic or andesitic units. Felsic tuff is mapped just off the margin of one of the highs.
iv. The inversion calculates low density cells at depth near the center of the cross-section. This anomaly reaches upward to align with a mapped dacite unit.

Figure 5.6d presents a north-south cross-section. Distinctive features are commented below:

i. This section shows the same shallow higher density features as in Figure 5.6c. Here they are aligned with coherent, flow-banded andesitic units.
ii. A low density anomaly that extends to depth appears to extend to surface to meet a mapped dacite. Such a large and deep low density anomaly could alternately represent a felsic intrusive body, or could indicate faulting.
iii. A localized high density anomaly occurs in the north-central part of the inversion area. Fig 5.6b shows the core of this high to be located between mapped dacitic and andesitic units.
iv. Lower density areas may signify more brecciated dacitic or andesitic facies, or could identify contacts or fault zones.

Again, density features appear to align with MT conductivity features at depth, when the two models are compared (Figure 5.6e). To the east a moderate density anomaly correlates with a conductivity high. Near the center of the cross-section low densities match low conductivities. In the west a density high matches a zone of, on average, high, but variable conductivity.

Figure 5.6f demonstrates coincidental horizontal changes in the gravity and MT inversion models.

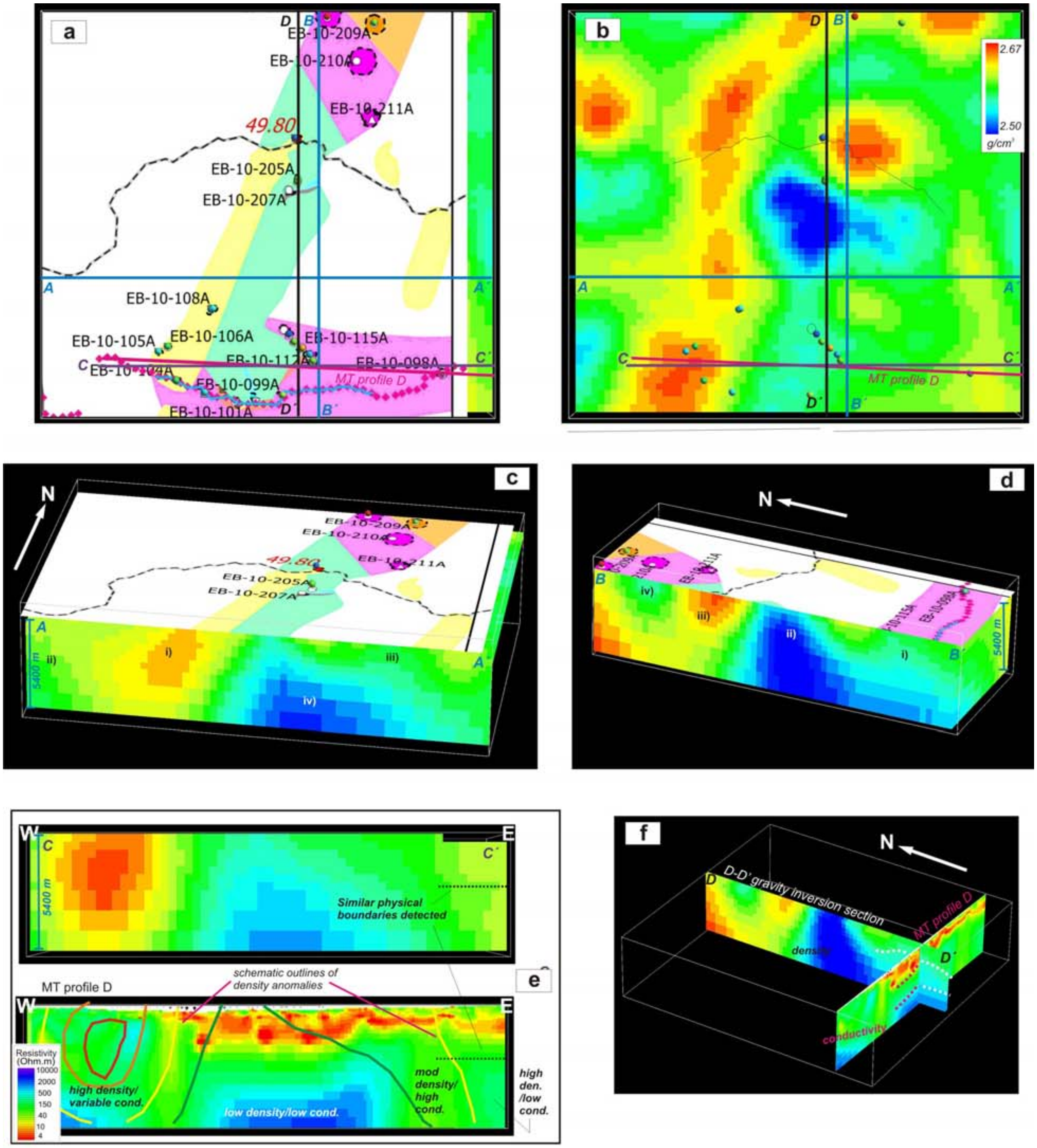


**Figure 5.6:Tibbles Road gravity inversion model. a) Geology of the Tibbles Road area, with locations of MT profile D, and inversion cross-sections A-A', B-B', C-C', and D-D'. Spheres represent density measurements made during this study. See figure 3.3 for geological and symbol legends. b) Horizontal slice through gravity inversion at 600 m elevation, with locations of MT profiles D, and inversion cross-sections A-A', B-B', C-C', and D-D'. c) A - A' Cross-section at 5865030 m N through gravity inversion, north-facing; see text for explanation of numbered features. d) B-B' Cross-section at 488570 m E through gravity inversion, east-facing; see text for explanation of numbered features. e) Cross-section through gravity inversion, north-facing; lower section shows MT profile D, roughly parallel to C-C' cross-section. f) Intersection of N-S density model slice with MT profile D.**

### 5.3.3 Aeromagnetic Maps

The Geological Survey of Canada conducted a high-resolution regional aeromagnetic survey in the Interior Plateau of British Columbia in 1993-1994 (GSC, 1994; Teskey et al., 1997). A number of salient features and trends were identified by Teskey et al. (1997) and include:

- The Yalakom and Tchaikazan faults are imaged in the southeastern part of the survey area, and merge on the southwestern boundary of the Tatla Lake Metamorphic Complex.
- A lineation, possibly the location of a major fault, can be traced across the survey area from southwest (51°, 125'50'W) to northeast (52"30'N, 122"30'W)
- “The general trend of magnetic patterns through the central part of the map area, northeast of the Yalakom fault, is north and northwest. This pattern is particularly evident along and parallel to the Fraser fault, which is seen as a dominant magnetic low, and its continuation north-northwest to the northern Fraser Plateau region, evident as parallel patterns of magnetic highs and lows.”
- “Major features evident at the 1:250 000 scale include the Tatla Lake Metamorphic Complex and major plutonic complexes of the Mount Waddington (NTS 92N; Tipper, 1969) and the southwest part of the Anahim Lake (NTS 93C) map areas. The latter areas contain complex aeromagnetic patterns, probably reflecting the presence of an intrusive complex comprising plutons of different compositions.”
- Several previously mapped plutons are clearly delineated by the aeromagnetic data.
- Several small aeromagnetic anomalies do not correspond to any mapped plutonic bodies or other indentified features. These may represent unexposed extensions of the known plutonic bodies or small unknown buried plutons.
- An Eocene volcanic centre interpreted by Metcalfe and Hickson (1995) in the Clisbako area corresponds to a broad positive magnetic anomaly. The anomaly lies at the intersection of two linear magnetic discontinuities, which possibly correspond to major pre-Eocene structures: one oriented SE-NW, the other parallel to the trend of the Anahim volcanic belt. Therefore, the location of the Clisbako volcanic centre could be controlled by such structures.
- “The Clisbako River area is also transected by numerous high-frequency north-bending trending anomalies, usually associated with areas underlain by Neogene Chilcotin Group basalts due to the abundance of magnetite in these rocks”

As part of this project, maps of the total magnetic field, residual magnetic field and magnetic first derivative were used to build a preliminary stratigraphic and structural framework of the Nechako region. The following steps were completed in order to highlight structural lineaments imaged by these surveys:

1- Form lines and fault sets were interpreted based mostly on the magnetic first derivative map (Figure 5.7), combined with the map of total magnetic field. Form lines illustrate the geometry of bedding, trends, breaks and constitute the framework of interpretation of the fault network.
2- The map of residual total field was used occasionally to constrain units contacts

3- Real magnetic values were checked locally in the original total field grid file. Zones of negative or low values usually match with green-blue areas. Outstanding zones of high values correspond to pink-light pink.

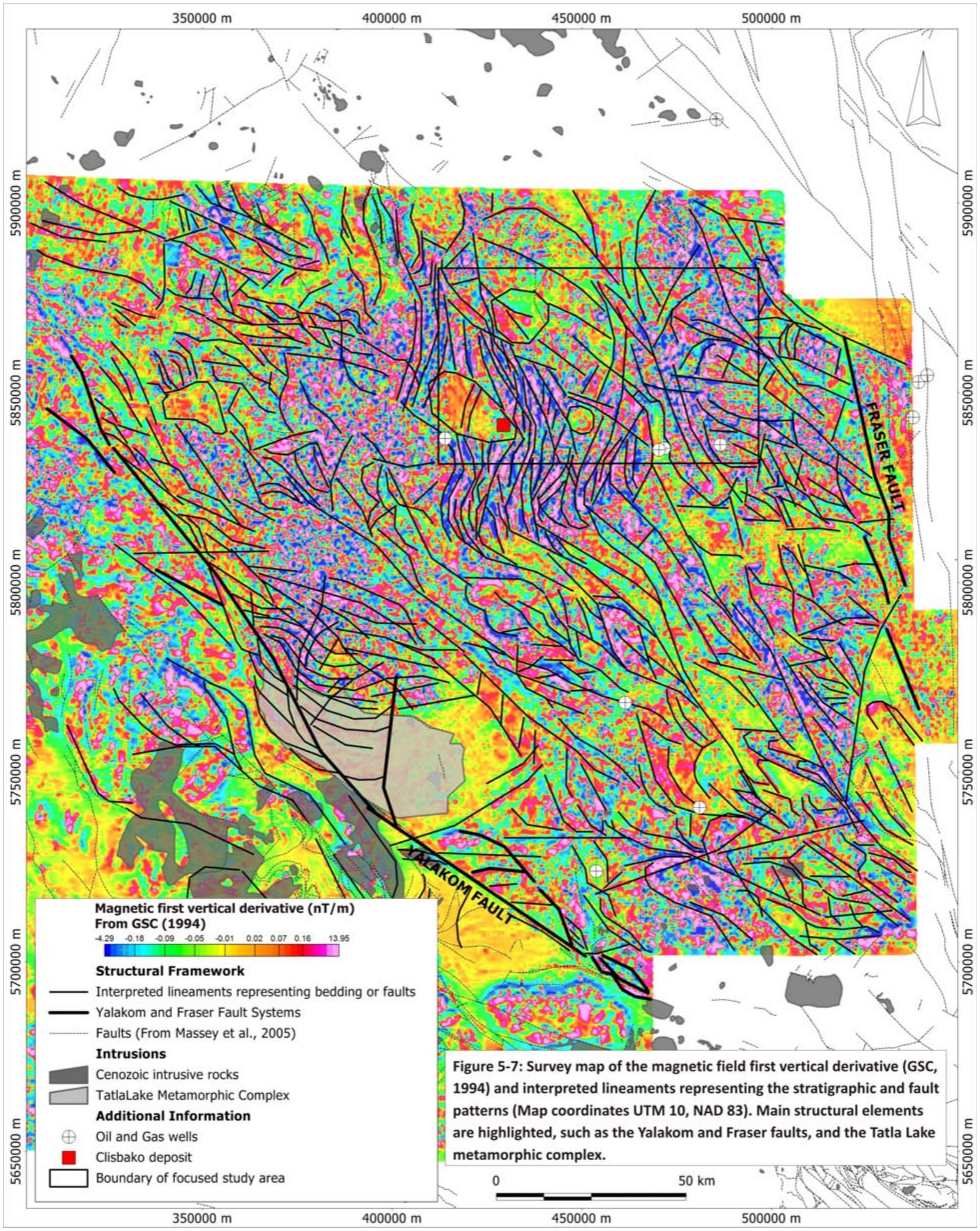


**Figure 5-7: Survey map of the magnetic field first vertical derivative (GSC, 1994) and interpreted lineaments representing the stratigraphic and fault patterns (Map coordinates UTM 10, NAD 83). Main structural elements are highlighted, such as the Yalakom and Fraser faults, and the Tatla Lake metamorphic complex.**

Distinctive structural elements from the aeromagnetic interpretation include the Yalakom and Fraser fault systems (Figure 5.7). Structural relationship between the Tatla Lake metamorphic complex and the Yalakom fault is also outlined on Figure 5.7. The general north and northwest trend of magnetic patterns outlined in Teskey et al. (1997) is also evidenced by the interpreted lineaments. However, there is a predominance of northwest-trending faults to the west, in the Yalakom fault area, compared to the Fraser fault area to the east where most structures trend north-northwest. In addition, east-west, west-northwest and west-southwest trending features are identified.

On the map of the magnetic field first vertical derivative (Figure 5.7), areas with distinctive patterns are identified and be used to constrain extent of lithological units. In particular, the “spotted” pattern on the western and southern half of the map corresponds in some places with subhorizontal Chilcotin basalt lava. Within and around the focused study area, a distinctive “banded” pattern corresponds to the mapped extent of Eocene volcanic rocks and could reflect flow-banding structures and tilting of these rocks.

A number of intrusions are imaged as well from the magnetic field first vertical derivative map. The focused study area contains two broad positive anomalies with dimensions ranging from about 7 x 7 km for the easternmost one, and 14 x 22 km for the westernmost one (Figure 5.7). The latter anomaly corresponds to the Eocene volcanic centre interpreted by Metcalfe and Hickson (1995) in the Clisbako area; the Clisbako epithermal deposit is located at the edge of this anomaly.

## 5.4 GIS-derived Eocene Thickness Model

### 5.4.1 Method

A GIS Eocene thickness model was computed using the GIS software Manifold. The method for building this model was adapted from Mihalynuk (2007) and is detailed below.

1. The thickness of the post-Eocene volcanic package, including the Chilcotin Group basalts and the Holocene Anahim volcanic rocks, is constrained using mapped and inferred contacts of these units (Massey et al., 2005), basalt plus drift thicknesses logged in water wells (Andrews and Russell, 2008; Dohaney et al., 2010b) and basalt logged in oil and gas wells (Riddell et al., 2007).
   - Contact depths from wells are converted to elevations: an elevation is assigned to each well locality representing the elevation of the basal contact of the post-Eocene package.
   - Intersection points are generated between the mapped boundary of the post-Eocene package and elevation contour lines (50 m spacing) generated from a Digital Elevation Model (Centre for Topographic Information, 1997). Each point is assigned an elevation which represent the intersection between the topography and the mapped contact of the post-Eocene package.

2. All elevation points generated at the previous step are pasted into a new surface. This surface represents the elevation base of the post-Eocene package. The surface is generated with the gravity interpolation method, using a cell size of 1km*1km and 10 neighbours. Initially, Kriging was used as

an interpolation method, but it seems to be flattening the negative elevations which end up not being represented.

3. The post-Eocene basal elevation surface is subtracted from the DEM surface; this result in a thickness model of the post-Eocene rock package.

4. The basal depths of the Paleocene-Eocene package are constrained using mapped and inferred contacts of Eocene and Paleocene volcanic rocks (Massey et al., 2005), contact depths established from oil and gas wells (Riddell et al., 2007; Riddell, 2010) and cross-sections constructed in the Chilanko Forks area by Mihalynuk et al. (2009). In some cases, a decision was made to integrate the Paleocene volcanic rocks logged in oil and gas wells to the Eocene package.
    - Contact depths from wells are converted to elevations: an elevation is assigned to each well locality representing the elevation of the basal contact of the Eocene-Paleocene package.
    - Intersection points are generated between the mapped contact of the Eocene-Paleocene package and elevation contour lines (50 m spacing) generated from the DEM. Each point is assigned an elevation which represents the intersection between the topography and the mapped contact of the Eocene-Paleocene package.

5. All elevation points generated at the previous step are pasted into a new surface. This surface represents the basal elevation of the Eocene-Paleocene package. The surface is generated with the Gravity interpolation method, using a cell size of 1km*1km and 10 neighbours.

6. The most constrained Eocene-Paleocene elevation surface is substracted from the DEM surface; this results in a thickness model of the Eocene plus post-Eocene package.

7. The thickness model of the post-Eocene package is then substracted from the thickness model of the Eocene plus post-Eocene package. The resulting model is an Eocene thickness model (Figure 5.8).

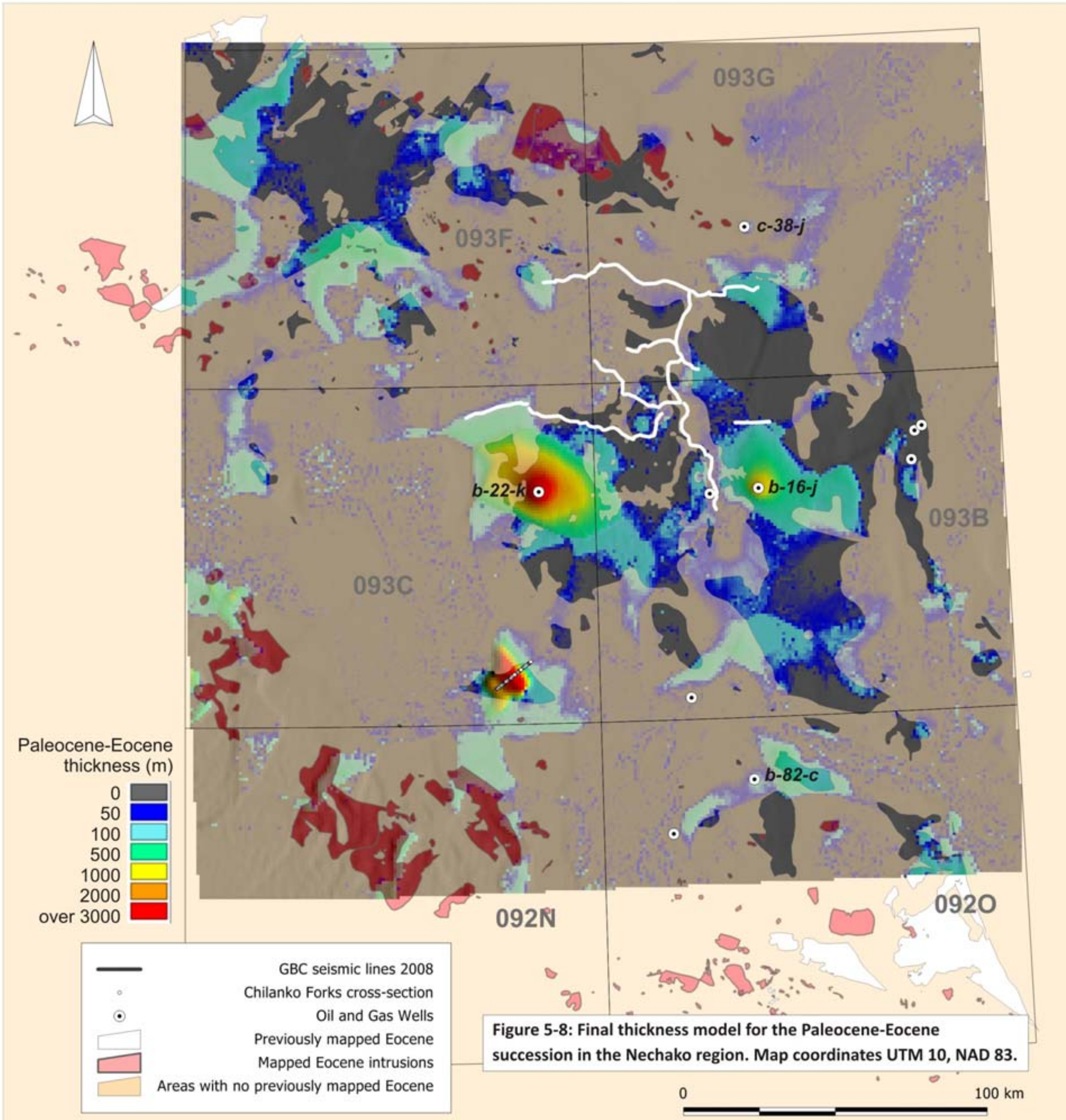

**Figure 5-8: Final thickness model for the Paleocene-Eocene succession in the Nechako region. Map coordinates UTM 10, NAD 83.**

### 5.4.2 Results

Several important observations resulted from the building process of this GIS model. First, the density of water wells used to constrain the thickness of Chilcotin basalt is more important in the southeast corner of the study area (NTS sheets 092P; 093A, B). In other areas, only two oil and gas wells sample basalt but there are no isotopic dates to confirm that they belong to Miocene Chilcotin basalts. As a result, the post-Eocene thickness model for the studied area displays variable levels of confidence.

Considerable thicknesses of Eocene volcanic rocks are recorded in oil and gas wells (Figure 5.1 and 5.2) and inferred from surface mapping (Mihalynuk et al., 2009). The successive addition of constraints from oil and gas wells and cross-sections shows local but important modifications of the basal elevation model of the Paleocene-Eocene package.

On the resulting Eocene thickness model (Figure 5.8), Eocene thicknesses are commonly between 50 and 100 meters within the previously mapped boundaries of Eocene-Paleocene rocks. However, thicknesses can reach 1000 to over 3000 meters in the better constrained areas: below wells B-22-K and B-16-J, and along the Chilanko Forks cross-section. These considerable thicknesses may correspond to Eocene calderas, pull-apart basins or paleo-depressions. However, these added constraints are isolated and localized compared to the extent of the study area; additional constraints will significantly modify the model.

A semi-transparent mask is applied to the resulting Eocene thickness model (Figure 5.8). Areas covered by the mask correspond to areas outside of known Eocene exposure. However, some of these masked areas display significant thickness of Paleocene-Eocene rocks. In these areas, Eocene rocks may be covered by the Neogene and Holocene basalts. Other possibilities include post-depositional structural disruption, erroneous mapping, or errors in unit assignment. Finally, some areas included in the mapped Paleocene-Eocene display a null elevation in the model.

### 5.4.3 Future Improvements of the Thickness Model

The following tasks will be undertaken in order to improve the quality of the Eocene thickness model for the Nechako region:

- Conduct detailed logging and sampling of existing core chips for wells B-16-J and B-22-K: description of lithologies and correlation with lithologies mapped in the surface, new U-Pb geochronology;
- Update Eocene and Neogene volcanic rocks contacts using recent mapping in the Chezacut and Chilanko Forks areas (Mihalynuk et al., 2008a and 2009), and mapping done as part of this study;
- Integrate seismic lines and MT lines information to the GIS thickness model;
- Constrain depth for the roots of Eocene intrusions.

# 6 Data Integration and Discussion

Main contributions from this project are reviewed below in light of the different objectives outlined in Chapter 1, including:

- Providing an improved stratigraphic model for the Eocene rocks
- Assessing the physical properties of Eocene volcanic rocks
- Assessing the variable thicknesses of Eocene volcanic rocks
- Proposing a structural framework of Eocene volcanic rocks

The applications of the different contributions are discussed, and their importance relative to improved understanding of the Nechako region geology.

## 6.1 Contribution from Recent Field Investigations

### 6.1.1 Stratigraphic Model

A preliminary stratigraphic model was developed for a focused study area part of the Nechako region of central BC (Chapter 3 of this report). The proposed stratigraphic model is based on field characteristics of mapped Eocene volcanic rocks including: lithologic characteristics and facies variations, geochemical signature, age, field relationships. Extensive literature review and existing datasets support new observations. The proposed stratigraphic model constitutes a basis for future investigations. Furthermore, improvements to this model will be proposed following additional field work.

Eocene volcanic rocks analyzed as part of this study display a clear high-potassium calc-alkaline geochemical signature. In addition, these rocks are geochemically characterized by linear trends for some of the major elements ($Fe_2O_3$, MgO, CaO, $K_2O$, $TiO_2$, $P_2O_5$) reflecting fractionation and evolution from a common magmatic source. These trends also suggest a contemporaneous tectonic evolution for the entire region because the rocks were sampled across the study area. Other elements, such as $Al_2O_3$ and $Na_2O$, display less variability in the range of concentrations for the different lithological units analyzed.

A series of preliminary maps, cross-sections and logs were produced following compilation of the field data and integration with geochemical and geochronological datasets. Eocene volcanic rocks mapped in this study display a range of textures and compositions and can be organized in a preliminary stratigraphic framework by lithological unit. The majority of mapped units are coherent and brecciated dacite interpreted as lava flows and domes. Several dacitic units have distinctive field characteristics and likely correspond to distinct volcanic events. However, the geochemical signature of these different dacitic units is quite similar. Future geochronology sampling will aim specifically at unravelling the age relationships between these different units. The other major rock units are coherent and brecciated andesite interpreted as lavas which are mapped mostly in the eastern part of the focused study area. The oldest mapped rocks are likely Early Eocene rhyolitic lavas observed in the Tibbles Road area.

### 6.1.2 Physical Properties

Physical properties constitute a direct link between the geology and geophysical models. In this project, a series of density measurements were conducted, in addition to systematic magnetic susceptibility measurements in the field (Chapter 4 of this report). Density and magnetic susceptibility values were analyzed in relation with lithologies, textures and identified mappable units. In addition, these results were compared to rock property measurements conducted as part of previous studies and compiled in the BC rock property database.

As a result, a physical property profile for the different units mapped in the field is proposed for both density and magnetic susceptibility measurements. Spatial variations of physical property values can be observed over the focused study area and correspond with changes in mapped units. Eocene volcanic rocks sampled as part of this study present a range of density and magnetic susceptibility values, and it may be challenging to establish distinctions between the different units based on physical properties only. However, the signatures of rock groups older and younger than the Eocene are more distinctive and present a narrower range of values. These distinct signatures are also visible in pre-existing physical property datasets.

Physical property profiles established for the different volcanic facies and units mapped as part of this project can be used together with the proposed maps to constrain seismic and magnetotelluric surveys interpretations. Relationships between mapping done as part of this study and MT profiles A, B, C, D from the Nazko area (from Spratt and Craven, in press ) are illustrated on Figure 6.1. The profiles are located on Figure 1.3. Spratt and Craven (2009 and 2010) interpreted three different groups of resistive layers underlying the Nechako region. A near surface resistive layer is interpreted as Chilcotin basalts (indicated as 1 on the profiles). The upper crust low resistivity layer, has two end members: a Cretaceous sedimentary package (2a on the profiles) and the Eocene volcaniclastic units (2b on the profiles). Finally an underlying resistive unit is identified by numbers 3 on the profiles. Black dashed lines represent interpreted crustal-scale faulting.

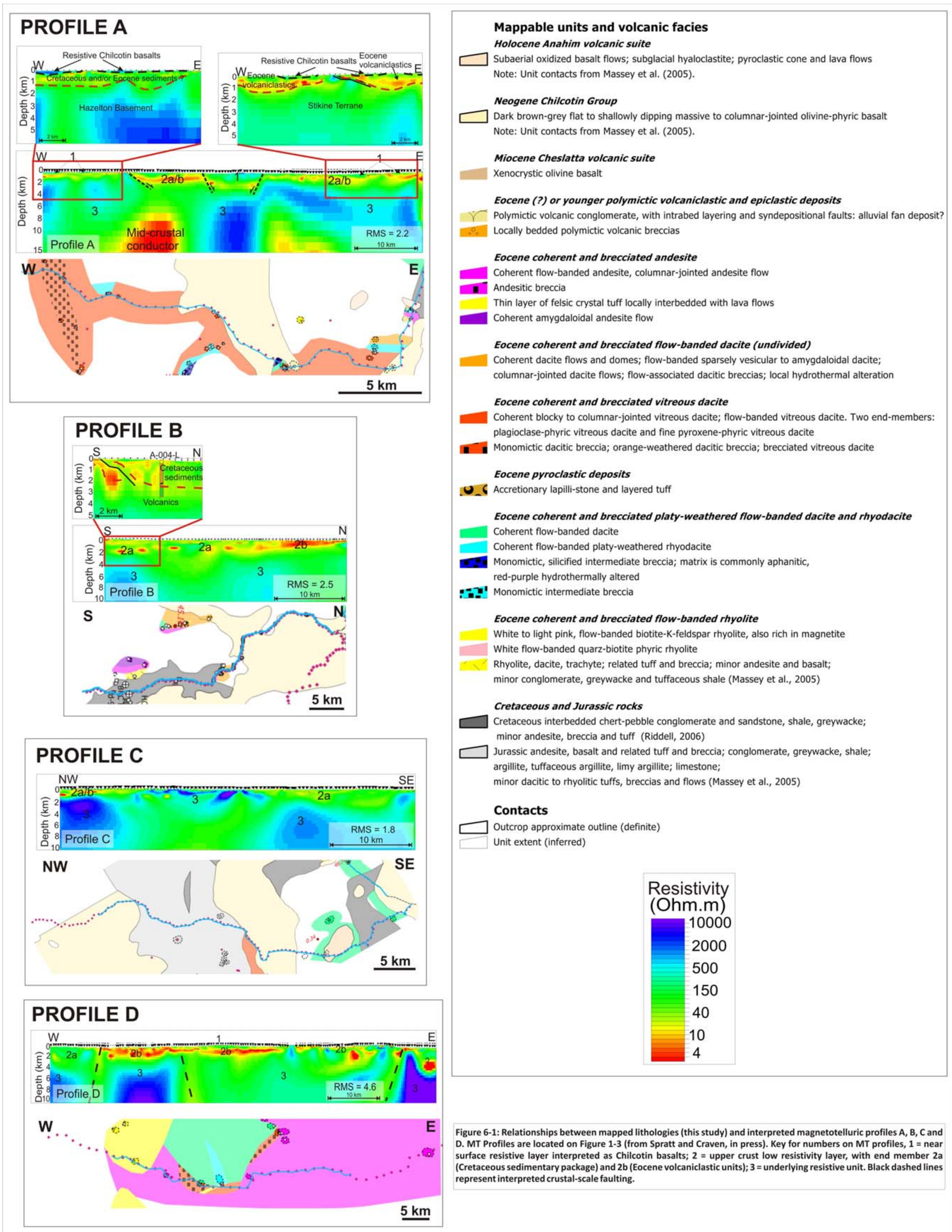


**Figure 6-1: Relationships between mapped lithologies (this study) and interpreted magnetotelluric profiles A, B, C and D. MT Profiles are located on Figure 1-3 (from Spratt and Craven, in press). Key for numbers on MT profiles, 1 = near surface resistive layer interpreted as Chilcotin basalts; 2 = upper crust low resistivity layer, with end member 2a (Cretaceous sedimentary package) and 2b (Eocene volcaniclastic units); 3 = underlying resistive unit. Black dashed lines represent interpreted crustal-scale faulting.**

### 6.1.3 Structural Framework and Thickness Model

In this project, evaluation of the variable thicknesses of Eocene volcanic sequences and their structural framework aims at providing insights into the underlying Jura-Cretaceous basin architecture and the tectonic evolution of the Nechako region.

Eocene volcanic rocks in the study area present a wide range of thicknesses, varying between several tens of meters up to 3000 meters in some places. The thickest sections are identified from the limited oil and gas wells (Chapter 5 of this report) located throughout the study area. It is likely that similarly thick sequences of Eocene volcanic rocks exist elsewhere but without further drilling it will be difficult to confirm. The proposed GIS thickness model (Chapter 5 of this report) is a first attempt at evaluating the regional thickness variations of the Paleocene-Eocene rock package. The model is constrained by geological data from wells and mapping, but later versions will include Eocene thicknesses evaluated from MT and seismic surveys. The MT method should be included in priority as it has proved to be useful for imaging the depth extent of basins, and also shows contrasting signatures between varying lithologies (Spratt and Craven, in press). In addition, mapping conducted as part of this project will also be included. The present thickness model indicates that the thickness of Eocene volcanic rocks can be highly variable across the Nechako region. In addition, mapped contacts are not always consistent with the model. This suggests that: 1) significant thicknesses of Eocene rocks may be masked either by drift or younger units; 2) Eocene contacts can be poorly defined in some places due to limited access and exposure.

Lineaments interpreted from an aeromagnetic survey (Chapter 5 of this report) constitute a preliminary stratigraphic and structural framework for the entire Nechako region. Stratigraphic contacts as well as dominant trends in the fault network are outlined on magnetic survey maps. Regional scale features such as the Yalakom and Fraser faults seem to control the distribution and orientation of the different fault sets interpreted.

The combination of the interpreted structural framework with the GIS thickness model (Figure 6.2) allows for the identification of a number of structural depressions which were infilled by the products of Eocene volcanism and bounded by faults. These faults are part of a regional network controlled to the east by the Fraser fault and to the west by the Yalakom fault. Areas with significant modelled thicknesses of Eocene volcanic rocks are generally bounded by interpreted faults and could represent pull-apart basins or calderas.

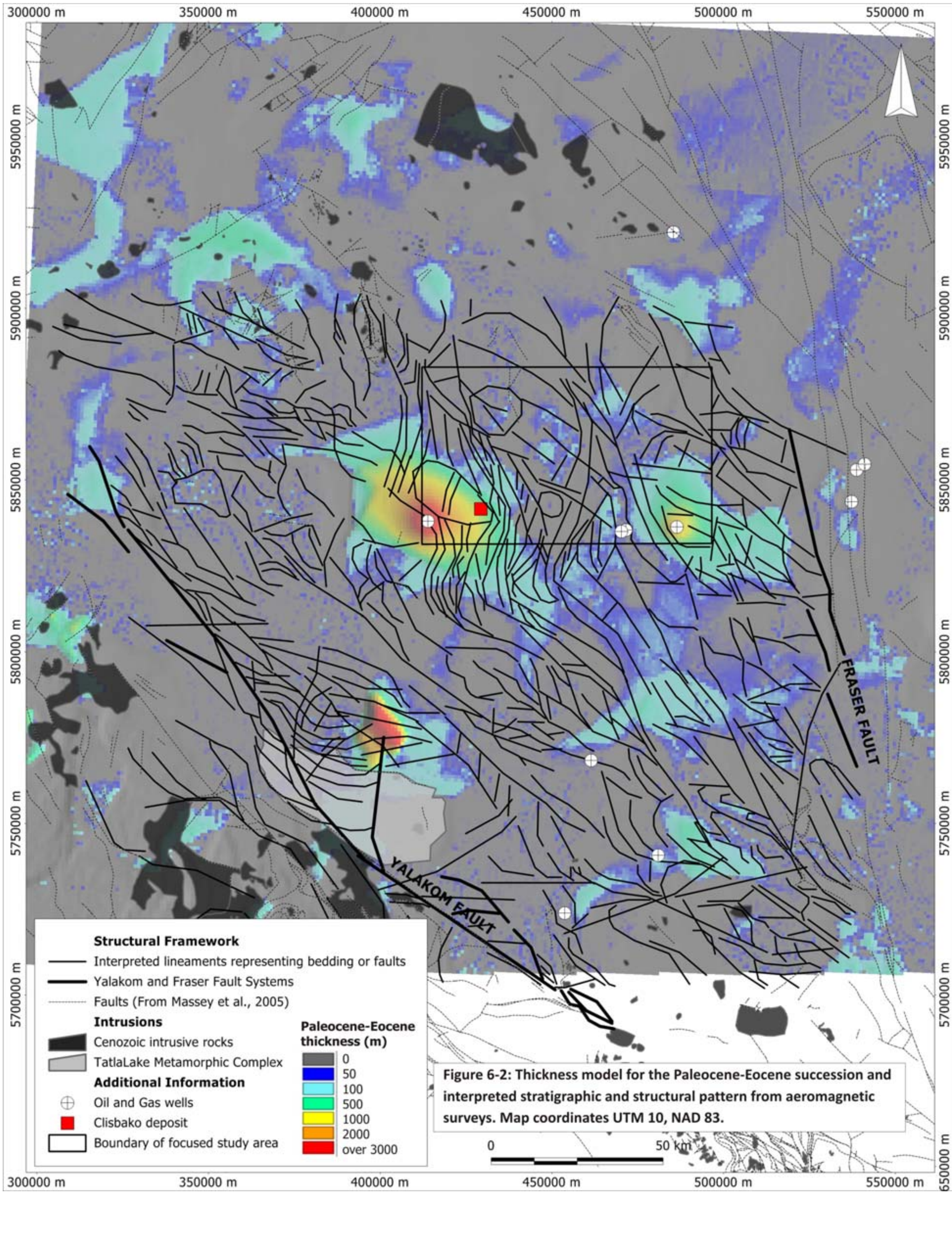


**Figure 6-2: Thickness model for the Paleocene-Eocene succession and interpreted stratigraphic and structural pattern from aeromagnetic surveys. Map coordinates UTM 10, NAD 83.**

## 6.2 Review of a Recent Tectonic Model and Comparison with New Dataset

The structural model for the Nechako region is proposed by Hayward and Calvert (in press) and is briefly reviewed here. This model is entirely based on geophysical data interpretation, including seismic surveys and Bouguer anomaly maps. Areas with great thicknesses of Eocene rocks, such as in the vicinity of well b-22-k, are interpreted as pull-apart basins bounded by en-échelon strike-slip faults linked by NE-trending structures. Based on isotopic dating conducted in well b-22-k (Riddell, 2010), basin initiation predates the Middle to Late Eocene Fraser Fault. Eocene volcanic rocks deposition is interpreted to be coeval or younger than Early Middle tectonism responsible for the Yalakom fault. This model is consistent with general dextral transtension taking place in the Cordillera during Eocene times (Ewing, 1980; Struik, 1993).

Observations, maps and models presented in this report are also consistent with a transtensional model involving the formation of local fault-bounded basins filled with Eocene volcanic rocks. However, several other hypotheses, including the caldera model, should be investigated and compared to Hayward and Calvert's model. Assessment of the different possible models will be one of the main objectives of the PhD research work conducted by Esther Bordet.

## 6.3 Implications for Exploration in the Nechako Region

In this report, many aspects of the Eocene volcanic rock package have been presented and can be applied to both oil and gas exploration, and mineral resources reconnaissance and exploration.

In the context of oil and gas exploration, the proposed GIS thickness model combined with interpreted structural and stratigraphic lineaments can be used to target areas where the underlying Cretaceous basin rocks are most accessible. In addition, these results can be associated with magnetotelluric and seismic 2D profiles to define the structure of the underlying basin and abrupt changes in the thickness of the overlying Paleocene and Eocene packages.

Interpretations of magnetotelluric and seismic surveys are more confidently constrained by the data, maps and cross-sections that are presented in this report. In addition, mapped lithologies can be associated with physical property signatures, and help constrain better the geophysical responses of these rocks.

The stratigraphic model proposed in this report can be compared to Eocene stratigraphic models proposed in other areas of the Nechako region. Lateral facies variations are to be expected at the regional scale. A stratigraphic and structural framework for the Eocene volcanic sequence will be a significant foundation for any future mineral exploration activity taking place in the Nechako region.

## References


Anderson, R.G., Snyder, L.D., Grainger, N.C., Resnick, J., and Barnes, E.M. (2000) Tertiary geology of the Takysie Lake and Marilla map area, central British Columbia; *in* Current Research 2000-A13, Geological Survey of Canada

Anderson, R.G., Resnick, J., Russell, J.K., Woodsworth, G.J., Villeneuve, M.E. and Grainger, N.C. (2001) The Cheslatta Lake suite: Miocene mafic, alkaline magmatism in central Bristish Columbia. Canadian Journal of Earth Sciences, vol. 38, p. 697-717.

Andrew, K.P.E. (1988) Geology and Genesis of the Wolf Precious Metal Epithermal Prospect and the Capoose Base and Precious Metal Porphyry-style Prospect: Unpublished M.Sc. thesis, University of British Columbia, 334 p.

Andrews, G.D.M. and Russell, J.K. (2007) Mineral exploration potential beneath the Chilcotin Group, south-central BC: preliminary insights from volcanic facies analysis; *in* Geological Fieldwork 2006, BC Ministry of Forests, Mines and Lands, Paper 2007-1 and Geoscience BC, Report 2007-1, p. 229–238.

Andrews, G.D.M. and Russell, J.K. (2008) Cover thickness across the southern Interior Plateau, British Columbia (NTS 092O, P, 093A, B, C, F): constraints from water-well records; *in* Geoscience BC Summary of Activities 2007, Geoscience BC, Report 2008-1, p. 11–19.

Andrews, G.D.M, Russell, J.K. and Dohaney, J. (2008) A preliminary physical property characterization of the Chilcotin Group basalts, south-central BC (092A, P, 093A, B). Vancouver Roundup poster presentation.

Awmack, H.J., Armitage, A. and Pawliuk, D. (2010) Technical report on the Capoose Project. Silver Quest Resources Ltd., 51 p.

Bevier, M.L. (1983) Implications of geochemical and isotopic composition for petrogenesis of Chilcotin Group basalts, British Columbia. Journal of Petrology, vol. 24, p. 207-226.

Bevier, M.L. (1989) A lead and strontium isotopic study of the Anahim volcanic belt, British Columbia: Additional evidence for widespread suboceanic mantle beneath western North America. Geological Society of America Bulletin, vol. 101, p. 973-981.

Breitsprecher, K., Thorkelson, D.J., Groome, W.G. and Dostal, J. (2003) Geochemical confirmation of the Kula-Farallon slab window in the Pacific Northwest, Data Repository Item 2003042. Geology, vol.31, no.4, p.351–354.

Breitsprecher, K. and Mortensen, J.K., (2004) BCAge 2004 A-1–a database of isotopic age determinations for rock units from British Columbia; BC Ministry of Forests, Mines and Lands, Open File 2004-3 (release 3.0), 9.3 Mb.

Bordet E. and Hart, C.J.R. (2010) Epigenetic Metallogeny of the Nechako Region, central British Columbia. Extented Abstract, SEG Annual Meeting, Keystone, Colorado October 2010.

Bordet E. and Hart, C.J.R. (2011) Characterization and structural frame work of Eocene volcanic sequences in the Nechako region, central British Columbia (NTS 092N, O, 093B, C, G); *in* Geoscience BC Summary of Activities 2010, Geoscience BC, Report 2011-1, p. 239–254.

Chapman, J. and Kushner, W. (2009) Geological assessment report on the Clisbako property, NTS 93C/9E, 47 p.

Clague, J.J. (1991) Quaternary glaciation and sedimentation, Chapter 12; *in* Geology of the Cordilleran Orogen in Canada; Geological Survey of Canada, J. Gabrielse and C.J. Yorath (editors),Geology of Canada, no. 4, (*also* Geological Society of America, Geology of North America, v. G-2), p. 421–434.

Clague, J.J. and James, T.S. (2001) History and isostatic effects of the last ice sheet in southern British Columbia. Quaternary Science Reviews, vol.21, p. 71-87.

Calvert, A.J., Hayward, N., Smithyman, B.R., and Takam Takougang, E.M. (2009) Vibroseis survey acquisition in the central Nechako Basin, south-central British Columbia (parts of 093B, C, F, G); *in* Geoscience BC Summary of Activities 2008, Geoscience BC, Report 2009-1, p. 145–150.

Centre for Topographic Information – Geomatics Canada (1997) Digital Elevation model for NTS sheets 093B, 093C, 093G, 093F, 092N, 092O, North American Datum of 1983. Canadian Digital Elevation Data, Level 1 (CDED1), Government of Canada, Natural Resources Canada, Centre for Topographic Information.

Cosgrove, T. (1981) Well history report on Canhunter Esso Nazko B-16-J/93-B-11, British Columbia.

Cosgrove, T. (1982) Well history report on Canhunter et al. Chilcotin B-22-K/93-C-9, British Columbia.

Dohaney, J., Andrews, G.D.M., Russell, J.K., and Anderson, R.G. (2010a) Distribution of the Chilcotin Group, Taseko Lakes and Bonaparte Lake map areas, British Columbia; Geological Survey of Canada Open File 6344 and Geoscience BC Map 2010-2-1; 1 sheet, scale 1:250 000.

Dohaney, J., Joseph, J.M.R., and Andrews, G.D.M. (2010b) Interactive bibliography and database for the Chilcotin Group basalts (NTS 82E, L, M; 83D; 92H, I, J, O, P; 93A, B, C, F, G, J, K, L), south-central British Columbia; Geological Survey of Canada, Open File 6286, 1 CD-ROM.

Diakow, L.J. and Levson, V.M. (1997) Bedrock and surficial geology of the southern Nechako plateau, central British Columbia; BC Ministry of Forests, Mines and Lands, Geoscience Map 1997-2, scale 1:100 000.

Diakow, L.J. and Mihalynuk, M.G. (1986) Geology of Whitesail Reach and Troitsa Lake map areas (93E/10W, 11E); *in* Geological Fieldwork 1986, BC Ministry of Forests, Mines and Lands, Paper 1987-1.

Enkin, R.J., Vidal, B.S., Baker, J. and Stuyk, N.M (2008) Physical properties and paleomagnetic Database for south-central British Columbia. GSC Geological Fieldwork 2007, paper 2008-1, p 5-8.

Ewing, T.E. (1980) Paleogene tectonic evolution of the Pacific Northwest. Journal of Geology, vol. 88, no. 6, p. 619-638.

Farrell, R.E. (2010) Volcanic facies architecture of the Chilcotin Group basalts at Chasm Provincial Park, British Columbia. Masters Thesis, University of British Columbia, 164 p.

Faulkner, E.L. (1986) Blackdome Deposit (92O/7E, 8W). In: BC-MEMPR Geological Fieldwork 1985, Paper 1986-1, p. 107-110.

Ferri, F. and Riddell, J. (2006) The Nechako Basin project: new insights from the southern Nechako Basin; *in* Summary of Activities 2006, BC Ministry of Forests, Mines and Lands, p. 89–124.

Friedlander, B. and Russell, J.K (2011) Wet/Dry Method for Determining Bulk Sample Density. Laboratory report, Centre for Experimental Studies of the Lithosphere, University of British Columbia, 1 p.

Friedman, R.M., Diakow, L.J., Lane, R.A. and Mortensen, J.K. (2001) New U-Pb age constraints on latest Cretaceous magmatism and associated mineralization in the Fawnie range, Nechako Plateau, central British Columbia: Canadian Journal of Earth Sciences, vol.38, p.619-637.

Gabrielse, J. and Yorath, C.J. (1991) Tectonic synthesis, Chapter 18; *in* Geology of the Cordilleran Orogen in Canada, Geological Survey of Canada, J. Gabrielse and C.J. Yorath (editors), Geology of Canada, no. 4, (*also* Geological Society of America, Geology of North America, v. G-2), p. 677–705.

Geological Survey of Canada (1994) Magnetic residual total field, Interior Plateau of British Columbia. GSC Open File 2785, 1994.

Gordee, S., Andrews, G., Simpson, K.A. and Russell, J.K. (2007). Subaqueous Channel-Confined Volcanism within the Chilcotin Group, Bull Canyon Provincial Park (NTS 093B/03), South-Central British Columbia. GSC *Geological Fieldwork 2006, Paper 2007-1, p. 285-290.*

Grainger, N.C., Villeneuve, M.E., Heaman, L.M. and Anderson, R.G. (2001): New U-Pb and Ar-Ar isotopic age constraints on the timing of Eocene magmatism, Fort Fraser and Nechako River map areas, central BC; Canadian Journal of Earth Sciences, v. 38., p. 679–696.

Haskin, M.L., Snyder, L.D., and Anderson, R.G. (1998) Tertiary Endako Group volcanic and sedimentary rocks at four sites in the Nechako River and Fort Fraser map areas, central British Columbia; in Current Research 1998-A; Geological Survey of Canada, p. 155-164.

Hayward, N. and Calvert, A.J. (2009) Preliminary first-arrival modelling constraints on the character, thickness and distribution of Neogene and Eocene volcanic rocks in the southeastern Nechako Basin, south-central British Columbia (NTS 092N, O, 093B, C); in Geoscience BC Summary of Activities 2008, Geoscience BC, Report 2009-1, p. 151–156.

Hayward, N. and Calvert, A.J. (in press) Interpretation of structures in the south-eastern Nechako Basin, British Columbia, from seismic reflection, well log and potential field data. Canadian Journal of Earth Sciences.

Irvine, T. N. and Baragar, W. R. A. (1971) A guide to the chemical classification of the common volcanic rocks. Canadian Journal of Earth Sciences 8, 523–548.

June M. Ryder, Robert J. Fulton et John J. Clague (1991) The Cordilleran Ice Sheet and the Glacial Geomorphology of Southern and Central British Colombia. Géographie physique et Quaternaire, vol. 45, n° 3, 1991, p. 365-377.

Le Maitre, R. W. (1989) A Classification of Igneous Rocks and Glossary of Terms. Recommendations of the IUGS Commission on the Systematics of Igneous Rocks. Oxford: Blackwell.

Lane, R.A. and Schroeter ,T.G. (1997) A review of metallic mineralization in the Interior Plateau, central British Columbia. In: L.J. Diakow, J.M. Newell (eds.) Interior Plateau Geoscience Project: Summary of Geological, Geochemical and Geophysical Studies, BCGS Survey Branch Open File 1996-2, p. 237-256.

Larocque, J.P. and Mihalynuk, M.G. (2009) Geochemical Character of Neogene Volcanic Rocks of the Central Beetle-Infested Zone, South-Central British Columbia (NTS 093B, C). BC Ministry of Energy, Mines and Petroleum Resources, Geological Fieldwork 2008, Paper 2009-1, p. 109-115.

Li, Y., and Oldenburg, D.W. (1996) 3-D inversion of magnetic data. Geophysics v. 61, p. 394-408.

Li, Y., and Oldenburg, D.W. (1998) 3D inversion of gravity data. Geophysics, v. 63, p.109-119.

Logan, J.M. and Moynihan, D.P. (2009) Geology and mineral occurrences of the Quesnel River map area, central British Columbia (NTS 093B/16); *in* Geological Fieldwork 2008, BC Ministry of Forests, Mines and Lands, Paper 2009-1.

Lowe, C., Enkin, R.J. and Struik, L.C. (2001) Tertiary extension in the central BC intermontane belt: magnetic and paleomagnetic evidence from the Endako region; Canadian Journal of Earth Sciences, v. 38, p. 657–678.

Massey, N.W.D., MacIntyre, D.G., Desjardins, P.J. and Cooney, R.T. (2005): Digital geology map of British Columbia: whole Province; BC Ministry of Forests, Mines and Lands, GeoFile 2005-1.

Mathews, W.H. (1989) Neogene Chilcotin basalts in south-central British Columbia: geology, ages, and geomorphic history. Canadian Journal of Earth Sciences, vol. 26, p. 969-982.

Mathews, W.H. (1991) Physiographic evolution of the Canadian Cordillera, Chapter 11; *in* Geology of the Cordilleran Orogen in Canada; Geological Survey of Canada, J. Gabrielse and C.J. Yorath (editors),Geology of Canada, no. 4, (*also* Geological Society of America, Geology of North America, v. G-2), p. 405–418.

Metcalfe, P. and Hickson, C. (1995) Tertiary Volcanic Stratigraphy of the Clisbako River Area, Central British Columbia, *in* Current Research 1995-4, Geological Survey of Canada, p. 67-73.

Metcalfe, P., Richards, T.A., Villeneuve, M.E., White, J.M. and Hickson, C.J. (1998) Physical and chemical volcanology of the Eocene Mount Clisbako volcano, central British Columbia. British Columbia Ministry of Energy, Mines and Petroleum Resources, Paper 1997-2, p. 31-61.

Mihalynuk, M.G. (2007) Neogene and Quaternary Chilcotin Group cover rocks in the Interior Plateau, south-central British Columbia: a preliminary 3D Thickness Model; *in* Geological Field Work 2006, Ministry of Energy, Mines and Petroleum Resources, paper 2007-1.

Mihalynuk, M.G., Orovan, E.A., Larocque, J.P, Bachiu, T. and Wardle, J. (2009): Chilanko Forks area geology (NTS 93C/8); BC Ministry of Forests, Mines and Lands, Open File 2009-6, scale 1:50 000.

Mihalynuk, M.G., Peat, C.R., Orovan, E.A., Terhune, K., Ferby, T. and McKeown, M.A. (2008a) Chezacut area geology (NTS 93C/8); BC Ministry of Forests, Mines and Lands, Open File 2008-2, scale 1:50 000.

Mihalynuk, M.G., Peat, C.R., Terhune, K. and Orovan, E.A. (2008b) Regional geology and resource potential of the Chezacut map area, central British Columbia (NTS 093C/08); *in* Geological Fieldwork 2007, Ministry of Energy, Mines and Petroleum Resources, Paper 2008-1.

Mihalynuk, M.G., Friedman, R.M. and Ullrich, T.D. (2008c) Geochronological results from reconnaissance investigations in the Beetle Infested zone, south-central British Columbia; in Geological Fieldwork 2007, Ministry of Energy, Mines and Petroleum Resources, Paper 2008-1.

Monger, J. and Price, R. (2002) The Canadian Cordillera: Geology and Tectonic Evolution; CSEG Recorder, URL <http://www.cseg.ca/publications/recorder/2002/02feb/feb02-canadian-cordillera.pdf> [September 2010].

Mwenifumbo, J. and Mwenifumbo, A.L. (2010) Analysis of well logs from the Nechako basin. Geological Survey of Canda, Open File 6542, 36 p.

Peccerillo, A. and Taylor, S. R. (1976) Geochemistry of Eocene calc-alkaline volcanic rocks from the Kastamonu area, Northern Turkey. Contributions to Mineralogy and Petrology, vol. 58, p. 63–81.

Quane, S., Andrews, G., Van de Reep, P., Enkin, R. and Russell, K. (2010) Rock physical property measurements : an aid to interpretation of geophysical surveys in the Nechako Basin oil and gas region, central British Columbia.

BC MINFILE, 2010. MINFILE BC mineral deposits database; BC Ministry of Energy, Mines and Petroleum Resources, URL (http://minfile.gov.bc.ca/) [June 2010].

Riddell, J.M. (2006) Geology of the southern Nechako Basin, NTS 92N, 92O, 93B, 93C, 93F, 93G. BC Ministry of Energy, Mines and Petroleum resources, Petroleum geology Map 2006-1, 3 sheets.

Riddell, J.M. (2010) Summary of apatite fission-track analyses and radiometric dates from the Nechako region, British Columbia (NTS 92O, N; 093B, C, E, F, G, L) and implications for oil and gas prospectivity. *In:* Geoscience Reports 2010, BC Ministry of Energy, Mines and Petroleum Resources, p. 123-131.

Riddell, J.M., Ferri, F., Sweet, A. and O'Sullivan, P. (2007) New geoscience data from the Nechako basin project. *In:* Ministry of Energy, Mines and Petroleum Resources: The Nechako Initiative – Geoscience Update 2007. Petroleum Geology Open File 2007-1, p. 59-98.

Riddell, J. and Ferri, F. (2008): Nechako Project Update; *in* Geoscience Reports 2008, BC Ministry of Forests, Mines and Lands, p. 67–77.

Rouse, G.E. and Mathews, W.H. (1988) Palynology and geochronology of Eocene beds from Cheslatta Falls and Nazko areas, central British Columbia. Canadian Journal of Earth Sciences, vol. 25, p. 1268-1276

Rouse, G. E. 1992. Appendix D, Palynology Results *in* Hunt, J.A. Stratigraphy, maturation and source rock potential of Cretaceous strata in the Chilcotin-Nechako region of British Columbia. M.Sc. thesis, *University of British Columbia,* Vancouver, B.C. Canada, 1992, pp. 448.

Smithyman, B.R. and Clowes, R.M. (2011): Improved near-surface velocity models from the Nechako Basin seismic survey, south-central British Columbia (parts of NTS 93B, C, F, G), part 2: full-wave form in version; *in* Geoscience BC Summary of Activities 2010, Geoscience BC, Report 2011-1, p. 255–264.

Souther, J.G., Clague, J.J. and Mathews, R.W. (1987) Nazko cone: a Quaternary volcano in the eastern Anahim Belt. Canadian Journal of Earth Sciences, vol. 24, p. 2477-2485.

Souther, J.G. (1991) Volcanic regimes, Chapter 14; *in* Geology of the Cordilleran Orogen in Canada; Geological Survey of Canada, J. Gabrielse and C.J. Yorath (editors),Geology of Canada, no. 4, (*also* Geological Society of America, Geology of North America, v. G-2), p. 457–490.

Spratt, J.E. and Craven, J.A. (2009) Preliminary images of the conductivity structure of the Nechako Basin, south-central British Columbia (NTS 092N, O, 093B, C, F, G) from the magnetotelluric method; *in* Geoscience BC Summary of Activities 2008, Geoscience BC, Report 2009-1, p. 175-182.

Spratt, J.E. and Craven, J.A. (2010) Magnetotellurique imaging of the Nechako Basin, British Columbia; *in* Current Research 2010-3, Geological Survey of Canada, 9 p.

Spratt, J.E. and Craven, J.A. (In press) Near surface and crustal-scale images of the Nechako Basin, British Columbia, Canada, from magnetotelluric investigations. Canadian Journal of Earth Sciences.

Steiner, R. (Hess D.W Consultants Ltd.) (1972) Vieco Texacal Punchaw c-38-j - Drilling report

Struik, L.C. (1993) Intersecting intracontinental Tertiary transform fault systems in the North American Cordillera; Canadian Journal of Earth Sciences, v. 30, p. 1262–1274.

Struik, L.C., and MacIntyre, G. (2001) Introduction to the special issue of Canadian Journal of Earth Sciences: The Nechako NATMAP Project of the central Canadian Cordillera: Canadian Journal of Earth Sciences, v. 38, p. 485-494.

Struik, L.C., MacIntyre, G. And Williams, S.P. (2007) Nechako NATMAP Project: A digital suite of geoscience information for central British Columbia. Geological Survey of Canada, Open File 5623, 2007.

Tempelman-Kluit, D. (2011) Blackwater: new gold mineralization style for British Columbia. MEG Abstract.

Teskey, D., Stone, P., Mustard, S. and Metcalfe, P. (1997) High-resolution regional aeromagnetic survey – Interior Plateau British Columbia. Geological Survey of Canada Paper 1997-2

Tipper, H.W. (1959) Geology , Quesnel, Cariboo District, British Columbia; Geological Survey of Canada, Map 12-1959, scale 1:253 440.

Tipper, H.W. (1969) Geology, Anahim Lake, British Columbia; Geological Survey of Canada, Map 1202A, scale 1:253 440.

Wang, K., Hole, J. A., Stephenson, A. L., Spence, G. D., Miller, K. C., Harder, S. H., Kaip, G. M. and Clowes, R. M. (2010): Controlled-source seismic investigation of the generation and collapse of a batholith complex, Coast Mountains, Western Canada

Whalen, J.B., Anderson, R.G., Struik, L.C. and Villeneuve, M.E. (2001) Geochemistry and Nd isotopes of the François Lake plutonic suite, Endako batholith: host and progenitor to the Endako molybdenum camp, central British Columbia. Canadian Journal of Earth Sciences, vol.38, p. 603–618.

WesternGeco MDIC (2010) 2D land joint inversion of seismic, magnetotelluric and gravity for pre-stack depth migration imaging, Nechako basin, British Columbia, lines 05, 10 and 15. Geoscience BC final project report, 49 p.

Westfall, J. (2004) Summary of forest health conditions in British Columbia. BC Ministry of Forests, Forest Practices Branch.

Wetherup, S. (1997) Geology of the Nulki Hills and surrounding area, central BC; *in* Current Research 1997-A, Geological Survey of Canada, p. 125–132.

Wetherup, S. and Struik, L.C. (1996) Vanderhoof Metamorphic Complex and surrounding rocks, central British Columbia; *in* Current Research 1996-A, Geological Survey of Canada, p. 63–70.

Williams, N.C. (2008) Geologically-constrained UBC–GIF gravity and magnetic inversions with examples from the Agnew-Wiluna greenstone belt, Western Australia: Unpublished Ph.D. Thesis, The University of British Columbia, 479 p.

# APPENDICES